AD_____

Award Number: DAMD17-00-1-0582

TITLE: Prenatal Alcohol Exposure Damages Brain Signal
         Transduction System

PRINCIPAL INVESTIGATOR: Kevin K. Caldwell, Ph.D.

CONTRACTING ORGANIZATION: The University of New Mexico
                            Albuquerque, New Mexico   87131-5041

REPORT DATE: September 2004

TYPE OF REPORT: Final

PREPARED FOR: U.S. Army Medical Research and Materiel Command
                Fort Detrick, Maryland   21702-5012

DISTRIBUTION STATEMENT: Approved for Public Release;
                        Distribution Unlimited

The views, opinions and/or findings contained in this report are
those of the author(s) and should not be construed as an official
Department of the Army position, policy or decision unless so
designated by other documentation.

20050712 041

REPORT DOCUMENTATION PAGE

Form Approved
OMB No. 074-0188

Public reporting burden for this collection of information is estimated to average 1 hour per response, including the time for reviewing instructions, searching existing data sources, gathering and maintaining the data needed, and completing and reviewing this collection of information. Send comments regarding this burden estimate or any other aspect of this collection of information, including suggestions for reducing this burden to Washington Headquarters Services, Directorate for Information Operations and Reports, 1215 Jefferson Davis Highway, Suite 1204, Arlington, VA 22202-4302, and to the Office of Management and Budget, Paperwork Reduction Project (0704-0188), Washington, DC 20503

1. AGENCY USE ONLY (Leave blank)	2. REPORT DATE September 2004	3. REPORT TYPE AND DATES COVERED Final (1 Sep 2000 – 31 Aug 2004)

4. TITLE AND SUBTITLE	5. FUNDING NUMBERS
Prenatal Alcohol Exposure Damages Brain Signal Transduction System	DAMD17-00-1-0582

6. AUTHOR(S)
Kevin K. Caldwell, Ph.D.

7. PERFORMING ORGANIZATION NAME(S) AND ADDRESS(ES)	8. PERFORMING ORGANIZATION REPORT NUMBER
The University of New Mexico Albuquerque, New Mexico *E-Mail:* kcaldwell@salud.unm.edu	

9. SPONSORING / MONITORING AGENCY NAME(S) AND ADDRESS(ES)	10. SPONSORING / MONITORING AGENCY REPORT NUMBER
U.S. Army Medical Research and Materiel Command Fort Detrick, Maryland 21702-5012	

11. SUPPLEMENTARY NOTES

12a. DISTRIBUTION / AVAILABILITY STATEMENT	12b. DISTRIBUTION CODE
Approved for Public Release; Distribution Unlimited	

13. ABSTRACT (Maximum 200 Words)

This final report details the results of our studies. The proposal's overall goal is to uncover biochemical mechanisms that underlie learning and memory. These studies have yielded novel information about the effects of fear conditioning on brain phospholipase C-β1a (PLC-β1a), indicating that PLC-β1a may play an important role in the biochemical processes underlying fear-conditioned learning and memory formation. We have uncovered the molecular basis of the observed association between PLC isozymes and extracellular signal-regulated protein kinase. In addition to increasing our understanding of the biochemical basis of learning and memory, these studies have yielded important information about the neurochemical mechanisms that underlie fear and stress, and, consequently, may provide insight into the neurochemical basis of posttraumatic stress syndrome.

14. SUBJECT TERMS		15. NUMBER OF PAGES
Fear, stress, alcohol, brain, enzyme		74
		16. PRICE CODE

17. SECURITY CLASSIFICATION OF REPORT	18. SECURITY CLASSIFICATION OF THIS PAGE	19. SECURITY CLASSIFICATION OF ABSTRACT	20. LIMITATION OF ABSTRACT
Unclassified	Unclassified	Unclassified	Unlimited

NSN 7540-01-280-5500

Standard Form 298 (Rev. 2-89)
Prescribed by ANSI Std. Z39-18
298-102

Table of Contents

INTRODUCTION

Phosphatidylinositol-specific phospholipase C (PLC) isozymes hydrolyze phosphatidylinositol 4,5-bisphosphate (PtdIns(4,5)P$_2$), yielding two intracellular second messengers: inositol 1,4,5-trisphosphate (Ins(1,4,5)P$_3$) and 1,2-diacylglycerol. Production of Ins(1,4,5)P$_3$ results in the release of Ca^{2+} from intracellular storage sites, while 1,2-diacylglycerol directly activates the conventional and novel isoforms of protein kinase C. Complementary DNA clones have been isolated for at least 11 distinct mammalian PLC isozymes (Rhee, 2001), which are grouped into four types: PLC-β, PLC-δ, PLC-γ and PLC-ε. PLC-β1 is the predominant PLC isozyme in brain, accounting for approximately 50% of the total PLC activity in this tissue (Takenawa et al., 1991). In a recently published study (Weeber et al., 2001), we reported that one-trial fear conditioning, a form of Pavlovian classical conditioning in which a conditioned stimulus (CS), a tone, is paired with an unconditioned stimulus (UCS), a brief electrical foot shock, is associated with changes in subcellular PLC-β1a enzyme activity and protein level in the hippocampal formation (HPF) and medial frontal cortex (MFC), and that these changes are altered in rats that were exposed prenatally to ethanol. Based on these observations, two goals were approved in the Statement of Work for this grant.

GOAL 1: To determine the time course of one trial fear conditioning-induced changes in PLC-β1a subcellular distribution and catalytic activity in adult rats who were exposed, or not, to moderate levels of ethanol throughout gestation.

Our previous work (Weeber et al. 2001), as well as several other lines of study, indicate that fear conditioning is associated with time-dependent changes in the subcellular distribution and activity of various cellular proteins. Studies undertaken in several laboratories have demonstrated that, under certain conditions, there are two temporal phases that are critical for long-term consolidation of fear memory: one period exists for the first few minutes up to one-hour following training, while the other period occurs between one- and six-hours after training, with the period from 2- to 4-hours most commonly being reported as important (Bernabeu et al., 1997; Bourtchuladze et al., 1998; Quevedo et al., 1999; Igaz et al., 2002). We sought to determine whether the time-dependency of fear-conditioned memory was correlated with changes in PLC-β1 enzyme activity and/or subcellular distribution and whether fetal alcohol exposure (FAE) altered this correlation.

GOAL 2: To determine whether one trial fear conditioning alters the phosphorylation state of PLC-β1a and, if so, whether fetal alcohol exposure modifies the changes in PLC-β1a phosphorylation.

Phosphorylation (i.e., the addition of a phosphate group to a serine, threonine or tyrosine residue) of proteins has been demonstrated to affect the catalytic activity and subcellular distribution of a variety of enzymes, including PLC isozymes. The phosphorylation of proteins is catalyzed by enzymes termed protein kinases, while the dephosphorylation (i.e., the removal of a phosphate group) is catalyzed by enzymes termed protein phosphatases. FAE has been reported to affect the activity of enzymes (e.g., protein kinase C, PKC) known to play an important role in protein phosphorylation. We sought to determine whether fear conditioning and/or prenatal exposure to alcohol altered the phosphorylation state of PLC; further, we sought to identify protein kinases or phosphatases that might play a role in this effect.

BODY

Progress made toward GOAL 1 is as follows.

We completed analyses of the alterations in phosphatidylinositol-specific phospholipase C-β1a (PLC-β1a) levels and enzyme activities in subcellular fractions prepared from the hippocampal formation (HPF) and medial frontal cortex (MFC) 1, 3, 5, 7, 24 and 72-hours following a single

4

trial of fear conditioning in control rats. We did not conduct the studies proposed for fetal alcohol-exposed rats primarily because we grossly underestimated the actual cost and amount of time required to perform these studies. In order to complete them, we would have been unable to pursue the studies related to GOAL 2 (see below), which proved to be extremely important. The results of our studies in control animals were published in the journal *Pharmacology, Biochemistry and Behavior* (please see Weeber and Caldwell 2004 in Appendix).

Conclusions

In summary, a single trial of fear conditioning was found to initiate complex and dynamic temporal changes in PLC-β1a enzyme activities and concentrations associated with the HPF and MFC. These results extend our previous study (Weeber et al., 2001) and correlate the regulation of PLC-β1a enzyme activity and subcellular distribution and the processes involved in learning and memory formation.

Progress made toward GOAL 2 is as follows.

We identified that extracellular signal-regulated protein kinase 2 (ERK2) associates with PLC-β1, -β2, -β4, -γ1 and −γ2 isozymes. Further, we identified potential mechanisms through which these associations may occur (please see Appendix for manuscript by Buckley and Caldwell that has been accepted for publication in *Pharmacology, Biochemistry and Behavior*). In addition to the data shown in the accepted manuscript, we found that prenatal alcohol exposure alters the interaction between ERK2 and PLC isozymes, indicating that this association may play a role in FAE-induced learning deficits (see Figure 1). In these studies, we found that fear conditioning increased the association of one or more PLC isozymes with ERK2 in control animals, whereas in FAE animals there was no increase in the association of ERK2 and PLC isozymes following fear conditioning. As ERK2 has been shown to play a critical role in fear-conditioned learning (Atkins et al., 1998; Selcher et al. 1999; Schafe et al. 2000), it follows that FAE-dependent disruption of the integration of ERK2 signaling may be an important mechanism underlying the learning deficits observed in animals exposed to alcohol prenatally.
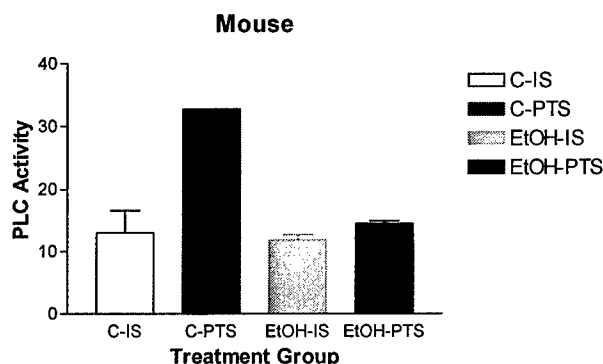
Figure 1   PLC activity present in anti-ERK2 immunoprecipitates isolated from mouse hippocampal formation postnuclear fractions. The hippocampal formation was isolated from adult mice that had been prenatally exposed to ethanol (EtOH), or not (control, C), following fear conditioning (paired tone-shock, PTS) or behavioral control (immediate shock, IS). Postnuclear fractions were prepared and ERK2 was immunoprecipitated. Immunecomplex PLC activity was measured and expressed as nmole Ins(1,4,5)P₃ product formed / min / μg tissue. Two-way ANOVA revealed a significant effect of diet [F(1,6)=13.3, p<.01], a significant effect of fear conditioning [F(1,6)=17.7, p<.01] and a significant interaction between diet and fear conditioning [F(1,6)=10.4, p<.02].

In addition to these studies, we made an important and novel observation that PLC-γ1 directly interacts with, and is a substrate for ERK2. Further, we found that ERK2-catalyzed phosphorylation of PLC-γ1 regulated PLC-γ1 catalytic activity. The results of these studies were recently published in the *Journal of Biological* Chemistry (please see Buckley et al. 2004 in the Appendix).

Section Conclusions:

These studies provide the basis to hypothesize that learning and memory are dependent on spatial and temporal alterations in the integration of PLC- and ERK2-dependent signaling in the rat brain, and that errors in the coordination of these signals may lead to cognitive and behavioral impairments.

Additional studies supported by the funds of this grant

Two lines of research directly related to the Statement of Work were developed using funds from this award.

1. Development of a method for capturing PLC isozymes on the surface of microtiter plates (Buckley and Caldwell 2003 Analytical Biochemistry; see Appendix)

In vitro quantification of the catalytic activity of an enzyme isoform requires the availability of selective agents that allow for either measurements in the presence of the other enzyme isoforms or the purification of the isoform and subsequent performance of these measurements on the purified enzyme. We developed a method for the measurement of phospholipase C-γ1 enzyme activity employing native enzyme that is immobilized on microtiter plates. We employed the technique to show that one or more tyrosine kinases co-purify with rat brain phospholipase C-γ1. The method is applicable to the study of any enzyme isoform (e.g., PLC-β1a, the focus of the Army grant) for which antibodies that capture the native form of the enzyme are available, and could easily be employed in high throughput procedures.

2. Development and characterization of a mouse model of fetal alcohol exposure (Allan et al 2003, Alcoholism: Clinical and Experimental Research; see Appendix)

Efforts to better understand the basis of prenatal ethanol-induced impairments in brain functioning, and the mechanism(s) by which ethanol produces these defects, rely on the use of animal models of FAE. Most studies on fetal alcohol effects have employed the rat, using a variety of ethanol administration paradigms and schedules. We sought to develop a mouse model of FAE that minimized problems that are associated with existing rat models of FAE (see Allan et al pp.4-5 for detailed discussion), as well as increase the opportunity to use the power of genetically defined and genetically altered mouse populations. We believe that the model complements and extends other available models for the study of FAE and will prove to be a useful tool in testing hypotheses about the neural mechanisms underlying the learning deficits present in fetal alcohol spectrum disorders (FASD).

KEY RESEARCH ACCOMPLISHMENTS

1. We completed the studies for GOAL 1 using control, but not FAE, rats. These studies have yielded novel information about the effects of fear conditioning on brain PLC-β1a. They indicate that PLC-β1a may play an important role in the biochemical processes underlying fear-conditioned learning and memory formation. These studies yielded one reportable outcome: Weeber and Caldwell 2004 (Appendix).

2. We conducted a series of studies related to GOAL 2. These studies identified previously unknown protein-protein interactions between PLC isozymes and ERK2, a protein kinase. Two reportable outcomes resulted from these studies: Buckley et al. 2004 (Appendix) and Buckley and Caldwell 2004 (Appendix).

3. We developed a method for rapid measurement of enzyme activity which will facilitate future studies on PLC isozymes. This research resulted in one reportable outcome: Buckley and Caldwell 2003 (see Appendix)

6

4. We assisted in the development of a mouse model of fetal alcohol exposure. This model will be extremely useful to us in the future, as it will allow for the testing of hypotheses in genetically defined and genetically altered mouse populations. One reportable outcome resulted from this work: Allan et al. 2003 (see Appendix).

REPORTABLE OUTCOMES

Buckley C.T. and Caldwell K.K. (2003) Two-layer antibody capture of enzymes on the surface of microtiter plates: application to the study of the regulation of phospholipase C-γ1 catalytic activity Anal. Biochem. 320: 193-198.

Allan, A.M., Paz R.D., and Caldwell K.K. (2003) Mouse fetal alcohol exposure impairs hippocampal-dependent learning. Alcohol. Clin. Exp. Res. 27 (Supplement to issue no. 5) 42A.

Allan A.M., Chynoweth J, Tyler L.A., and Caldwell K.K. (2003) A mouse model of prenatal ethanol exposure using a voluntary drinking paradigm. Alcohol. Clin. Exp. Res. 27: 2009-2016.

Weeber, E.J. and Caldwell, K.K. (2004) Delay fear conditioning modifies phospholipase C-β1a signaling in the hippocampus and frontal cortex. Pharmacol. Biochem. Behav. 78: 155-164

Buckley, C.T., Caldwell K.K. (2004) Fear conditioning is associated with altered integration of PLC and ERK signaling in the hippocampus. Pharmacol. Biochem. Behav.

Buckley, C.T., Sekiya, F., Kim· Y.J., Rhee, S.G., Caldwell· K.K. (2004)) Identification of phospholipase C-γ1 as a mitogen-activated protein kinase substrate. J. Biol. Chem. 279: 41807-41814.

CONCLUSIONS

We made substantial progress toward GOAL1. The results that we obtained in our studies on control animals are both significant and novel. They indicate that a single trial of fear conditioning initiates complex and dynamic temporal changes in PLC-β1a enzyme activities and concentrations in the brain.

We made several important discoveries in studies related to GOAL 2. We demonstrated that PLC isozymes and ERK2 form signaling complexes in brain and that these complexes are functionally relevant to learning and memory. Further, we found that fetal alcohol exposure impacted these complexes and that this may play a role in the learning and memory deficits that are associated with prenatal alcohol exposure. Finally, we found that PLC-γ1 and ERK2 directly interact, that PLC-γ1 is a substrate for ERK2-catalyzed phosphorylation, and that ERK2 regulates PLC-γ1 enzyme activity.

REFERENCES

Atkins CM, Selcher JC, Petraitis JJ, Trzaskos JM, Sweatt JD (1998). The MAPK cascade is required for mammalian associative learning. Nat Neurosci 1: 602-609.

Bernabeu R, Bevilaqua L, Ardenghi P, Bromberg E, Schmitz P, Bianchin M, Izquierdo I, Medina JH. Involvement of hippocampal cAMP/cAMP-dependent protein kinase signaling pathways in a late memory consolidation phase of aversively motivated learning in rats. Proc. Natl. Acad. Sci. USA 1997;94:7041-7046.

Bourtchuladze R, Abel T, Berman N, Gordon R, Lapidus K, Kandel ER. Different training procedures recruit either one or two critical periods for contextual memory consolidation, each of which requires protein synthesis and PKA. Learning & Memory 1998;5:365-374.

Igaz LM, Vianna MRM, Medina JH, Izquierdo I. Two time periods of hippocampal mRNA synthesis are required for memory consolidation of fear-motivated learning. J. Neurosci. 2002;22:6781-6789

Quevedo J, Vianna MRM, Roesler R, de-Paris F., Izquierdo I, Rose SPR. Two time windows of anisomycin-induced amnesia for inhibitory avoidance training in rats: protection from amnesia by pretraining but not pre-exposure to the task apparatus. Learning & Memory 1999;6:600-607.

Rhee SG. Regulation of phosphoinositide-specific phospholipase C. Annu. Rev. Biochem. 2001;70:281-312.

Schafe GE, Atkins CM, Swank MW, Bauer EP, Sweatt JD, LeDoux JE (2000) Activation of ERK/MAP kinase in the amygdala is required for memory consolidation of Pavlovian fear conditioning. J Neurosci 20: 8177-8187.

Selcher JC, Atkins CM, Trzaskos JM, Paylor R, Sweatt JD (1999). A necessity for MAP kinase activation in mammalian spatial learning. Learning & Memory 6: 478-490.

Takenawa T, Homma Y, Emori Y. (1991). Properties of phospholipase C isozymes. Methods Enzymol. 1991;197:511-518.

Weeber EJ, Savage DD, Sutherland RJ, Caldwell KK. Fear conditioning-induced alterations of phospholipase C-β1a protein level and enzyme activity in rat hippocampal formation and medial frontal cortex. Neurobiol. Learn. Mem. 2001;76:151-182.

PERSONNEL WHO RECEIVED PAY FROM THIS GRANT

Kevin K. Caldwell, Ph.D.

Colin T. Buckley

APPENDIX FOR FINAL REPORT FOR U.S. DEPARTMENT OF ARMY AWARD
#DAMD17-00-1-0582.

CONTENTS

ACADEMIC
PRESS

Two-layer antibody capture of enzymes on the surface of microtiter plates: application to the study of the regulation of phospholipase C-γ1 catalytic activity☆

Colin T. Buckley and Kevin K. Caldwell*

Department of Neurosciences, University of New Mexico Health Sciences Center, Albuquerque, NM 87131, USA

Received 26 February 2003

Abstract

In vitro quantification of the catalytic activity of an enzyme isoform requires the availability of selective agents that allow for either measurements in the presence of the other enzyme isoforms or purification of the isoform and subsequent performance of these measurements on the purified enzyme. Isozyme-specific antibodies are useful tools for these types of analyses. In the present report, we detail a method for the measurement of phospholipase C-γ1 enzyme activity employing native enzyme that is immobilized on microtiter plates. The method uses biotinylated antiglobulin bound to streptavidin-coated microtiter plates to immobilize antiphospholipase C-γ1 antibody and subsequently capture phospholipase C-γ1 from brain tissue lysates. This method avoids biotinylation of the primary (antiphospholipase C-γ1) antibody, making it less labor intensive than previously described methods for using streptavidin-coated plates; in addition, it is highly reproducible and sensitive and allows for quantification of enzyme activity. We employ the technique to show that one or more tyrosine kinases copurify with rat brain phospholipase C-γ1. The method is applicable to the study of any enzyme isoform for which antibodies that capture the native form of the enzyme are available and could easily be employed in high-throughput procedures.
© 2003 Elsevier Inc. All rights reserved.

Keywords: Phospholipase C; Affinity capture; Enzyme; Activity; Microtiter

Enzyme isoforms are commonly present in nature. In many cases, multiple approaches (e.g., purification, pharmacologic, and molecular) can be employed to characterize these individual isoforms. Each of these approaches has unique advantages and disadvantages. The present report details a method that is technically simple and applicable to the in vitro characterization of a wide variety of enzyme isoforms.

Current approaches used for the separation of an enzyme from a complex mixture (e.g., cell or tissue extract) employ chromatographic, electrophoretic, or immunologic methods. Compared to chromatographic and electrophoretic techniques, immunologic techniques are often easier, may allow for increased yields, and are applicable to the processing of a wide range of sample sizes. Antibodies that are capable of separating a native (cf. denatured) form of an enzyme may allow for in vitro measurements of enzyme activity.

Here we describe the development of a method that immunochemically immobilizes an enzyme using biotinylated antiglobulin bound to streptavidin-coated microtiter plates to immobilize antibodies directed against the enzyme of interest. Specifically, we employed biotinylated anti-rabbit IgG bound to streptavidin-coated microtiter plates to immobilize rabbit polyclonal antiphospholipase C-γ1 antibodies, which, in turn, were used to capture phospholipase C-γ1 from rat brain lysates, thus immobilizing the immune complex on the solid-phase support of the microtiter plate (Fig. 1). It should be noted that the biotinylation step is applied to the secondary antiglobulin, so that the primary antibody remains unaffected by the biotinylation process.
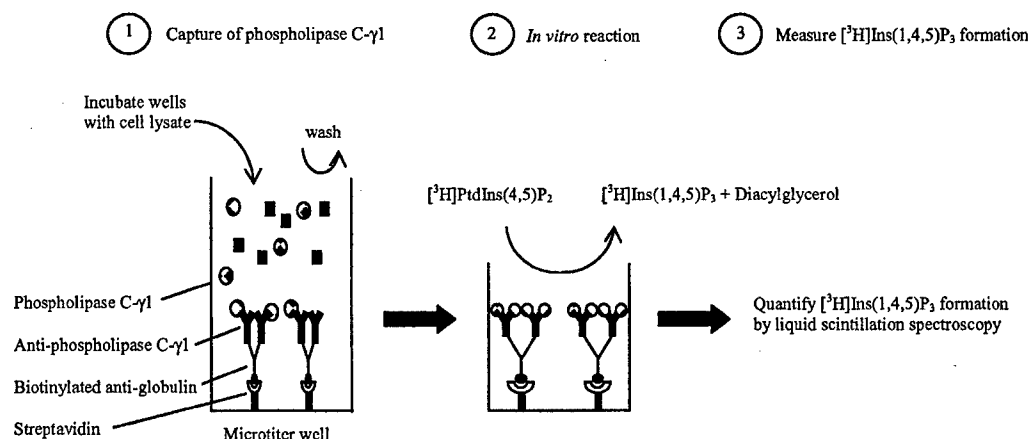
Fig. 1. Schematic of phospholipase C-γ1 immobilization and activity assay using biotinylated goat anti-rabbit IgG and streptavidin-coated microtiter wells. The procedure consists of three steps: (i) phospholipase C-γ1 is captured from the cellular lysate using rabbit antiphospholipase C-γ1 IgG, which is bound by biotinylated goat anti-rabbit IgG immobilized onto streptavidin-coated microtiter plates; (ii) an in vitro reaction in which the lipase substrate, [³H]PtdIns(4,5)P₂, is hydrolyzed into [³H]Ins (1,4,5)P₃ and 1,2-diacylglycerol; and (iii) the [³H]Ins (1,4,5)P₃ product is quantified as a measure of phospholipase C enzyme activity using liquid scintillation spectroscopy.

Biotinylated antiglobulins are a common reagent used to identify primary antibodies bound to antigens in immunohistochemistry and Western blotting. Thus, biotinylated antibodies are commercially available and have been developed with specificity for immunoglobulins, allowing for the application of this procedure for immobilizing a variety of antibodies from different species and different immunoglobulin isotypes quickly and uniformly. It is worth noting that the antibody configuration that we describe in this report could be used to capture proteins of interest during the capture phase of a sandwich enzyme-linked immunosorbent assay.

We demonstrate the validity of the method for the study of one of the primary phosphatidylinositol-specific phospholipase C isozymes, phospholipase C-γ1, found in rodent brain. Phospholipase C isozymes catalyze the hydrolysis of phosphatidylinositol 4,5-bisphosphate (PtdIns(4,5)P₂),[1] yielding inositol 1,4,5-trisphosphate (Ins(1,4,5)P₃) and 1,2-diacylglycerol [1,2]. Complementary DNA clones have been isolated for 11 distinct mammalian phospholipase C isozymes [3]. Comparison of the predicted amino acid sequences of these clones reveals that phospholipase C isozymes may be grouped into four types: phospholipase C-β, -δ, -γ, and -ε. Most, if not all, of these phospholipase C isozymes are present in brain [4–7], making studies of the individual isoforms present in this tissue difficult.

Phosphorylation has been shown to influence the catalytic activity of a variety of enzymes, including phospholipase C-γ and -β isozymes. Several studies have demonstrated that phospholipase C-γ catalytic activity

is regulated by tyrosine phosphorylation [3,8]. We demonstrate that the study of the role of protein kinase-dependent regulation of phospholipase C-γ1 is possible employing the method that we describe for the immobilization of the enzyme on microtiter plates.

In summary, the method detailed in this report is applicable to the in vitro study of any enzyme for which specific antibodies are available. The method is applicable to the high-throughput screening of regulators (e.g., inhibitors) of enzyme activity, antibodies, and the identification of interacting proteins.

Materials and methods

Materials

Rabbit polyclonal antibodies against phospholipase C-γ1, biotin-conjugated goat anti-rabbit IgG, and normal rabbit IgG were purchased from Santa Cruz Biotechnology (Santa Cruz, CA). Aprotinin, 4-(2-aminoethyl)benzenesulfonylfluoride, leupeptin, calpain III, and genistein were from Calbiochem (San Diego, CA). Sodium vanadate was purchased from Fisher Chemical (Fair Lawn, NJ). Immunoware microtubes and bovine serum albumin, fraction V, were purchased from Pierce (Rockford, IL). Dulbecco's phosphate-buffered saline (PBS) was obtained from Biowhittaker (Walkersville, MD). Triton X-100, PtdIns(4,5)P₂, and Streptawells (streptavidin-coated microtiter plates) were from Roche (Indianapolis, IN). [³H]PtdIns(4,5)P₂ was obtained from Perkin–Elmer (Boston, MA). Assay Dilution Buffer I, Kinase Inhibitor Cocktail, and Magnesium/ATP Cocktail were from Upstate Biotechnology (Lake Placid, NY).

---

[1] Abbreviations used: PtdIns(4,5)P₂, phosphatidylinositol 4,5-bisphosphate; Ins(1,4,5)P₃, inositol 1,4,5-trisphosphate; PBS, phosphate-buffered saline.

Animals

All procedures involving rats were approved by the University of New Mexico Health Sciences Center Laboratory Animal Care and Use Committee; 4- to 7-month-old female Sprague–Dawley rats (Harlan Industries, Indianapolis, IN) were housed in a constant (22 °C) temperature room on a 16-h dark/8-h light schedule (lights off from 17:30 to 09:30 h). All rats were provided ad libitum access to standard rat chow and tap water.

Preparation of Triton X-100-soluble extracts from rat brain

Brains from five rats were removed and homogenized as described in Weeber et al. [9], except that the volume of homogenization buffer (20 mM Tris–HCl, pH 7.4, 1 mM EDTA, 320 mM sucrose, 40 µg leupeptin/mL, 20 µg aprotinin/mL, 30 µM calpain III inhibitor, 0.5 mM 4-(2-aminoethyl)benzenesulfonylfluoride, and 200 µM sodium orthovanadate) was 45 mL. Homogenates were centrifuged ($1000g_{max}$, 10 min, 4 °C) to separate crude soluble (S1) and particulate (P1) fractions. The supernatant was decanted and stored in ice. The pellet was resuspended in 10 mL of homogenization buffer, homogenized, and spun as before. The supernatant was decanted, combined with the supernatant from above to form the S1 fraction, and brought to 16 mM (1.0% v/v) Triton X-100, 75 mM KCl, and 75 mM NaCl. The mixture was left at 4 °C for 20 min, and then centrifuged ($20,000g_{max}$, 20 min, 4 °C) to remove the Triton X-100-insoluble material. The Triton X-100-soluble material was collected, rapidly frozen in liquid nitrogen, and stored at −80 °C until further analysis. The total protein concentration of the sample was determined by the method of Bradford [10], using the Bio-Rad (Richmond, CA) protein assay kit; bovine serum albumin served as the protein standard for these determinations.

Tissue preparation and subcellular fractionation of rat hippocampus

The preparation of the Triton X-100 extract of the $200,000g_{max}$, postnuclear particulate (P2) preparation derived from rat hippocampal formation was performed essentially as described in Weeber et al. [9]. Briefly, the hippocampal formation was removed and homogenized as described. Homogenates were frozen in liquid nitrogen and stored at −80 °C until further fractionated. Frozen rat hippocampal tissue homogenates were thawed on ice and then centrifuged ($1000g_{max}$, 7 min, 4 °C). The supernatant was decanted and stored in ice. The pellet was resuspended in 0.5 mL homogenization buffer and then homogenized and centrifuged as before. The supernatant was decanted, combined with the su-

pernatant from the first centrifugation to form the S1 fraction, and centrifuged ($200,000g_{max}$, 30 min, 4 °C). The soluble (S2) fraction was decanted from the pellet (P2) fraction. The P2 pellet was resuspended in 0.5 mL of extraction buffer (homogenization buffer supplemented with 75 mM NaCl, 75 mM KCl, and 16 mM (1%, v/v) Triton X-100), homogenized, and left in ice. After 20 min, the suspended P2 pellet was spun in an ultracentrifuge ($200,000g_{max}$, 20 min, 4 °C). The Triton X-100-soluble P2 extract was decanted, aliquoted into storage tubes, snap-frozen in liquid nitrogen, and stored at −80 °C. The protein concentration was determined as described above.

Optimization of rabbit phospholipase C-γ1 antibody concentrations

Biotinylated goat anti-rabbit IgG at 1.0 µg of antibody/100 µL of PBS per well was coated onto streptavidin-coated microtiter wells, as recommended by the manufacturer. Wells were incubated overnight at 4 °C and then washed three times (5 min per wash) with PBS at room temperature. Rabbit antiphospholipase C-γ1 antibody was serially diluted in PBS from a stock solution of 10 µg/mL to a final dilution of 0.31 µg/mL, and a volume of 100 µL of each solution was incubated with the biotinylated goat anti-rabbit IgG-coated streptavidin plates overnight at 4 °C. The strips were washed three times (5 min per wash) with PBS at room temperature. Rat brain S1 fraction was loaded at 20 µg/100 µL PBS per well and incubated overnight at 4 °C. Control wells contained normal rabbit IgG coated at 1.0 µg/100 µL per well and received rat brain S1 fraction (20 µg/100 µL). Unbound proteins were removed by washing the wells three times (5 min per wash) with 1.25X phospholipase C assay buffer (see below) at room temperature. Phospholipase C activity was then quantified as described below.

Stability studies of phospholipase C-γ1 enzyme

Phospholipase C-γ1 was captured from a volume of 100 µL of a 200 µg/mL solution of rat brain S1 preparation using antiphospholipase C-γ1 immobilized with biotin-conjugated anti-rabbit immunoglobulin on streptavidin-coated microtiter plates, as described above. The wells were incubated with phospholipase C substrate, as described below, for the following times: 15, 30, 45, or 60 min. At the indicated time, the enzyme activity was quantified as described below.

Optimization of the amount of tissue curve

Biotinylated anti-rabbit immunoglobulin was immobilized onto streptavidin-coated wells as described above. A volume of 100 µL/well of antiphospholipase

C-γ1 antibody, at a concentration of 2.0 μg/mL of PBS, was then coated onto the immobilized biotin-conjugated anti-rabbit immunoglobulin and left for 18 h at 4 °C, at which time the strips were washed three times (5 min each) with PBS at room temperature. Wells were incubated with hippocampal P2 extract: 0–100 μg of protein diluted to 100 μL in PBS per well. Control wells were coated with a volume of 100 μL normal rabbit IgG at 2.0 μg/mL of PBS and received 100 μg of hippocampal P2 protein per 100 μL of PBS. All wells were incubated overnight at 4 °C. Immobilized enzyme was assayed as described below.

Effect of tyrosine kinase inhibitor on phospholipase C-γ1 catalytic activity

Antiphospholipase C-γ1 antibodies were coated onto biotinylated antiglobulin immobilized on streptavidin at 200 ng of rabbit polyclonal antibody/100 μL per well. Each well was then incubated with 20 μg of rat hippocampal P2 extract overnight and, subsequently, washed three times (5 min each) with room-temperature PBS buffer. Wells were then incubated (20 min, 35 °C) in the presence of one of the following four solutions: Assay Dilution Buffer I (20 mM 3-(N-morpholino)propanesulfonic acid, pH 7.2, 25 mM β-glycerol phosphate, 5 mM EGTA, 1 mM sodium orthovanadate, a phosphatase inhibitor, 1 mM dithiothreitol); 100 μM ATP, 15 mM MgCl$_2$ in Assay Dilution Buffer I; 0.5% (v/v) dimethyl sulfoxide in Assay Dilution Buffer I; or 50 μM genistein, a tyrosine kinase inhibitor, in Assay Dilution Buffer I containing 0.5% (v/v) dimethyl sulfoxide. The wells were rinsed three times (5 min each) in room-temperature 1.25X phospholipase C assay buffer and assayed for enzyme activity as described below.

Phospholipase C-γ1 enzyme activity assay

Phospholipase C-γ1 enzyme activity was quantified essentially as described in Weeber et al. [9]. Briefly, phospholipase C-γ1 enzyme was affinity-purified from rat brain extracts and washed with 1.25X phospholipase C assay buffer (final assay concentration: 35 mM sodium phosphate, pH 6.8, 70 mM KCl, 0.8 mM EGTA, 0.8 mM CaCl$_2$), as described above. One hundred microliters of 1.25X phospholipase C assay buffer was then added to each well, and the well was incubated for 5 min at 37 °C prior to adding the enzyme substrate. Twenty-five microliters of [^{3}H]PtdIns(4,5)P$_2$/Triton X-100 solution (final assay concentration: 0.200 mM PtdIns(4,5)P$_2$, 10,000–15,000 cpm/nmol, and 0.32 mM (0.02%, v/v) Triton X-100) was added and the incubation was continued for 30 min (unless otherwise noted). At the end of the reaction, 100 μL was removed from each well and transfered into tubes containing 125 μL of 1.0% (w/v) bovine serum albumin. Proteins and lipids were precip-

itated with 300 μL of ice-cold 10% (v/v) trichloroacetic acid and centrifuged at room temperature (14,000g$_{max}$ for 4 min); 300 μL of the supernatant containing the reaction product ([^{3}H]Ins(1,4,5)P$_3$) was removed and quantified by liquid scintillation spectroscopy. Immune complex-dependent activity was calculated by subtracting background [^{3}H]Ins(1,4,5)P$_3$ (release present in normal rabbit IgG antibody control samples) from the activity measured in wells containing antiphospholipase C-γ1 antibody. Data were calculated as nmol Ins(1,4,5)P$_3$ product formed per min, or per mg protein, or per min per mg protein present in the extract from which the enzyme was affinity-purified.

Results and discussion

Fig. 1 depicts the experimental design used in these studies. Biotinylated anti-rabbit IgG was bound to streptavidin-coated microtiter plate wells, creating a solid phase for immobilizing rabbit polyclonal antibodies against phospholipase C-γ1. The immobilized antiphospholipase C-γ1 antibodies were used to capture enzyme from rat brain tissue samples. Enzyme activity was determined using a conventional method to measure PtdIns(4,5)P$_2$ hydrolysis.

The optimal dilution of the rabbit antiphospholipase C-γ1 antibody was determined by serial dilution of the antibody between 10.0 and 0.31 μg/mL of PBS (Fig. 2). Subsequent measurements of phospholipase C activity revealed increased formation of the reaction product, [^{3}H]Ins(1,4,5)P$_3$, with increasing antibody amounts

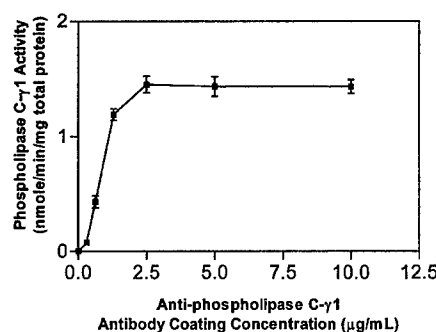Fig. 2. Determination of the quantity of rabbit antiphospholipase C-γ1 antibody that can be adhered to the surface of biotinylated anti-rabbit IgG-coated streptavidin plates. Streptavidin-coated microtiter wells were first coated with 1.0 μg of biotinylated goat anti-rabbit IgG in 100 μL PBS and then coated with rabbit antiphospholipase C-γ1 antibody in a dilution series starting at 10.0 μg/mL and ending at 0.31 μg/mL. The wells were rinsed with PBS and then incubated (18 h, 4 °C) with 20 μg of rat brain S1 fraction diluted in 100 μL of PBS. After the incubation, the wells were rinsed and phospholipase C activity was measured as described under Materials and methods. The reaction mix was incubated for 30 min. Each point is the average (n = 3), after background subtraction. Some error bars are obstructed by symbols for the points.

from 31 to 125 ng antibody per well, reaching a saturating plateau at antibody amounts greater than 125 ng per well. Therefore, the optimal coating concentration of antibody is approximately 1.25 μg/mL. In subsequent assays, we coated the wells with 100 μL of a 2.0 μg/mL solution of rabbit phospholipase C-γ1 antibody per well. This concentration of antibody was used to saturate efficiently the binding sites on the wells and to avoid creating transient monolayers of antibody that can occur at higher concentrations of antibody due to nonspecific protein–protein interactions.

The stability of the immobilized phospholipase C-γ1 over time (Fig. 3) was determined by measuring enzyme activity associated with a constant amount of immobilized phospholipase C-γ1 captured from a 100-μL volume of rat brain S1 (200 μg/mL), for varying periods of time ranging from 0 to 60 min. The results demonstrate that the hydrolysis of substrate increased in a linear fashion for 60 min, demonstrating that immobilized phospholipase C-γ1 is stable for at least this length of incubation. Subsequent studies were performed employing a 30-min incubation due to the ease of product detection at this time.

After the optimization of the immunoassay parameters, the linearity of the assay with increasing protein amounts was determined. The results (Fig. 4) demonstrate a linear trend in phospholipase C-γ1 enzyme activity between 2 μg and approximately 25 μg of hippocampal formation P2 extract protein. Although the phospholipase C-γ1 enzyme activity curve fails to reach a plateau, it appears to be tending toward saturation. Higher tissue concentrations were not tested since it is not practical to use tissue samples in that range.

We sought to determine whether the technique that we used for the affinity capture of phospholipase C-γ1

Fig. 4. Determination of the PLC-γ1 activity captured from increasing tissue concentrations. Phospholipase C-γ1 was captured from protein amounts ranging from 1.56 to 100 μg of rat hippocampal P2 fraction. Unbound proteins were rinsed from the wells and phospholipase C activity was measured as described under Materials and methods. The reaction was incubated for 30 min. Each point is the average ($n = 3$), after background subtraction. Some error bars are obstructed by symbols for the points.

allowed for the detection of tyrosine kinase(s) that associate with the phospholipase C-γ1. To do this, we affinity captured phospholipase C-γ1 and incubated immune complexes under conditions that allowed for substrate phosphorylation (i.e., in the presence of Mg^{2+} and ATP) or not. The wells were then rinsed with 1.25X phospholipase C assay buffer and the catalytic activity of the isozyme was determined. Incubation of anti-phospholipase C-γ1 immune complexes with Mg^{2+}–ATP increased phospholipase C enzyme activity (Fig. 5). To determine the type of protein kinase responsible for the stimulation, we employed specific protein kinase inhibitors. In the presence of selective inhibitors of Ca^{2+}–calmodulin-dependent protein kinase II, protein kinase C, and protein kinase A, ATP-dependent stimulation of phospholipase C-γ1 catalytic activity was still observed (data not shown), whereas the tyrosine kinase inhibitor, genistein, in the presence of Ca^{2+}–calmodulin-dependent protein kinase II, protein kinase
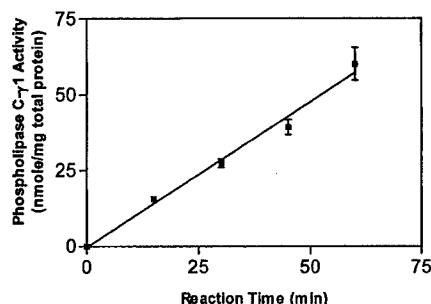

Fig. 3. Time course of phospholipase C-γ1 activity captured from rat brain S1 fraction. Streptavidin-coated microtiter wells were coated with 1.0 μg biotinylated goat anti-rabbit IgG followed by coating with 0.2 μg rabbit antiphospholipase C-γ1 antibody. Phospholipase C-γ1 was captured from 20 μg of rat brain S1 fraction. Phospholipase C activity was measured as described under Materials and methods. Reactions were incubated for the following times: 15, 30, 45, and 60 min. Each point is the average ($n = 3$), after background subtraction. Some error bars are obstructed by symbols for the points.
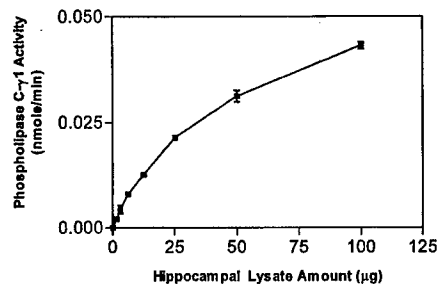

Fig. 5. Tyrosine kinase inhibitor, genistein, blocks ATP-dependent stimulation of hippocampal formation of P2 fraction phospholipase C-γ1 catalytic activity. Phospholipase C-γ1 captured by antiphospholipase C-γ1 antibody was treated with or without ATP and/or genistein and phospholipase C activity was subsequently determined as described under Materials and methods. (a) Buffer without genistein or ATP; (b) buffer with genistein minus ATP; (c) buffer plus ATP minus genistein; (d) buffer with ATP and genistein. Each point is the average ± SE ($n = 7$), after background subtraction.

C, and protein kinase A inhibitors completely inhibited the ATP-dependent stimulation of phospholipase C-γ1 catalytic activity. These results demonstrate that a tyrosine protein kinase copurifies with immunoseparated phospholipase C-γ1, and the effect of this kinase on phospholipase C-γ1 catalytic activity can be blocked using a specific tyrosine protein kinase inhibitor.

These studies have described the development of an immunochemical immobilization method for enzymes. This nonadsorbent, noncovalent, microtiter plate assay offers several advantages over solid-phase immunoassays in which the capture antibody is coated directly to the surface of a microtiter plate well and nonadsorbent, noncovalent methods in which the capture antibody is first biotinylated and then immobilized onto microtiter plates coated with streptavidin. First, we tried direct adsorption of the phospholipase C antibody onto NUNC-Immuno MaxiSorp 96-well plates under various conditions (e.g., various buffers, pH, temperature, and antibody concentrations) and we were not able to detect phospholipase C enzyme activity under any of the conditions that we used. We, therefore, concluded that the most likely explanation for this result was that the antibody had become denatured by the surface, so that it was unable to bind phospholipase C. Subsequently, when we used the solid-phase support described in this report, a catalytically active form of the enzyme was captured in the well. For the application of studying phospholipase C enzyme activity, the use of biotinylated antiglobulin to immobilize antiphospholipase C antibodies was better than direct adsorption of antiphospholipase C antibody onto plastic. Therefore, this technique allows for antibodies that bind poorly to plastic or that become denatured by plastic surfaces to be of use in the assay. Second, the technique described herein offers an advantage over the direct absorption of antiglobulin onto the plastic surface of a microtiter plate by removing the antiglobulin from direct contact with the hydrophobic surface using a streptavidin–biotin bridge. This linkage is hydrophilic in nature and has been shown to greatly increase the reactivity of antibodies bound to the surface of a microtiter plate [11,12]. Third, this method avoids biotinylation of the capture antibody, which is both time consuming and requires using materials that are known carcinogens.

In conclusion, this novel microtiter plate assay allows for the rapid capture and determination of catalytic activity of enzyme isoforms from tissue or cellular ho-

mogenates. It is technically simple to perform and could be employed in the study of any enzyme or protein for which affinity capture antibodies are available.

Acknowledgments

References

[1] P.W. Majerus, T.S. Ross, T.W. Cunningham, K.K. Caldwell, A.B. Jefferson, V.S. Bansal, Recent insights in phosphatidylinositol signaling, Cell 63 (1990) 459–465.

[2] R.L. Williams, Mammalian phosphoinositide-specific phospholipase C, Biochim. Biophys. Acta 1441 (1999) 255–267.

[3] S.G. Rhee, Regulation of phosphoinositide-specific phospholipase C, Annu. Rev. Biochem. 70 (2001) 281–312.

[4] M. Watanabe, M. Nakamura, K. Sato, M. Kano, M.I. Simon, Y. Inoue, Patterns of expression for the mRNA corresponding to the four isoforms of phospholipase Cβ in mouse brain, Eur. J. Neurosci. 10 (1998) 2016–2025.

[5] Y. Homma, T. Takenawa, Y. Emori, H. Sorimachi, K. Suzuki, Tissue- and cell type-specific expression of mRNAs for four types of inositol phospholipid-specific phospholipase C, Biochem. Biophys. Res. Commun. 164 (1989) 406–412.

[6] S.B. Lee, S.G. Rhee, Molecular cloning, splice variants, expression, and purification of phospholipase C-δ4, J. Biol. Chem. 271 (1996) 25–31.

[7] G.G. Kelley, S.E. Reks, J.M. Ondrako, A.V. Smrcka, Phospholipase Cε: a novel Ras effector, EMBO J. 20 (2001) 743–754.

[8] M.I. Wahl, G.A. Jones, S. Nishibe, S.G. Rhee, G.J. Carpenter, Growth factor stimulation of phospholipase C-gamma 1 activity. Comparative properties of control and activated enzymes, J. Biol. Chem. 267 (1992) 10447–10456.

[9] E.J. Weeber, D.D. Savage, R.J. Sutherland, K.K. Caldwell, Fear conditioning-induced alterations of phospholipase C-β1a protein level and enzyme activity in rat hippocampal formation and medial frontal cortex, Neurobiol. Learn. Mem. 76 (2001) 151–182.

[10] M. Bradford, A rapid and sensitive method for the quantification of microgram quantities of protein utilizing the principle of protein-dye binding, Anal. Biochem. 72 (1976) 248–254.

[11] M. Suter, J.E. Butler, The Immunochemistry of sandwich ELISAs. II. A novel system prevents the denaturation of capture antibodies, Immunol. Lett. 13 (1986) 313–316.

[12] J.H. Peterman, P.J. Tarcha, V.P. Chu, J.E. Butler, The immunochemistry of sandwich-ELISAs. IV. The antigen capture capacity of antibody covalently attached to bromoaceyl surface-functionalized polystyrene, J. Immunol. Methods. 111 (1988) 271–275.

A Mouse Model of Prenatal Ethanol Exposure Using a Voluntary Drinking Paradigm

Andrea M. Allan, Julie Chynoweth, Lani A. Tyler, and Kevin K. Caldwell

Background: The incidence of fetal alcohol spectrum disorders is estimated to be as high as 1 in 100 births. Efforts to better understand the basis of prenatal ethanol-induced impairments in brain functioning, and the mechanisms by which ethanol produces these defects, will rely on the use of animal models of fetal alcohol exposure (FAE).

Methods: Using a saccharin-sweetened alcohol solution, we developed a free-choice, moderate alcohol access model of prenatal alcohol exposure. Stable drinking of a saccharin solution (0.066%) was established in female mice. Ethanol then was added to the saccharin in increasing concentrations (2%, 5%, 10% w/v) every 2 days. Water was always available, and mice consumed standard pellet chow. Control mice drank saccharin solution without ethanol. After a stable baseline of ethanol consumption (14 g/kg/day) was obtained, females were impregnated. Ethanol consumption continued throughout pregnancy and then was decreased to 0% in a step-wise fashion over a period of 6 days after pups were delivered. Characterization of the model included measurements of maternal drinking patterns, blood alcohol levels, food consumption, litter size, pup weight, pup retrieval times for the dams, and effects of FAE on performance in fear-conditioned learning and novelty exploration.

Results: Maternal food consumption, maternal care, and litter size and number were all found to be similar for the alcohol-exposed and saccharin control animals. FAE did not alter locomotor activity in an open field but did increase the time spent inspecting a novel object introduced into the open field. FAE mice displayed reduced contextual fear when trained using a delay fear conditioning procedure.

Conclusions: The mouse model should be a useful tool in testing hypotheses about the neural mechanisms underlying the learning deficits present in fetal alcohol spectrum disorders. Moreover, a mouse prenatal ethanol model should increase the opportunity to use the power of genetically defined and genetically altered mouse populations.

Key Words: Fetal Alcohol Syndrome, Ethanol, Mouse, Voluntary Drinking Behavior.

THE INCIDENCE OF fetal alcohol spectrum disorders (FASD), which includes fetal alcohol syndrome and alcohol-related neurodevelopmental disorder (Streissguth and O'Malley, 2000), is estimated to be as high as 1 in 100 births (Sampson et al., 1997). Children with FASD display a variety of cognitive and behavioral aberrations, ranging from severe mental retardation to subtle deficits that become apparent under stressful conditions (Mattson and Riley, 1998; Streissguth et al., 1990, 1994). Efforts to better understand the basis of prenatal ethanol-induced impairments in brain functioning, and the mechanisms by which

ethanol produces these defects, will rely on the use of animal models of fetal alcohol exposure (FAE).

Most studies on fetal alcohol effects have employed the rat using a variety of ethanol administration paradigms and schedules. Prenatal ethanol exposure paradigms commonly require dams either to ingest an ethanol-containing liquid diet or to be intubated, or injected, with ethanol. These procedures produce variable degrees of maternal stress, which, in turn, may modify the effects of prenatal drug exposure on the developing fetus (Slone and Redei, 2002; Ward and Wainwright, 1989). The use of liquid diets also limits the amount of ethanol that can administered without inducing malnutrition. An additional confound associated with many existing paradigms of FAE is that cross-fostering of the pups is used to avoid introducing differences in maternal care that may occur between control (non–alcohol-consuming) and alcohol-drinking moms, whether alcohol availability is continued postpartum or whether alcohol is withdrawn. The quality of maternal care has been shown to produce significant changes in hippocampal synaptophysin immunoreactivity and Morris water maze performance in the offspring (Liu et al., 2000). Even brief maternal separation (45 min) has been shown to increase

the expression of nerve growth factor in the dentate gyrus and hilus regions of the hippocampal (Cirulli et al., 1998).

We sought to develop a mouse model of FAE that minimized these problems. In the present studies, we used saccharin-sweetened ethanol solutions (Czachowski et al., 1999; Roberts et al., 1999; Tomie et al., 2002) and a modification of the sucrose fading approach (Slawecki et al., 1997) to establish consistent, voluntary alcohol consumption patterns before impregnating female mice and then maintained alcohol consumption throughout gestation. Nutrition was provided using a standard pellet diet. After delivery of the offspring, stepwise decreases in ethanol concentrations in the saccharin solution prevented the display of ethanol withdrawal signs in the mother and eliminated the need to cross-foster the pups. This procedure did not significantly affect various measures of maternal or neonatal well-being or maternal care for the pups yet resulted in cognitive and behavioral impairments in the offspring consistent with other models of FAE.

MATERIALS AND METHODS

Ethanol Drinking and Fetal Alcohol Exposure Paradigms

All of the procedures used in the current studies were approved by the University of New Mexico Health Sciences Center Laboratory Animal Care and Use Committee.

Sixty day-old B6SJL/F1 (Harlan Industries, Indianapolis, IN) female mice were individually housed in plastic cages in a temperature-controlled room (22°C) on a 12 hr dark/12 hr light schedule (lights on from 0700 to 1900 hr). Standard chow and water were available ad libitum.

Prenatal exposure of mice to ethanol was performed using saccharin-sweetened solutions (Czachowski et al., 1999; Roberts et al., 1999; Tomie et al., 2002). Female mice were offered 22 hr free access to either 0.066% saccharin or water for 2 weeks. Subsequently, ethanol was added to the saccharin tube for the experimental groups, whereas the control group continued to have access to saccharin alone. The concentration of ethanol was increased in a stepwise fashion every 2 days, from 0% to 2%, to 5%, and then finally to 10% (w/v). After 2 weeks of drinking, a male was introduced into the female's cage. Once the female was determined to be pregnant by the presence of vaginal plug, the male was removed and nesting material was placed in the cage. Ethanol consumption was not measured for the 1 to 2 days while the male was present in the cage. Females continued to drink stably throughout pregnancy. Within 1 day of birth, the alcohol and the saccharin concentrations were reduced by one-half every 2 days, until the mice were consuming only water. Saccharin-consuming mothers were weaned off of the sweetened water in a similar step-down fashion. Litter sizes and litter weights were determined on postnatal day 7. Pups were weaned at 23 days and maintained in same-sex, littermate housed cages with free access to water and chow. Offspring (both male and female) were 60 to 100 days old when used in the present experiments. No more than two littermates were represented in any single treatment condition.

Characterization of Maternal Care

Maternal grooming (frequency and duration) and care for the pups (latency to retrieve pups removed from the nest and time spent on the nest) were evaluated at postnatal days 3 to 5 between 1000 and 1300 hr by videotape monitoring.

Blood Ethanol Measurement

Maternal blood ethanol concentrations produced by ad libitum consumption of the 10% ethanol/0.066% saccharin solutions were measured using saphenous vein puncture (a 10 μl sample) and determined enzymatically (Farr et al., 1988). Blood samples were collected from nine separate groups of mice at 15 different times between 0000 and 2400 hr during the second week of gestation; each dam gave a maximum of three different samples. Blood alcohol was determined for three separate breeding rounds of FAE animals. Because restraint and blood taking are stressful, these measures were performed on a separate group of dams that were drinking at a rate similar to the experimental dams; the pups from these dams were not used in these studies.

Whole blood was collected from the saphenous vein and immediately mixed with 0.2 ml of 6.6% perchloric acid and stored frozen at −20°C until assayed. Blood ethanol standards were created by mixing whole blood from untreated mice with known amounts of ethanol ranging from 0 to 240 mg/dl and then mixing 0.1 ml aliquots of each standard with perchloric acid and storing the standards frozen with the samples. Blood ethanol samples were assayed using a modification of the method of Lundquist (1959). The ethanol standard curve was linear over the 0 to 240 mg/dl range. Sample blood ethanol values were determined by regression analysis.

Corticosterone Radioimmunoassay and Adrenal Weights

After we obtained body weights, adult mice were rapidly decapitated, blood was collected, and the adrenal glands were dissected, separated from the capsule, and wet weighed. Trunk blood was collected into chilled tubes containing ethylenediaminetetraacetic acid (7.5 mg) and aprotinin (0.2 ml/0.5 ml blood) and centrifuged at 2200 × g for 10 min at 4°C. Supernatant (plasma) then was collected into clean tubes and stored at −80°C until used in the assay. Corticosterone levels were analyzed in duplicate using a mouse corticosterone radioimmunoassay kit (ICN Biochemicals, Costa Mesa, CA). The detection limit for the kit was determined to be 3 ng of corticosterone/ml with a within-assay variance of 4.5% and a between-assay variance of 6.5%.

Novel Object Exploration

The novel object test was adapted from the protocol previously described by Grailhe et al. (1999). An open field apparatus, measuring 17 inches × 17 inches with 8 inch high Plexiglas sidewalls, was used. The floor of the apparatus was black and divided into five areas: four equal quadrants and one center area having a diameter of 14 cm. The experiments were carried out in a dimly lit room with the aid of a video camera to minimize effects of stress and anxiety. The floor and walls were wiped with 70% isopropanol before each test session. The test session consisted of two 5 min periods. At the start of the first 5 min session, mice were placed into the center area, and the latency to leave the center, the total time spent in the center, and the total number of center line crosses and the number of total lines crossed were recorded as measures of exploration. At the start of the second 5 min period, a pink and green striped gray cube, one cubic inch, with an open side was placed into the center of the apparatus, with the open side facing the mouse. Measurements were made of the latency to approach the novel object, the total time spent in the center area, the total number of center line crosses, and the number of total line crosses.

Delay Fear Conditioning

Fear conditioning was conducted using a procedure similar to that described by Wehner and colleagues (Lu and Wehner, 1997; Smith and Wehner, 2002). A Coulbourn Instruments (Allentown, PA) Habitest® System with two metal walls, two Plexiglas walls, and a stainless steel grid floor for administration of the foot shock was used for conditioning. The apparatus was located within a sound-attenuated chamber.

Mice were trained as follows. After 90 sec of habituation in the conditioning context, the conditioned stimulus (CS), an 80 dB, 6 Hz clicker,

was initiated. For the unconditioned stimulus (US), an electric foot shock (0.55 mA) was delivered during the last 2 sec of the 30 sec CS. Ninety seconds later, the CS/US sequence was repeated. Thirty seconds after cotermination of the second CS/US pairing, the animal was removed from the conditioning context and returned to its home cage.

Approximately 24 hr later, we assessed mice for their conditioned responses to the context and to the CS by measuring freezing behavior (defined by the absence of movements other than those necessary for respiration; Bouton and Bolles, 1980; Fanselow, 1980) after reintroduction into the context in which conditioning occurred and exposure to the CS in a novel context (a clear plastic container with orange-scented bedding). Freezing was measured using a time-sampling procedure in which every 10 sec the mouse was scored as either moving or freezing. The amount of freezing (expressed as a percentage) was calculated by dividing the number of observation periods where the mouse was frozen by the total number of observation periods. Freezing in the conditioning context (in the absence of the CS and US) was measured for 4 min. Freezing to the CS in the novel context was determined approximately 1 hr after assessment of contextual conditioning. Basal levels of freezing in the novel context were scored for 3 min without presentation of the CS. After basal scoring, the CS was initiated and remained on while freezing was scored for an additional 3 min.
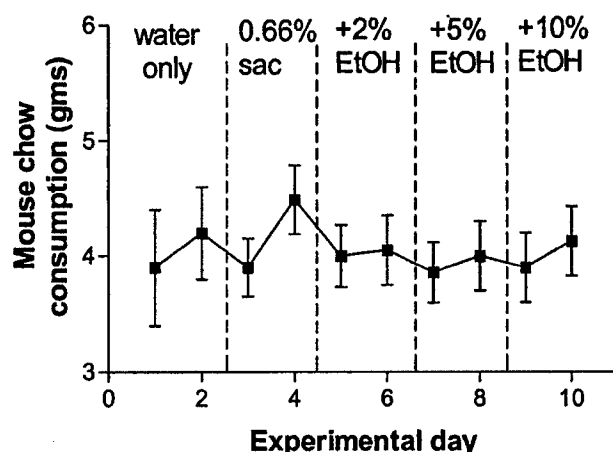
RESULTS

Effect of Saccharin Fading Ethanol Exposure Paradigm on Food and Fluid Consumption

We monitored the consumption of standard breeder chow and water as the ethanol was introduced. Although there was a small increase in food consumption on introduction of the saccharin (Fig. 1A), there were no significant alterations in either the eating (Fig. 1A) or drinking (Fig. 1B) patterns of the mice. Figure 1B shows that the gradual introduction of ethanol was readily accepted by the mice, with a slight reduction in intake once the 10% (w/v) ethanol was introduced into the bottles. Saccharin-drinking control mothers maintained a stable level of preference for the saccharin across their pregnancy (Fig. 2), drinking almost exclusively from the saccharin-sweetened water tubes. Similarly, the 10% (w/v) ethanol-drinking mothers developed a stable preference for the sweetened ethanol solution before pregnancy and maintained this preference throughout the pregnancy (Fig. 2). Although there was a clear preference for the sweetened solutions, the mice reduced their water intake such that there was no significant increase in their total fluid consumption.

Effect of Saccharin Fading Ethanol Exposure Paradigm on Maternal Blood Alcohol Levels

Blood alcohol levels, measured in a separate group of ethanol-drinking dams, were evaluated over a 24 hr period (Fig. 3). Peak blood alcohol levels were achieved between 1600 hr and 0100 hr, during the dark cycle. The average daily consumption of ethanol by mouse dams on the 10% ethanol saccharin solutions was 14.0 g ethanol/kg body weight/day, generating average peak blood alcohol levels of 120 ($\pm$9) mg/dl consistently throughout the pregnancy (Fig. 3). The average calorie equivalent of the ethanol consumed was about 10% the daily diet intake.
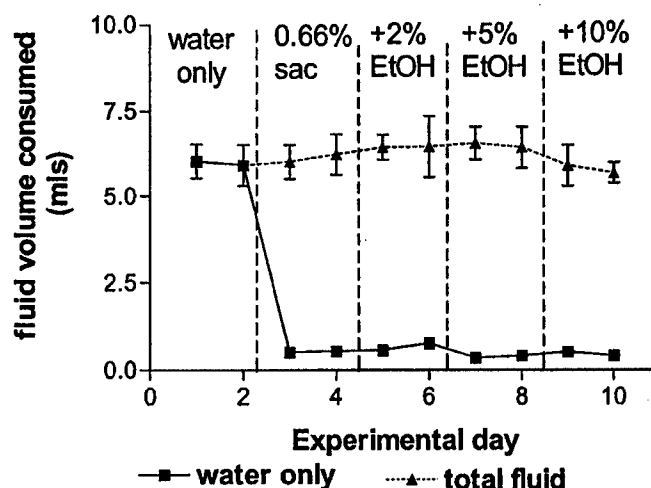
Fig. 1. Effect of the saccharin fading ethanol exposure paradigm on food and fluid consumption. (A) Amount (mean $\pm$ SEM, n = 12) of food consumed by the female mice assigned to the ethanol-drinking condition. Consumption of the standard breeder block chow was measured every day for a total of 10 days while saccharin and ethanol were introduced. (B) Volumes (mean $\pm$ SEM, n = 12) of fluid consumed from the water (square symbols) and saccharin or saccharin/ethanol tubes (triangle symbols) for a total of 10 days for the same set of female mice.

Effect of Saccharin Fading Ethanol Exposure Paradigm on Pup Weight, Litter Size, and Maternal Weight

Food consumption (Table 1) was monitored every other day, and no difference in average daily food consumption was noted between the females that drank saccharin-sweetened ethanol and those drinking saccharin alone. Additionally, there was no significant difference in the change of material weight from day 1, the start of 10% (w/v) ethanol, to day 17, the day that the male was introduced into the cage. Average pup weights and litter sizes did not significantly differ between the ethanol- and saccharin-drinking groups (Table 1). No gross anatomic abnormalities were noted at birth in the fetal ethanol-exposed mice.
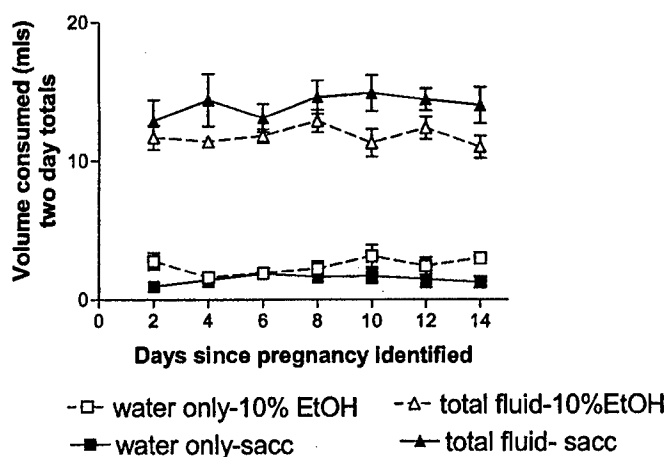
Fig. 2. Effect of the saccharin fading ethanol exposure paradigm on fluid consumption during pregnancy. Two day total amount (mean ± SEM, *n* = 12) of water only (squares) and total fluid (triangles) consumed by pregnant dams in the saccharin-drinking group (filled symbols) and the 10% w/v ethanol-drinking (open symbols) conditions. Water and total fluid consumption (2 day totals; mean ± SEM, *n* = 12) are given from day 2 to day 14 of their pregnancies.
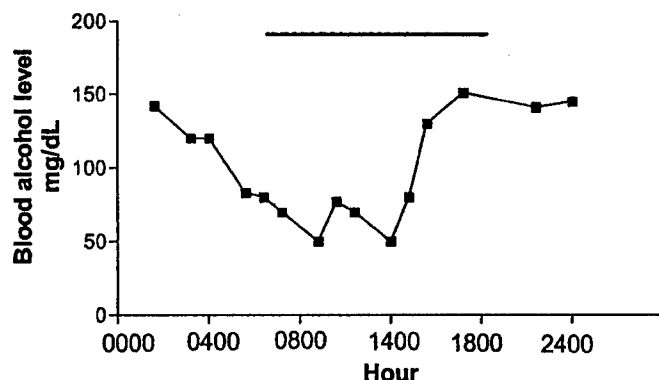

Fig. 3. Effect of the saccharin fading ethanol exposure paradigm on blood alcohol levels. Blood alcohol level determinations from saphenous vein blood of dams drinking 10% (w/v) ethanol in 0.06% saccharin across a 24 hr access period. Each point is mean ± SEM from six to eight dams per time point. Each dam is represented at no more than three time points. Solid horizontal bar indicates the lights-on period.

Effect of Saccharin Fading Ethanol Exposure Paradigm on Maternal Grooming and Latency to Retrieve Pups

Although pup weights and growth are good indicators of maternal care, we also addressed maternal care using a pup retrieval test as well as monitoring grooming frequencies over four 1 hr observation sessions (Table 2). The ethanol-drinking mothers retrieved pups that were deliberately removed from the nest with a similar latency to that of the saccharin-drinking mothers (Table 2). Furthermore,

ethanol-consuming females did not differ from controls in the percent time spent on the nest or grooming pups.

Effect of Saccharin Fading Ethanol Exposure Paradigm on Offspring Basal Corticosterone Levels

Several studies have shown that rats prenatally exposed to ethanol demonstrate changes in hypothalamic-pituitary-adrenal responsiveness, as indicated by elevations of adrenocorticotropin and corticosterone, especially after stress (Glavas et al., 2001; Osborn et al., 1996). Levels of corticosterone in blood were determined without using any activating stress other than handling the mouse just before decapitation. In our study, FAE females had a significantly higher plasma corticosterone level than did control females (Table 3). Although a similar difference was observed for males, it did not achieve significance. This was demonstrated by a significant sex × prenatal treatment condition interaction [$F(1,28) = 5.67, p < 0.03$]. No differences were observed in adrenal weights of FAE and control offspring.

Effect of Saccharin Fading Ethanol Exposure Paradigm on Novelty Exploration

Exploratory behavior within the testing environment (initial 5 min segment, without object present) and exploratory behavior in response to introduction of a novel object (second 5 min segment, with novel object) were assessed by recording the number of transitions, time spent in center, and number of entries into the center area (Fig. 4). In these studies, adult male offspring were used. Data were analyzed by analysis of variance with Bonferroni correction. Prenatal condition (ethanol versus saccharin) did not significantly affect the number of entries into the center, regardless of the object presence (Fig. 4B); thus, this dependent variable was not analyzed by ANOVA. There was no effect of prenatal condition on the number of transitions (Fig. 4C), but a significant decrease in number of transitions occurred when the object was present for both of the prenatal treatment conditions [$F(1,12) = 17.3, p < 0.01$]. This suggested that there was no significant difference between the prenatal treatment groups in general locomotor activity under these conditions. Time spent in the center with the object present was significantly greater for the FAE mice (Fig. 4A), as indicated by the significant interaction between prenatal condition and object presence [$F(1,12) = 169.58\ p < 0.0001$], suggesting greater exploratory activity.

Table 1. Maternal Weight Change, Food Consumption, Pup Weights and Litter Size, From Four Separate Studies

Treatment condition	Change in maternal weight (g)	Daily food consumption (g)	Pup weight (g)	Litter size
10% (w/v) EtOH in saccharin	+1.08 (±0.2)	4.4 (±0.38)	4.3 (±0.4)	8.4 (±1.3)
Saccharin only	+1.02 (±0.4)	4.2 (±0.13)	4.1 (±0.2)	8.2 (±2.0)

Values are mean ± SEM, *n* = 6 mothers per study.

Table 2. Pup Retrieval Time and Percent Time Nesting and Pup Grooming From Four Separate Studies

Treatment condition	Pup retrieval time (sec)	Percent time on nest (min/2 hr observation)	Percent time grooming pup
10% (w/v) EtOH in saccharin	62 (±8)	52 (±3)	7.2 (±1.0)
Saccharin only	57 (±1)	49 (±4)	9.7 (±0.9)

Values are mean ± SEM, n = 6 mothers per study.

Table 3. Average Adrenal Weights and Plasma Corticosterone Levels in Offspring From Saccharin and Ethanol-Drinking Dams Taken at 0900–1000 hr

	Average single adrenal weight (mg)	Total adrenal wt/body wt × 100	Plasma corticosterone level, μg/dl
Saccharin female	3.10 (±0.25)	0.0261 (±0.003)	3.00 (±0.4)
10% EtOH female	2.74 (±0.20)	0.0253 (±0.004)	5.06 (±0.4)*
Saccharin male	1.46 (±0.18)	0.0196 (±0.009)	2.78 (±0.3)
10% EtOH male	1.35 (±0.21)	0.0163 (±0.006)	3.30 (±0.4)

Values are mean (±SEM, n = 10).
* Statistically different from saccharin females, p < 0.03.

Effect of Saccharin Fading Ethanol Exposure Paradigm on Delay Fear Conditioning

FAE mice and control pups were reared to adulthood and trained using a delay conditioning paradigm. Twenty-four hours later, mice were assessed for their conditioned responses to the context and to the CS by measuring freezing behavior in response to reintroduction into the context in which conditioning occurred and exposure to the CS in a novel (altered) context (Fig. 5). As can be seen in Fig. 5, FAE mice froze less to the context than did saccharin controls, whereas freezing to the auditory CS was nearly identical in the two groups. An ANOVA revealed a significant effect of prenatal treatment condition [$F(1,36)$ = 18.3, $p < 0.001$] and a significant interaction between prenatal treatment and stimulus condition (tone versus context) [$F(1,36)$ = 19.5, $p < 0.001$], indicating that the FAE mice froze less to the context than saccharin mice but there were no differences between the prenatal treatment conditions in freezing to the tone.

DISCUSSION

Our goal was to develop a prenatal alcohol exposure model that would (1) produce a voluntary and stable drinking of moderate concentrations of ethanol throughout pregnancy, (2) not significantly affect maternal care, and (3) replicate the behavioral effects found previously in the rat moderate alcohol drinking model. We believe that we have developed a mouse model of FAE that accomplishes these goals. Using a moderate dose of ethanol (10%, w/v), this paradigm did not affect fetal birth weight, litter size, maternal care, or locomotor activity of the offspring, yet characterization of the behavioral phenotype of the offspring revealed deficits in contextual fear conditioning as well as increased novelty exploratory behavior. In addition, we found no effect on pup mortality rates. This is in sharp contrast to earlier mouse models, which reported a marked decrease in the number of viable pups among the alcohol diet groups (Boggan et al., 1979; Fish et al., 1981; Randall and Taylor, 1979).

The paradigm described herein developed drinking behavior in females before impregnation. Thus, stable drinking patterns and blood levels were established before the beginning of pregnancy. We believe that this more closely models human alcohol drinking patterns than do paradigms in which alcohol consumption is initiated once pregnancy has been established.

An additional goal of our model was to permit the mothers to care for their own pups, thereby reducing the stress of cross-fostering. To accomplish this, we needed to reduce the alcohol concentration after the pups were delivered as quickly as possible but without precipitating any withdrawal signs. In several pilot studies we determined that reducing both the ethanol and saccharin concentrations by one half every 2 days was slow enough to prevent any signs of handling-induced seizures or maternal neglect. Although gross measurements, such as pup retrieval times, pup weights, pup grooming, and litter sizes, suggest that maternal care was appropriate, other subtle differences between 10% ethanol- and saccharin-drinking mothers are likely to exist. In humans, it is well known that maternal alcohol consumption may slightly reduce milk production and that some of the alcohol consumed is transferred in the milk (for review, see Mennella, 2001). Using a rat model of prenatal and postnatal 20% alcohol exposure, Murillo-Fuentes et al. (2001) found no significant effect of ethanol on birth weight, but milk consumption and suckling behavior were reduced in pups whose mother continued to consume 20% ethanol. In our model, the nursing mothers were tapered off the ethanol solution and this may be why we did not see a significant difference in the pup weight between the 10% ethanol- and saccharin-drinking control groups.

Performance in the novel object task is an indication of exploratory responsiveness to novel stimuli, and although it is not a standard measure of anxiety, results of this task are influenced by anxiety. The test begins similar to a standard open field, spontaneous locomotion study, where entries into the center of the field are suggestive of lower levels of anxiety in the mouse. Mice generally display neophobia and, although attracted by novel objects, typically keep a
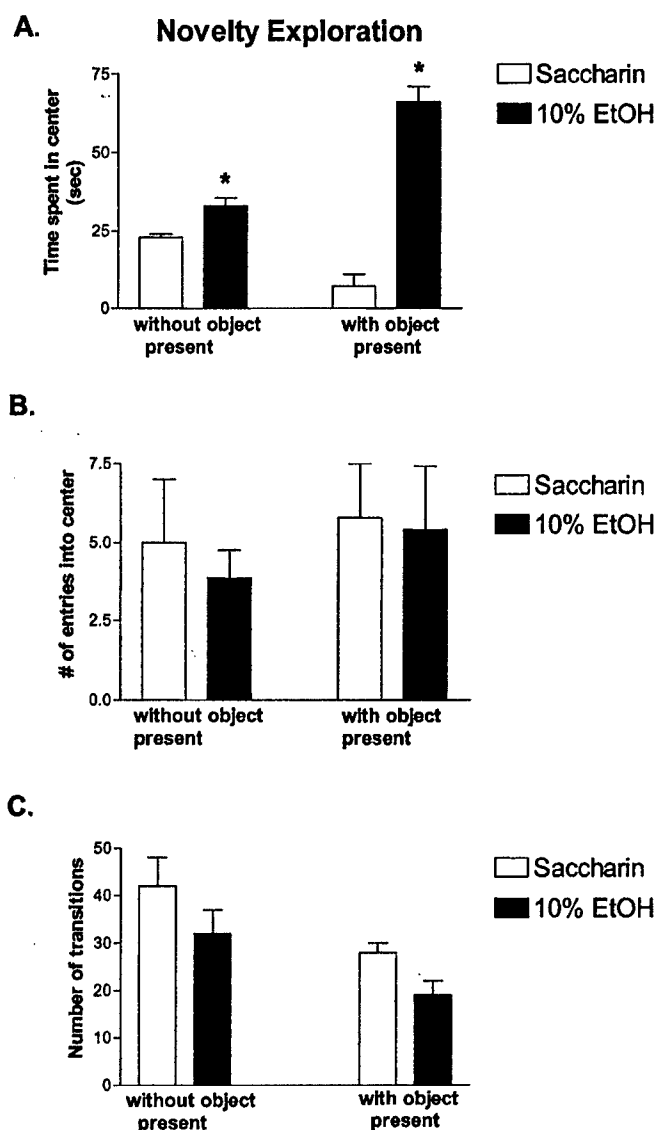
A. Novelty Exploration

B.

C.

Fig. 4. Effect of the saccharin fading ethanol exposure paradigm on novelty exploration. Novelty exploration was measured in adult male mice and expressed as mean (± SEM, n = 7 per group) time spent in the center (within 5 cm of the object, A), number of entries into the center area (B), and number of transitions across the quadrants of the open field (C). Data are presented as activity during the first 5 min without the object present in the first pair of bars and the behavioral activity during the last 5 min while the novel object was present in the last pair of bars. *p < 0.01 by ANOVA.
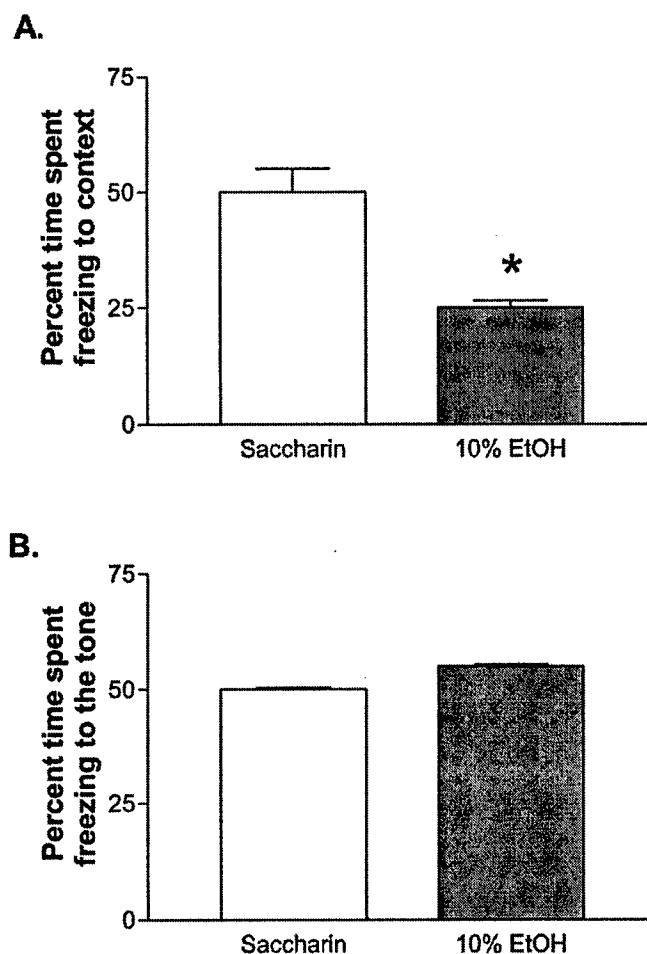
A.

B.

Fig. 5. Effect of the saccharin fading ethanol exposure paradigm on contextual fear learning and memory. Freezing to the training context (A) and to the conditioned stimulus in a novel context (B) in saccharin control and 10% EtOH mice trained with a paired tone shock. Adult male offspring of dams consuming either 0.066% saccharin (control; n = 10) or 10% (w/v) ethanol in 0.066% saccharin (10% EtOH; n = 10) were trained using a delay fear conditioning paradigm. (A) Twenty-four hours after training, the animals were returned to the training context, and the conditioned response (freezing) was assessed. Data are expressed as the percent freezing (number of freezing intervals ÷ total intervals). (B) Freezing to the CS tone was measured in a novel context. Data are expressed as in A. *p < 0.001 by ANOVA.

safe distance from them (see File, 2001, for review). Mice that perform with reduced anxiety on other tests (e.g., elevated plus and social interaction) typically will spend more time in close proximity of the novel object. An increase in number of entries into close proximity to a novel object indicates increased inquisitive behavior, whereas increased time spent near the novel object indicates inspective behavior (Dellu et al., 2000; Grailhe et al., 1999). In our study, the 10% ethanol mice reacted to the presentation of a novel object with increased inspective behavior compared with saccharin animals. It is not likely that the increase in time spent in proximity to the novel object was

due to decreased locomotor activity, because entries into the center and the number of transitions in the open field were not different in the 10% ethanol and saccharin mice. The higher level of inspective behavior may be due to a failure in the formation of associations and information processing, as suggested by their impaired performance in the fear conditioning task (discussed subsequently). Another interpretation of these data is that the 10% ethanol mice display a reduced level of anxiety.

The hippocampal formation has long been a focus of studies attempting to uncover the basis of ethanol-induced learning and memory deficits. In rodents, FAE is associated with impaired learning and/or memory in a variety of hippocampal-dependent tasks, including radial arm maze paradigms (Reyes et al., 1989), the Morris water maze task (Gabriel et al., 2002; Savage et al., 2002), and avoidance

learning (Furuya et al., 1996). In a recent group of studies, we found that rats exposed prenatally to moderate levels of ethanol displayed deficits in contextual fear conditioning but not fear of a discrete CS (Weeber et al., 2001). Similar to the findings of Weeber et al. (2001) using the rat model, the 10% ethanol mice displayed significant deficits in single-trial fear conditioning (Fig. 5). However, with the mouse model, a more robust attenuation of fear conditioned freezing was seen here (Fig. 5) compared with that reported in the rat (Weeber et al., 2001). Impaired contextual conditioning, but unaltered CS (tone) conditioning, indicates that FAE disrupts hippocampal functioning while leaving amygdalar functioning intact. The hippocampal formation plays a critical role in the consolidation and expression of contextual fear memory, whereas the amygdala plays an essential role in the acquisition and consolidation of information about both the elemental CS and the training context as well as the expression of both CS fear and contextual fear responses (see Weeber et al., 2001, for discussion). These results indicate that the 10% ethanol mice have impaired formation of the association between the context and the US. Identification of a learning/memory deficit in adult offspring demonstrates that the mouse, as well as the previously described rat, FAE model produces learning and memory impairments that persist into adulthood, similar to the clinical course of FASD in humans. It is interesting to note that Green et al. (2002) reported that eye-blink delay conditioning is impaired in rats that were exposed to alcohol as neonates, approximating the human third trimester period. Thus, FAE-induced deficits in associative learning measured using delay conditioning paradigms are reproducible across species and seem to be a useful behavioral endpoint for studying the effects of therapeutic interventions on FAE-induced learning and memory deficits.

An advantage of this mouse paradigm is that it will support drinking of high, moderate, and low ethanol amounts in a voluntary design. The procedure that we describe could be modified to study effects of binge-like drinking, as we have found that, by limiting alcohol availability to a 2 hr period, females will display higher alcohol drinking. For example, we have found that mothers will drink saccharin-sweetened 15% (w/v) ethanol in a 2 hr restricted access paradigm and generate blood alcohol levels of 150 to 180 mg/dL. In addition, a voluntary drinking approach can be used to study the effects of high blood alcohol levels because it avoids the problems of malnutrition that are a consequence of using higher concentrations of ethanol in liquid diets or the stress associated with oral intubation, which often is used to administer larger quantities of ethanol to dams.

The mouse FAE model described herein should prove useful in studies that exploit the availability of genetically modified, as well as several well-characterized, mouse strains to assess the interplay between different genes in determining susceptibility to and the outcome of FAE. The

studies presented here were performed using B6SJL/F1 mice because of our interest in developing a model that could be used with genetically altered mouse populations. However, it was important to demonstrate that similar results could be obtained in a genetically stable inbred strain. In a series of pilot studies we have obtained similar results on drinking levels, litter sizes, and pup weights using the C57 BL/6 J mice (data not shown). It is important to note that although the mouse does offer certain important advantages over other animal models of FAE, it will be important to study outcomes in a variety of models.

Finally, it is possible that one model may more closely replicate certain characteristics of human FASD (e.g., attention deficits), whereas another model more closely reproduces other characteristics (e.g., impaired spatial learning). Extensive characterization of the effects of FAE on various neurochemical, electrophysiological, and behavioral endpoints in other models has identified several targets for therapeutic intervention, which could be tested in our mouse model. Furthermore, thorough characterization of the effects of FAE in different animal models may identify distinct endpoints, which, in light of known differences in rodent brain neurochemistry and neurophysiology (e.g., differences in hippocampal GAP-43 expression; McNamara et al., 1996), may provide clues to the effects of genetic influence on the effects of FAE, and, thus identify therapeutic targets.

CONCLUSION

We describe the development and initial characterization of a mouse model of FAE. This model complements and extends other available models for the study of FAE. The paradigm that we used will facilitate the study of the impact of FAE without negatively influencing diet or natural consumption routes or requiring surrogate maternal care, all of which are thought to contribute to maternal stress. The mouse FAE model allows the use of genetically altered mice, as well as genetically defined inbred mouse strains, to identify risk factors that are associated with FASD cognitive deficits.

REFERENCES

Boggan WO, Randall CM, DeBeukelaer M, Smith R (1979) Renal anomalies in mice prenatally exposed to ethanol. Res Commun Chem Pathol Pharmacol 23:127–142.

Bouton ME, Bolles RC (1980) Conditioned fear assessed by freezing and by the suppression of three different baselines. Anim Learn Behav 8:429–434.

Cirulli F, Micera A, Alleva E, Aloe L (1998) Early maternal separation increases NGF expression in the developing rat hippocampus. Pharmacol Biochem Behav 59:853–858.

Czachowski CL, Samson HH, Denning CE (1999) Blood ethanol concentrations in rats drinking sucrose/ethanol solutions. Alcohol Clin Exp Res 23:1331–1335.

Dellu F, Contarino A, Simon H, Koob GF, Gold LH (2000) Genetic differences in response to novelty and spatial memory using a two-trial recognition task in mice. Neurobiol Learn Mem 73:31–48.

Fanselow MS (1980) Conditional and unconditional components of post-shock freezing. Pavlov J Biol Sci 15:177–182.

Farr KL, Montano CY, Paxton LL, Savage DD (1988) Prenatal ethanol exposure decreases hippocampal 3H-glutamate binding in 45-day-old rats. Alcohol 5:125–133.

Fish BS, Rank SA, Wilson JR, Collins AC (1981) Viability and sensorimotor development of mice exposed to prenatal short-term ethanol. Pharmacol Biochem Behav 14:57–65.

File SE (2001) Factors controlling measures of anxiety and responses to novelty in the mouse. Behav Brain Res 125:151–157.

Furuya H, Aikawa H, Yoshida T, Okazaki I (1996) Effects of ethyl alcohol administration to THA rat dams during their gestation period on learning behavior and on levels of monoamines and metabolites in the brain of pups after birth. Alcohol Clin Exp Res 20:305A–310A.

Gabriel KI, Johnston S, Weinberg J (2002) Prenatal ethanol exposure and spatial navigation: effects of postnatal handling and aging. Dev Psychobiol 40:345–357.

Glavas MM, Hofmann CE, Yu WK, Weinberg J (2001) Effects of prenatal ethanol exposure on hypothalamic-pituitary-adrenal regulation after adrenalectomy and corticosterone replacement. Alcohol Clin Exp Res 25:890–897.

Grailhe R, Waeber C, Dulawa SC, Hornung JP, Zhuang X, Brunner D, Geyer MA, Hen R (1999) Increased exploratory activity and altered response to LSD in mice lacking the 5-HT$_{5A}$ receptor. Neuron 22:581–591.

Green JT, Johnson TB, Goodlett CR, Steinmetz JE (2002) Eyeblink classical conditioning and interpositus nucleus activity are disrupted in adult rats exposed to ethanol as neonates. Learn Mem 9:304–320.

Liu D, Diorio J, Day JC, Francis DD, Meaney MJ (2000) Maternal care, hippocampal synaptogenesis and cognitive development in rats. Nat Neurosci 3:799–806.

Lu Y, Wehner JM (1997) Enhancement of contextual fear-conditioning by putative (±)-α-3-hydroxy-5-methylisoxazole-4-propionic acid (AMPA) receptor mediators and N-methyl-d-aspartate (NMDA) receptor antagonists in DBA/2J mice. Brain Res 768:197–207.

Lundquist F (1959) The determination of ethyl alcohol in blood and tissues. Methods Biochem Anal 7:217–251.

Mattson SN, Riley EP (1998) A review of the neurobehavioral deficits in children with fetal alcohol syndrome or prenatal exposure to alcohol. Alcohol Clin Exp Res 22:279–294.

McNamara RK, Namgung U, Routtenberg A (1996) Distinctions between hippocampus of mouse and rat: protein F1/GAP-43 gene expression, promoter activity, and spatial memory. Mol Brain Res 40:177–187.

Mennella J (2001) Alcohol's effect on lactation. Alcohol Res Health 25:230–234.

Murillo-Fuentes L, Artillo R, Carreras O, Murillo L (2001) Effects of maternal chronic alcohol administration in the rat: lactation performance and pup's growth. Eur J Nutr 40:147–154.

Osborn JA, Kim CK, Steiger J, Weinberg J (1996) Prenatal ethanol exposure differentially alters behavior in males and females on the elevated plus maze. Alcohol Clin Exp Res 22:685–696.

Randall CL, Taylor WJ (1979) Prenatal ethanol exposure in mice: teratogenic effects. Teratology 19:305–311.

Reyes E, Wolfe J, Savage DD (1989) The effects of prenatal alcohol exposure on radial arm maze performance in adult rats. Physiol Behav 46:45–48.

Roberts AJ, Heuser CJ, Koob GF (1999) Operant self-administration of sweetened versus unsweetened ethanol: effects on blood alcohol levels. Alcohol Clin Exp Res 23:1151–1157.

Sampson PD, Streissguth AP, Bookstein FL, Little RE, Clarren SK, Dehaene P, Hanson JW, Graham JM (1997) Incidence of fetal alcohol syndrome and prevalence of alcohol-related neurodevelopmental disorder. Teratology 56:317–326.

Savage DD, Belcher M, de la Torre AJ, Sutherland RJ (2002) Dose-dependant effects of prenatal ethanol exposure on synaptic plasticity and learning in mature offspring. Alcohol Clin Exp Res 26:1752–1758.

Slawecki CJ, Samson HH, Hodge CW (1997) Differential changes in sucrose/ethanol and sucrose maintained responding by independently altering ethanol or sucrose concentration. Alcohol Clin Exp Res 21: 250–260.

Slone JL, Redei EE (2002) Maternal alcohol and adrenalectomy: asynchrony of stress response and forced swim behavior. Neurotoxicol Teratol 24:173–178.

Smith AM, Wehner JM (2002) Aniracetam improves contextual fear conditioning and increases hippocampal γ-PKC activation in DBA/2J mice. Hippocampus 12:76–85.

Streissguth AP, Barr HM, Sampson PD (1990) Moderate prenatal alcohol exposure: Effects on child I.Q. and learning problems at age 7 1/2 years. Alcohol Clin Exp Res 14:662–669.

Streissguth AP, O'Malley K (2000) Neuropsychiatric implications and long-term consequences of fetal alcohol spectrum disorders. Semin Clin Neuropsychiatry 5:177–190.

Streissguth AP, Sampson PD, Olson HC, Bookstein FL, Barr HM, Scott M, Feldman J, Mirsky AF (1994) Maternal drinking during pregnancy: attention and short-term memory in 14 year old offspring. Alcohol Clin Exp Res 18:202–218.

Tomie A, diPoce J, Derenzo CC, Pohorecky LA (2002) Autoshaping of ethanol drinking: an animal model of binge drinking. Alcohol Alcohol 37:138–146.

Ward GR, Wainwright PE (1989) Prenatal ethanol and stress in mice: 1. Pup behavioral development and maternal physiology. Physiol Behav 45:533–540.

Weeber EJ, Savage DD, Sutherland RJ, Caldwell KK (2001) Fear conditioning-induced alterations of phospholipase C-beta 1a protein level and enzyme activity in rat hippocampal formation and medial frontal cortex. Neurobiol Learn Mem 76:151–182.

ELSEVIER

Delay fear conditioning modifies phospholipase C-β1a signaling in the hippocampus and frontal cortex

Edwin J. Weeber[a,b,1], Kevin K. Caldwell[a,*]

[a]*Department of Neurosciences, MSC08 4740, University of New Mexico, Albuquerque, 1 University of New Mexico, Albuquerque, NM 87131-0001, USA*
[b]*Department of Biology, University of New Mexico, Albuquerque, NM 87131, USA*

Abstract

The use of the single-trial fear conditioning paradigm allows for control over the exact moment when an animal is exposed to a learning event, making it possible to study both the initial neurobiological changes that are associated with learning and changes that take place over long periods of time. In the present study, we performed detailed analyses of the alterations in phosphatidylinositol-specific phospholipase C-β1a (PLC-β1a) levels and enzyme activities in subcellular fractions prepared from the hippocampal formation (HPF) and medial frontal cortex (MFC) 1, 3, 5, 7, 24, and 72 h following single-trial fear conditioning. We observed tissue- and time-dependent changes in both PLC-β1a enzyme activity and anti-PLC-β1a immunoreactivity in each subcellular fraction. Based on these observations, we hypothesize that changes in PLC-β1a catalytic activity and subcellular distribution play important roles in neuronal signaling processes that are required for fear-conditioned learning and memory.
© 2004 Elsevier Inc. All rights reserved.

Keywords: Fear conditioning; Phospholipase C; Subcellular fractionation

1. Introduction

Phosphatidylinositol-specific phospholipase C (PLC) isozymes hydrolyze phosphatidylinositol 4,5-bisphosphate [PtdIns(4,5)P_2], yielding two intracellular second messengers: inositol 1,4,5-trisphosphate [Ins(1,4,5)P_3] and 1,2-diacylglycerol (Majerus et al., 1990; Williams, 1999). Production of Ins(1,4,5)P_3 results in the release of Ca^{2+} from intracellular storage sites, while 1,2-diacylglycerol directly activates the conventional and novel isoforms of protein kinase C (Berridge, 1993; Nishizuka, 2001). Complementary DNA clones have been isolated for at least 11 distinct mammalian PLC isozymes (Rhee, 2001), which are grouped into four types: β, δ, γ, and ε. For each of these types, multiple subtypes have been identified. For example, there are four known PLC-β isoforms designated as PLC-β1–4. PLC-β1 is the predominant PLC isozyme in the brain,

accounting for approximately 50% of the total PLC activity in this tissue (Takenawa et al., 1991). PLC-β1 exists as two splice variants consisting of the 150-kDa PLC-β1a, which represents the preponderance of the PLC-β1 complement, and the 140-kDa PLC-β1b (Bahk et al., 1994).

There are a growing number of studies examining the roles of protein kinases in the induction and maintenance of long-lasting memories. Much of this research is focused on the four major protein kinase families present in the post-synaptic density: protein kinase C, protein kinase A, Ca^{2+}-calmodulin-dependent protein kinase, and extracellular signal-regulated protein kinase. Members of each of these families have been shown to be necessary for memory formation and synaptic plasticity in various capacities. In contrast, the role of phospholipases in learning and memory has often been overlooked. Support for a role for one or more PLC isozyme in fear conditioning comes from studies showing that the turnover rates of inositol phosphates and 1,2-diacylglycerol in the dentate gyrus and areas CA1 and CA3 of the hippocampus are increased following fear conditioning. (Laroche et al., 1990). Despite the presence of most, if not all, of the known members of the PLC family in the brain (Homma et al., 1989; Kelley et al., 2001; Lee

---

and Rhee, 1996; Watanabe et al., 1998), PLC-β1 stands out as a potentially important player in neuronal signaling (see Weeber et al., 2001, for discussion) due to its highly elevated expression in the CNS (Bahk et al., 1994; Ross et al., 1989; Smrcka and Sternweis, 1993; Takenawa et al., 1991). This hypothesis is supported by our earlier studies showing changes in hippocampal formation (HPF) and cortical PLC-β1a regulation following fear conditioning (Weeber et al., 2001).

The present experiments were aimed at investigating whether there are time-dependent changes in PLC-β1a enzyme activity and protein level associated with learning and memory formation in the rat HPF and medial frontal cortex (MFC). For these studies, we employed single-trial fear conditioning, which makes it possible to identify the exact moment that learning is initiated (Bevins and Ayres, 1994; Fanselow and Bolles, 1979), and thus facilitates the identification of biochemical changes that occur in conjunction with in vivo learning and memory processes.

Fear-induced long-term memory is dependent on de novo RNA and protein synthesis (Barrientos et al., 2002; Davis and Squire, 1984; Lattal and Abel, 2001; Stiedl et al., 1999). Recent studies have demonstrated that under certain conditions, there are two temporal phases that are critical for long-term consolidation of fear memory: one period exists for the first few minutes up to 1 h following training, while the other period occurs between 1 and 6 h after training, with the period from 2 to 4 h most commonly being reported as important (Bernabeu et al., 1997; Bourtchuladze et al., 1998; Igaz et al., 2002; Quevedo et al., 1999). The ability to observe these two phases depends on the strength of the training procedure that has been employed. Bourtchuladze et al. (1998) reported that a weak fear conditioning procedure, such as one in which the test subject experiences only a single pairing of a conditioned stimulus (CS) and an unconditioned stimulus (US), is associated with two periods of protein-synthesis-sensitive memory formation—immediately after training and 4 h after training. In contrast, if a strong training procedure (e.g., one in which the subject experiences multiple pairings of the CS and US) is used, inhibition of protein synthesis affects long-term memory only if the inhibitor is administered immediately after training. These studies indicate that long-term memory formation occurs at different rates, depending on the intensity of the training experience. One interpretation of these results is that strong training procedures regulate multiple signal transduction pathways, which in turn regulate transcriptional and translational processes required for long-term memory formation. Weaker training procedures can either regulate these same pathways less robustly or regulate fewer signal transduction pathways, which, as a result, causes a second period of protein-synthesis-dependent consolidation to occur. There is an astonishingly incomplete picture of the upstream signaling events that may control pathways leading to transcription- and translation-dependent memory formation.

We show that the temporal profiles of changes in subcellular PLC-β1a enzyme activity and protein levels associated with fear-conditioned learning and memory are remarkably dynamic with prominent changes 3 to 5 h following conditioning. Based on these results and the known dependence of learning and memory on molecules known to be controlled by PLC-β1a signaling, we speculate on the role that PLC-β1a may play in fear-conditioned learning and memory.

2. Materials and methods

2.1. Animals

Female Sprague–Dawley rats (90–150 days of age) obtained from Harlan Industries (Indianapolis, IN) were used in these studies. Following delivery from the distributor, all experimental rats were housed in groups of two or three per cage and allowed to adjust to the animal housing room for at least 7 days prior to being assigned to an experimental group and housed individually. Animals were housed in the same room, which was maintained at 22 °C on an 8-h dim light–16-h dark cycle (lights on from 0930 to 1730 h), and were given 24-h access to standard rat chow and tap water. All procedures and methods for housing, fear conditioning, and sacrificing rats were approved by the University of New Mexico Health Science Center Animal Care and Use Committee.

2.2. Fear conditioning

The procedures used for fear conditioning and treatment of control groups were performed as previously described in Weeber et al. (2001). Briefly, rats were randomly assigned to one of three experimental groups: single-trial fear-conditioned [paired tone–shock (PTS)], unpaired control (UPC), or unhandled (UH). Fear-conditioned rats were exposed to a 30-s tone (the CS), which terminated with a 2-s, 1-mA foot shock (the US). UPC rats received all of the same stimuli as the fear-conditioned rats (i.e., transportation, handling, context, tone, and shock), but the context, CS, and US experiences were separated by a minimum interval of 60 min, with the US being delivered in the animal's home cage. The UPC procedure allowed us to control for the unconditioned effects of foot shock, as well as handling, tone, and context exposures. The third experimental group consisted of naive, UH control rats, which did not receive any of the experiences associated with the fear conditioning paradigm prior to sacrifice.

At the appropriate time following exposure to the foot shock, PTS and UPC rats were taken directly from the housing room to an adjacent room and were sacrificed by decapitation without anesthesia. UH rats were sacrificed in the same manner. The brains were rapidly removed, and the HPF and MFC (identified as all areas rostral to the fornix and optic chiasm with the olfactory region previously removed) were dissected.

2.3. Analyses of PLC-β1a enzyme activity and immunoreactivity in subcellular fractions

All procedures for the preparation of HPF and MFC subcellular fractions, isolation of PLC-β1a by immunoprecipitation, and quantification of PLC-β1a enzyme activity and anti-PLC-β1a immunoreactivity were as described in Weeber et al. (2001). Immunoreactivity was determined using 20, 25, and 5 μg, respectively, of HPF S2 (200,000 × g soluble), P2 (200,000 × g postnuclear particulate), and P1 (1000 × g particulate) fractions, and 40, 40, and 10 μg of MFC S2, P2, and P1 fractions.

2.4. Calculation of PLC-β1a enzyme specific activity

Specific activities were calculated as the quotient of PLC-β1a enzyme activity divided by anti-PLC-β1a immunoreactivity in the subcellular fraction being analyzed. Both enzyme activity [pmol Ins(1,4,5)P$_3$ product formed/min/μg protein] and immunoreactivity (Unit; "units" were calculated as the immunoreactivity/μg protein fraction) were expressed relative to the total protein content of the subcellular fraction being analyzed, and thus, specific activity was expressed as pmol Ins(1,4,5)P$_3$ product formed/min/"unit" of enzyme.

2.5. Statistical analyses

For ease of presentation and clarity of results, graphs are presented at the 95% confidence level (95% CL). Data analysis using two-way ANOVA was performed on UPC and PTS animal groups to determine significant differences with variables of behavioral treatment and time. In addition, a Tukey multiple comparisons test was performed to verify statistical significance at experimental times where error bars do not overlap ($P < .05$), and these are the only time points that are marked with an asterisk.

2.6. Materials

Polyclonal antibodies for PLCβ-1a were purchased from Santa Cruz Biotechnology. PtdIns(4,5)P$_2$ and Triton X-100 were purchased from Boehringer-Mannheim. [H^3] PtdIns(4,5)P$_2$ was purchased from NEN. Protein A–Sepharose CL4B was purchased from Pharmacia. All other chemicals and supplies were obtained from commercial sources.

3. Results and discussion

3.1. Overview of experimental design

To determine the time dependence of the effects of fear conditioning on PLC-β1a, we measured the catalytic activity and level of the enzyme in HPF and MFC subcellular fractions (nuclear, cytosolic, and postnuclear membrane) at six times (1, 3, 5, 7, 24, and 72 h) following CS delivery. Because rodent brain contains multiple PLC isozymes, we chose to isolate PLC-β1a from other PLC isoforms present in HPF and MFC subcellular fractions by affinity capture using isozyme-specific antibodies. Specificity of the antibody has been previously established (Weeber et al., 2001). Immune complex-associated PLC activity was determined by measuring the in vitro hydrolysis of PtdIns(4,5)P$_2$. Subcellular PLC-β1a levels were assessed by semiquantitative immunoblotting. From these two measures, we calculated enzyme specific activity (i.e., PLC catalytic activity per unit of enzyme). Changes in PLC-β1a specific activity revealed alterations in the catalytic activity of the enzyme that could not be accounted for by changes in PLC-β1a levels, thus implicating the regulation of enzyme activity during memory formation. This method of analysis was employed by Wahl et al. (1992) to demonstrate that tyrosine phosphorylation increases the catalytic activity of PLC-γ1.

Two groups of control animals were employed in these studies: UPC and UH. UPC animals were exposed to each of the stimuli that comprise the single-trial fear conditioning paradigm without the pairing of the US with either the CS or the context. UH animals did not experience the CS, context, or US. Importantly, there were no significant differences between PLC-β1a enzyme activities or concentrations in subcellular fractions prepared from UH tissues and UPC tissues at any of the times tested (Figs. 1–3). The consistent measurements from UPC samples indicate that the changes in PLC-β1a recorded following fear conditioning (see below) are not the result of handling, exposure to the context, auditory cue, or foot shock.

3.2. HPF postnuclear membrane and cytosolic fractions

Contextual fear-conditioned learning is dependent upon normal HPF function (Sanders et al., 2003). We have previously shown that changes in the subcellular distribution and catalytic activity of HPF PLC-β1a occur after fear conditioning (Weeber et al., 2001). However, as our previous study assessed changes at 1 and 24 h following conditioning, it gave a rather incomplete picture of the time dependence of changes in PLC-β1a signaling associated with fear conditioning. Therefore, we sought to profile these changes with time.

Measurements of PLC-β1a enzyme activities in the HPF membrane and cytosolic fractions revealed a biphasic profile. The membrane fraction showed a significant decrease in PLC-β1a activity 3 h after fear conditioning, followed by an increase 5 and 7 h after training (Fig. 1A). Interestingly, this appears to be a mirror image of the biphasic activity profile observed for PLC-β1a isolated from the cytosolic fraction (Fig. 1D). By 72 h following conditioning, PLC-β1a enzyme activity returned to baseline levels both in the membrane and cytosolic fractions.
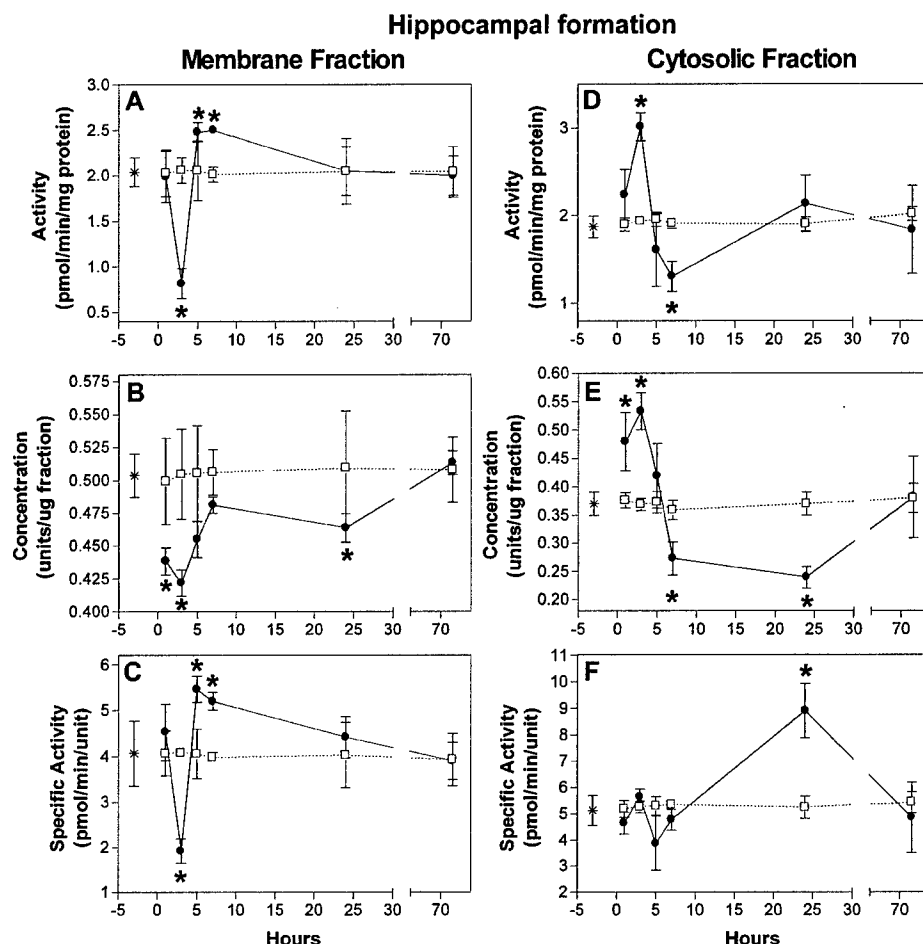
Fig. 1. Changes in HPF membrane- and cytosolic-associated PLC-β1a following single-trial fear conditioning. PLC-β1a enzyme activities were measured in the membrane (A) or the cytosolic fraction (D). Anti-PLC-β1a immunoreactivities were used to quantify PLC-β1a concentrations in the membrane (B) and cytosolic (E) fractions. Measurements were made from HPF subcellular fractions derived from fear-conditioned [PTS (□); $n = 6$] and unpaired control [UPC (□); $n = 6$] animals that were sacrificed 1, 3, 5, 7, 24, or 72 h after fear conditioning. In addition, enzyme activities and concentrations were measured in fractions derived from naive rats, not behaviorally manipulated [UH (*); $n = 4$]. Activity and concentration measurements were used to calculate PLC-β1a specific activities for membrane-associated (C) and cytosolic-associated (F) enzyme. Data are shown as mean ± S.E.M., 95% CL. Data were analyzed by two-way ANOVA (see table for results) followed by post hoc analysis using Tukey multiple comparisons test. Asterisks signify significance determined by both nonoverlapping error bars and by Tukey multiple comparisons test ($P>.05$).
Results of two-way ANOVA:

	Membrane fraction			Cytosolic fraction		
	Activity	Concentration	Specific activity	Activity	Concentration	Specific activity
Time $F(5,60)$, P	22.48, <.001	4.48, .0016	26.76, .0001	16.22, <.0001	18.46, <.0001	14.46, <.0001
Treatment $F(1,60)$, P	1.72, NS	42.18, <.0001	4.76, .033	2.09, NS	2.44, NS	.70, NS
Interaction $F(5,60)$, P	23.92, <.0001	3.49, .0078	27.93, <0.0001	16.76, <.0001	20.42, <.0001	15.24, <.0001

We found that, like the activity profiles, anti-PLC-β1a immunoreactivity changed with time in the membrane and cytosolic subcellular fractions. In both compartments, the greatest change occurred 3 h following fear conditioning, with a decrease in PLC-β1a protein associated with the membrane fraction and an increase in the cytosolic fraction; 72 h following conditioning PLC-β1a levels had returned to baseline concentrations (Fig. 1B and E). In the initial few hours after conditioning, changes in HPF PLC-β1a concentrations in the membrane fraction gener-

ally were equal to, and in an opposite direction to, changes in concentrations in the cytosolic fractions. This observation indicates that the reductions in membrane PLC-β1a concentrations were the result of translocation of the enzyme to the cytosol and that this translocation event was initiated by fear conditioning. However, it should be noted that the membrane fraction isolated in these studies is in fact composed of all cellular membranes, excluding nuclear membranes. Thus, we are unable to identify unequivocally the membrane type(s) [e.g., plasma, Golgi]
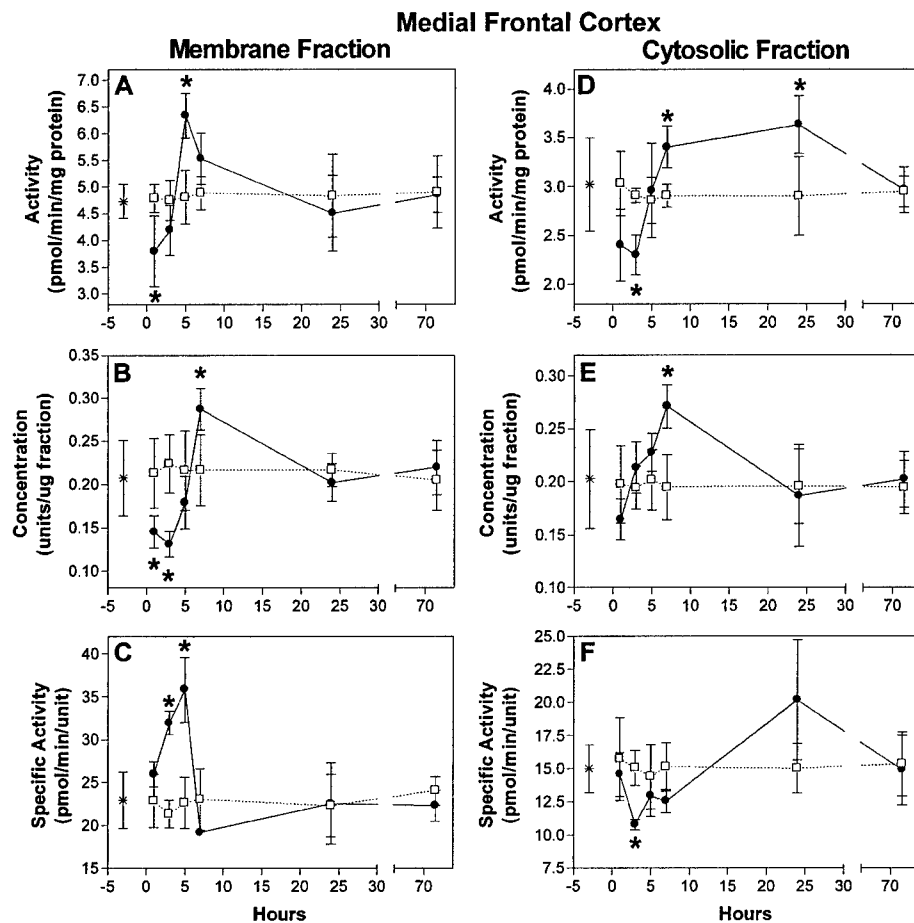
Fig. 2. Changes in MFC membrane- and cytosolic-associated PLC-β1a following single-trial fear conditioning. PLC-β1a enzyme activities were measured in the membrane (A) or the cytosolic fraction (D). Anti-PLC-β1a immunoreactivities were used to quantify PLC-β1a concentrations in the membrane (B) and cytosolic (E) fractions. Measurements were made from MFC subcellular fractions derived from fear-conditioned [PTS (□); $n=6$] and unpaired control [UPC (□); $n=6$] animals that were sacrificed 1, 3, 5, 7, 24, or 72 h after fear conditioning. In addition, enzyme activities and concentrations were measured in fractions derived from naive rats, not behaviorally manipulated [UH (*); $n=4$]. Activity and concentration measurements were used to calculate PLC-β1a specific activities for membrane-associated (C) and cytosolic-associated (F) enzyme. Data are shown as mean ± S.E.M., 95% CL. Data were analyzed by two-way ANOVA (see table for results) followed by post hoc analysis using Tukey multiple comparisons test. Asterisks signify significance determined by both nonoverlapping error bars and by Tukey multiple comparisons test ($P>.05$).
Results of two-way ANOVA:

	Membrane fraction			Cytosolic fraction		
	Activity	Concentration	Specific activity	Activity	Concentration	Specific Activity
Time $F(5,60)$, P	10.94, <.001	10.22, <.0001	15.14, <.0001	10.31, <.0001	5.32, .0004	6.40, <.0001
Treatment $F(1,60)$, P	0.13, NS	9.18, .0036	32.69, <.0001	0.08, NS	5.03, .0286	2.21, NS
Interaction $F(5,60)$, P	9.98, <.0001	11.86, <.0001	20.04, <.0001	12.66, <.0001	5.4, .0004	15.24, <.0001

from which the enzyme dissociated. The idea of PLC translocation following a signaling event is not novel. Redistribution of PLC-β isozymes between subcellular fractions has been reported following cell activation in various nonneuronal cells and cell lines. For example, PLC-β1 (Zini et al., 1996) and PLC-β2 (Bertagnolo et al., 1997) have been reported to translocate from the cytosol to the nucleus; PLC-β2 and PLC-β3 have been reported to move from a cytosolic to a cytoskeletal fraction (Banno et al., 1996; Coburn et al., 1997). However, to our

knowledge, our studies are the first evidence of the subcellular translocation of a PLC-β isozyme in brain tissue following behavioral activation.

In the cytosolic compartment at times up to 7 h following conditioning, the profile of concentration changes is similar to that of the changes in enzyme activity, suggesting that most of the activity differences are due to concentration changes (Fig. 1D and E). This conclusion is supported by a lack of change in enzyme specific activity (Fig. 1F). In contrast, visual inspection indicated that in the membrane
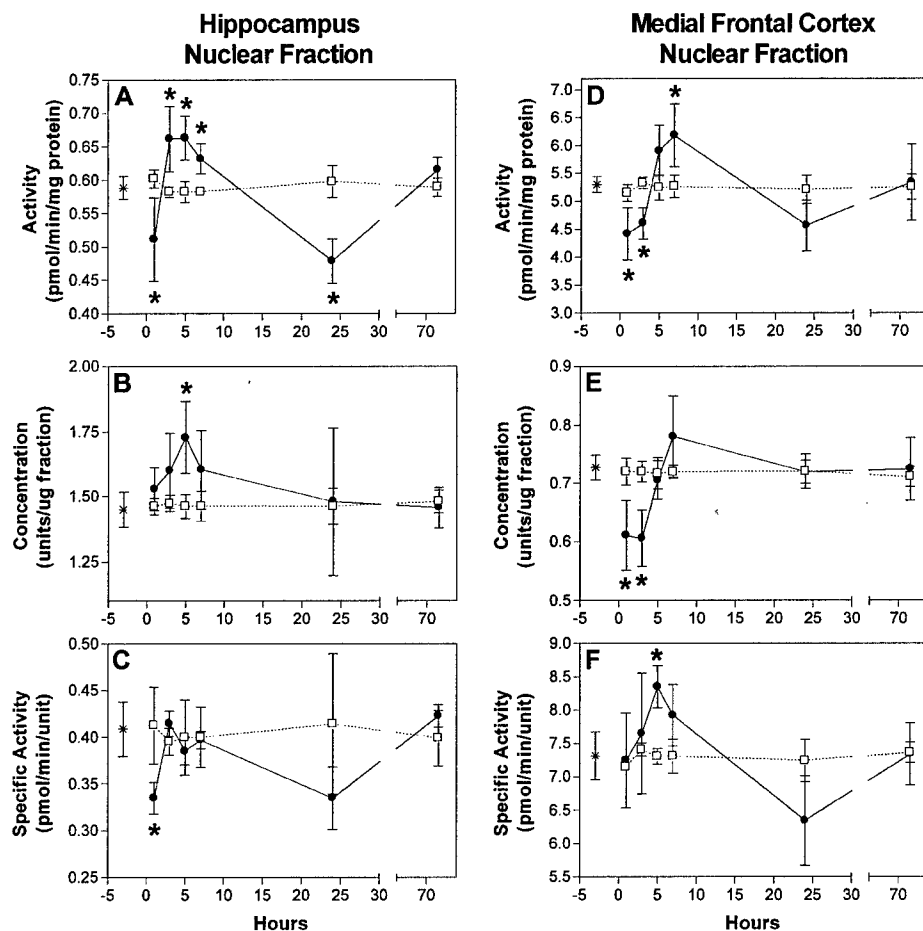
Fig. 3. Changes in nuclear-associated PLC-β1 isolated from the hippocampus and MFC following single-trial fear conditioning. HPF nuclear fraction PLC-β1a activity (A), anti-PLC-β1a immunoreactivity (B), and specific activity (C) were determined as described in the Methods section. Similarly, MFC nuclear fraction PLC-β1a enzyme activity (D), anti-PLC-β1 immunoreactivity (E), and specific activity (F) were determined as described. Measurements were made from fear-conditioned [PTS (□); $n=6$] and unpaired control [UPC (□); $n=6$] animals that were sacrificed 1, 3, 5, 7, 24, or 72 h after receiving a fear conditioning. Control rats not behaviorally manipulated are also shown [UH (*); $n=4$]. Data are shown as mean ± S.E.M., 95% CL. Data were analyzed by two-way ANOVA (see table for results) followed by post hoc analysis using Tukey multiple comparisons test. Asterisks signify significance determined by both nonoverlapping error bars and by Tukey multiple comparisons test ($P>.05$).
Results of two-way ANOVA:

	Membrane fraction			Cytosolic fraction		
	Activity	Concentration	Specific activity	Activity	Concentration	Specific activity
Time $F(5,60)$, P	11.32, <.001	1.49, NS	1.57, NS	7.60, <.0001	5.40, .0004	5.58, .0003
Treatment $F(1,60)$, P	0.25, NS	9.35, .0033	4.65, .0351	0.42, NS	5.05, .0283	2.04, NS
Interaction $F(5,60)$, P	17.06, <.0001	1.68, NS	3.43, .0083	6.97, <.0001	5.73, .0002	4.60, .0013

fraction, changes in concentration were not of sufficient magnitude to account for the changes in enzyme activities at these same times. Thus, the profile of the calculated specific activity of the enzyme (Fig. 1C) was similar to the enzyme activity profile (Fig. 1A) for this fraction. This result indicates that enzyme activity in the membrane fraction is subject to regulation (see below). Finally, the significant decrease in cytosolic fraction PLC-β1a concentration 24 h following conditioning resulted in a prominent increase in the specific activity of the enzyme associated with the fraction (Fig. 1F).

3.3. MFC postnuclear membrane and cytosolic fractions

In the rodent, the MFC has extensive neuronal connectivity with limbic structures and is important in the acquisition and consolidation of fear-conditioned learning (Morgan and LeDoux, 1995; Morrow et al., 1999; Sacchetti et al., 2002). We previously reported that 1 and 24 h after single-trial fear conditioning, PLC-β1a activity and concentration in MFC subcellular fractions were altered (Weeber et al., 2001). In the present study, we more fully assessed the temporal pattern of these changes.

The profiles generated from activity (Fig. 2A) and concentration (Fig. 2B) measurements of membrane PLC-β1a in the MFC were, in general, similar to those of the cytosolic fraction (Fig. 2D and E). However, there appears to be a temporal delay of PLC-β1a activity changes in the cytosolic fraction, being 1 to 3 h behind those of the membrane fraction. In addition, PLC-β1a levels were decreased in the membrane fraction, but not the cytosolic fraction, at early (1–5 h) times. Interestingly, this is in contrast to the mirror-like profiles seen in the membrane and cytosolic fractions isolated from the HPF. The PLC-β1a enzyme activity and concentration profiles for the membrane fraction in the MFC were similar to those observed in the HPF, except that there was not a significant decrease in PLC activity associated with the MFC fraction 3 h following conditioning. For the first 7 h posttraining, the profile of cytosolic PLC-β1a enzyme activity (Fig. 2D) was similar to changes in PLC-β1a levels (Fig. 2E) in the MFC, except at the 3-h time point, where activity is still decreased but concentrations are on the rise. This observation is supported by a minimal change in enzyme specific activity in this fraction at these times, except again for the 3-h time point, which was the only time a statistically significant change in PLC specific activity was seen (Fig. 2F). A striking difference between HPF and MFC was seen at the 24-h post-fear-conditioning time, at which time we observed that both the MFC membrane and cytosolic concentrations of PLC-β1a had returned to baseline levels (Fig. 2B, E), whereas the HPF membrane and cytosolic PLC-β1a concentrations were significantly downregulated at the 24-h time point (Fig. 1B and E).

Another major difference between the MFC and HPF was seen in the profile of the calculated PLC-β1a specific activities of the membrane fraction (Fig. 2C). We observed a significant increase in specific activity in the MFC 3 to 5 h after training, then a sharp decrease in specific activity by 7 h. Although the calculated specific activity at the 7-h time point was not statistically different from UPC or UH specific activities, there was a significant reduction of approximately 50% in specific activity between the 5- and 7-h time points. The appearance of this profile is quite different from that recorded in the HPF (Fig. 1C). Interestingly, the specific activity graphs generated from the MFC cytosolic fraction (Fig. 2F) closely resembles that of the HPF cytosolic PLC-β1a specific activity graph (Fig. 1F).

Taken together, these differences in the activity, concentration, and specific activities of cortical PLC-β1a suggest that the mechanisms controlling PLC-β1a in the MFC may be similar to, but distinctly different from, those in the HPF. Many of these differences appear to be temporal differences, with MFC increases in concentrations and activities occurring later than in the hippocampus. Beyond the temporal divergence is the significant increase in the percent change in PLC-β1a activity and concentration between the HPF and the MFC at time points up to 5 h.

3.4. Nuclear-associated PLC-β1a

There are several reports examining the possible role of PLC-β1 in signal transduction in the nucleus of various cells and cell lines (Bertagnolo et al., 1995; Divecha et al., 1993; Manzoli et al., 1997; Marmiroli et al., 1996). This research suggests that PLC-β1 translocation and involvement in nuclear signaling events are important in normal cellular function and signaling from the membrane to the nucleus. However, there are no reports of PLC-β1 involvement in nuclear signaling correlated with synaptic transmission, plasticity, or learning and memory processes. We reasoned that analysis of the effects of fear conditioning on nuclear PLC-β1a might assist in interpreting the results obtained in the analyses of cytosolic, as well as membrane, PLC-β1a.

When PLC-β1a activity was measured in isolated nuclei from HPF and MFC, a strikingly similar pattern of activity was seen over time. However, unlike the temporal patterns seen in the membrane and cytosolic fractions, the changes in nuclear-associated PLC-β1a activity appeared to have a triphasic profile (Fig. 3A and D). In both tissues, activities were reduced (relative to behavioral controls) 1 h after fear conditioning, followed by a significant increase in the 5- to 7-h time range, then another decrease 24 h after training, albeit significant only in the hippocampus, and a return to baseline levels 72 h after conditioning. This unexpected activity profile suggests a great degree of temporal control of nuclear phosphatidylinositols and PtdIns(4,5)P-derived second messenger production. HPF nuclear PLC-β1a concentrations were statistically different at the 5-h time point only (Fig. 3B). However, only the significant decrease in HPF activity at the 1-h time point resulted in a major change in the calculated enzyme specific activity at that time (Fig. 3C). In the MFC, the only significant increase in specific activity was seen at the 5-h time point after conditioning.

Changes in the amount of PLC-β enzyme associated with the nuclear compartment may result from (1) altered metabolism of enzyme already associated with the nucleus, (2) altered targeting of newly synthesized enzyme, or (3) translocation of preexisting enzyme from a nonnuclear compartment (e.g., the cytosol) to the nucleus. We found that the total amount of PLC-β1 in the nuclear fraction is 8- to 10-fold greater than that associated with the cytosolic and membrane fractions, which contain approximately equal amounts of enzyme (data not shown). Further purification of nuclei from the nuclear fractions revealed that, indeed, PLC-β1a is present in nuclei (Weeber et al., 2001). This suggests that a significant increase in the amount of PLC-β1a in the nuclear fraction is not likely to result from translocation of enzyme from the cytosolic or membrane fraction; rather, it may in part be due to altered turnover (translation and catabolism) and/or targeting of newly synthesized protein at early times and the same events, as well as transcriptional events, at later times. This does not discount the possibility of translocation of cytosolic or membrane PLC-β1 to the nucleus; however, it is unlikely

that it would be an amount capable of causing significant changes in nuclear PLC-β1 concentrations.

The amount of data presented here makes an overview of the dynamic temporal-dependent changes and overall trends of subcellular PLC-β1a activities and concentrations difficult to visualize. This becomes a greater challenge when differences in brain tissues are also introduced. To address this limitation, we graphed (Fig. 4) fear-conditioning-dependent changes in PLC-β1a concentrations and activities: [(PTS value/UPC value) × 100%]. This dramatically illustrates the acute increases and decreases in PLC-β1a activities and concentrations in the 0- to 7-h range after fear conditioning. Further, a correlation is seen between temporal fluctuations in PLC-β1a concentrations that are loosely synchronized with PLC-β1a activities. Fig. 4 also demonstrates the differences between HPC and MFC tissues. This may reflect the differences in the dependence on PLC-β1a for the induction of specific pathways for proper memory encoding in the HPF and MFC.

3.5. PLC-β1a may play a role in protein-synthesis-dependent fear-conditioned memory formation

It is a generally held belief that the formation of memories is due, at least in part, to changes in the synaptic strength of specific neuronal pathways (Bailey and Kandel, 1993). Changes in synaptic strength would undoubtedly involve transcription and translation of the necessary proteins to enhance synaptic connections. As noted in the Introduction, several studies have demonstrated that a protein-synthesis-dependent phase of fear-conditioned memory formation exists between 1 and 6 h after training. The demonstration that HPF and MFC PLC-β1a catalytic activity and subcellular distribution are significantly altered during this period (especially 3 and 5 h after conditioning) implicates PLC-β1a as an important component of the signaling pathway(s) involved in transcription- and/or translation-dependent consolidation of fear memories in these two brain regions. These effects of PLC-β1a could result from either direct effects on the translational and transcriptional machinery, or indirect effects mediated by alterations in the levels of the substrates [e.g., PtdIns(4,5)P$_2$] and products [e.g., Ins(1,4,5)P$_3$ and 1,2-diacylglycerols] of the reactions that it catalyzes.

It is important to note that two C-terminal splice variants of PLC-β1 exist: a and b (Bahk et al., 1994). In most studies published to date, effects of treatments (e.g., pharmacologic or molecular) on these two variants have not been distinguished. Thus, it cannot be unequivocally determined whether observed effects are attributable to one or both of these subtypes. In this context, we note that our studies analyzed the PLC-β1a isoform.

PLC-β1 has been shown to couple to receptors (e.g., metabotropic glutamate receptors) known to regulate gene expression and protein synthesis (Mao and Wang, 2003; Raymond et al., 2000). Microinjection of PLC-β1 into
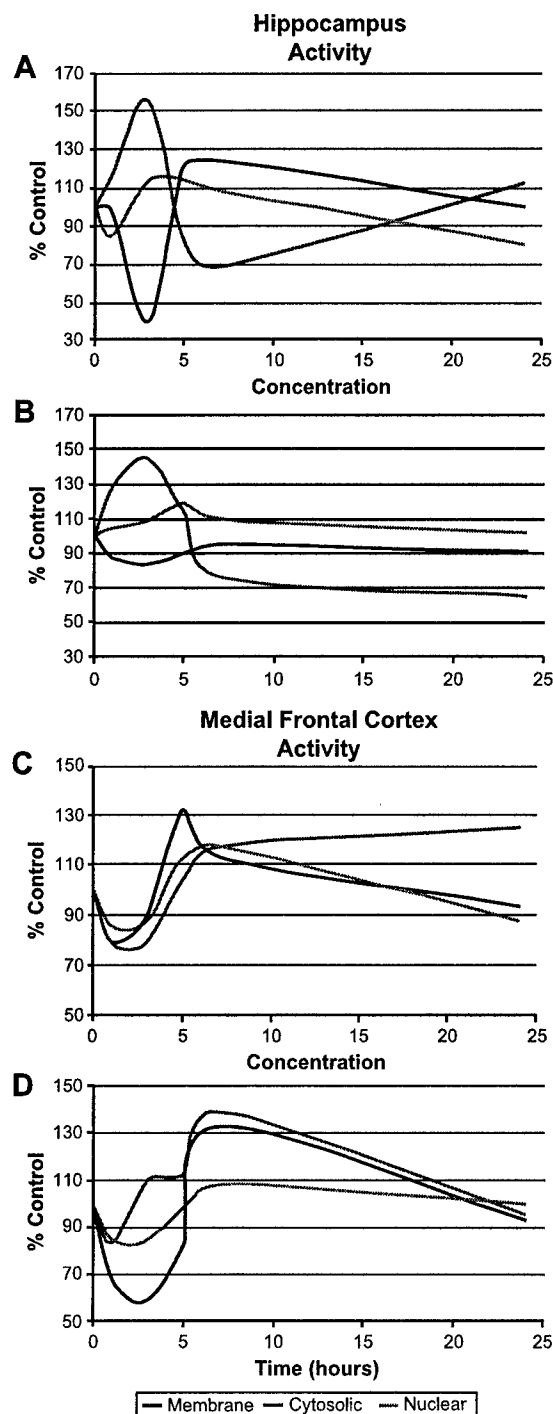
Fig. 4. Comparison of subcellular PLC-β1a activity and concentration profiles from the hippocampus and MFC over time. The percent change of PTS animals compared to the UPC animals at each time point was calculated and graphed. Best fit lines are drawn for changes in HPF PLC-β1a activity (A) and concentration (B), and MFC PLC-β1a activity (C) and concentration (D) for the membrane (blue), cytosolic (red), and nuclear (green) fractions. Time 0 was determined by the average of all time points determined from the UPC group.

quiescent NIH 3T3 cells induces DNA synthesis (Smith et al., 1989). Underexpression of PLC-β1 in Swiss 3T3 cells blocks IGF-1-stimulated DNA synthesis (Manzoli et al., 1997). Overexpression of both PLC-β1a and PLC-β1b reduces expression of the p45/NF-E2 transcription factor in murine erythroleukemia cells (Faenza et al., 2002). Finally, ultrastructural studies of human osteosarcoma Saos-2 cells have shown that PLC-β1 is present in the interchromatin domain and at the interheterochromatin border (Marmiroli et al., 1996; Zini et al., 1996), implicating it in the regulation of gene transcription.

PLC-β1a may regulate transcription and translation as the result of catalyzing the production of Ins(1,4,5)P$_3$ and 1,2-diacylglycerol, which are key regulators of Ca^{2+}-dependent and 1,2-diacylglycerol-dependent protein kinases, respectively. Both of these families of protein kinases have been shown to control transcription and translation (Angenstein et al. 2002; Ventura and Maioli, 2001; West et al., 2001). The potential importance of PLC-β1 in the regulation of gene transcription becomes more compelling in light of work establishing the existence of a nuclear PtdIns(4,5)P$_2$ signaling system (Divecha et al., 1991; Irvine, 2003; Sun et al., 1997).

3.6. Fear-conditioning-dependent regulation of PLC-β1a catalytic activity

Some of the most interesting results to arise from these studies were the cases where changes in enzyme activity could not be accounted for by concurrent changes in enzyme concentrations. In these instances, the calculated specific activity of PLC-β1a was altered. An association between the regulation of the specific activity of a PLC isoform and the formation of a specific memory has not been previously reported. Changes in the calculated enzyme specific activities seen following fear conditioning may be due to direct modification (e.g., phosphorylation) of PLC-β1a, association of the enzyme with an activity-modifying molecule (e.g., G-protein subunit), or changes in enzyme state (e.g., oligomerization). It has been shown that PLC-β1 activity is regulated by protein kinase C (Filtz et al., 1999; Litosch, 1997; Ryu et al., 1990), mitogen-activated protein kinase (Vitale et al., 2001), interaction with G-proteins (Blayney et al., 1996; Boyer et al., 1994; Jhon et al., 1993; Lee et al., 1994), and self-association (Morris and Scarlata, 1997; Paulssen et al., 1998). The mechanisms underlying the observed changes in PLC-β1a specific activity in response to fear conditioning are presently under investigation.

4. Conclusion

In summary, single-trial fear conditioning was found to initiate complex and dynamic temporal changes in PLC-β1a enzyme activities and concentrations associated with the HPF and MFC. These results extend our previous study

(Weeber et al., 2001) and correlate the regulation of PLC-β1a enzyme activity and subcellular distribution and the processes involved in learning and memory formation.

References

Angenstein F, Evans AM, Settlage RE, Moran ST, Ling SC, Klintsova AY, et al. A receptor for activated C kinase is part of messenger ribonucleoprotein complexes associated with poly-mRNAs in neurons. J Neurosci 2002;22:8827–37.

Bahk YY, Lee YH, Lee TG, Seo J, Ryu SH, Suh P-G. Two forms of phospholipase C-β1 generated by alternative splicing. J Biol Chem 1994;269:8240–5.

Bailey CH, Kandel ER. Structural changes accompanying memory storage. Annu Rev Physiol 1993;55:397–426.

Banno Y, Nakashima S, Ohzawa M, Nozawa Y. Differential translocation of phospholipase C isozymes to integrin-mediated cytoskeletal complexes in thrombin-stimulated human platelets. J Biol Chem 1996;271: 14989–94.

Barrientos RM, O'Reilly RC, Rudy JW. Memory for context is impaired by injecting anisomycin into dorsal hippocampus following context exploration. Behav Brain Res 2002;134:299–306.

Bernabeu R, Bevilaqua L, Ardenghi P, Bromberg E, Schmitz P, Bianchin M, et al. Involvement of hippocampal cAMP/cAMP-dependent protein kinase signaling pathways in a late memory consolidation phase of aversively motivated learning in rats. Proc Natl Acad Sci U S A 1997;94:7041–6.

Berridge MJ. Inositol trisphosphate and calcium signalling. Nature 1993; 361:315–25.

Bertagnolo V, Mazzoni M, Ricci D, Carini C, Neri LM, Previati M, et al. Identification of PI-PLC β1, γ1, and δ1 in rat liver: subcellular distribution and relationship to inositol lipid nuclear signalling. Cell Signal 1995;7:669–78.

Bertagnolo V, Marchisio M, Capitani S, Neri LM. Intranuclear translocation of phospholipase C β2 during HL-60 myeloid differentiation. Biochem Biophys Res Commun 1997;235:831–7.

Bevins RA, Ayres JJB. A deficit in one-trial context fear conditioning is not due to opioid analgesia. Pharmacol Biochem Behav 1994;49:183–6.

Blayney LM, Gapper PW, Newby AC. Phospholipase C isoforms in vascular smooth muscle and their regulation by G-proteins. Br J Pharmacol 1996;118:1003–11.

Bourtchuladze R, Abel T, Berman N, Gordon R, Lapidus K, Kandel ER. Different training procedures recruit either one or two critical periods for contextual memory consolidation, each of which requires protein synthesis and PKA. Learn Mem 1998;5:365–74.

Boyer JL, Graber SG, Waldo GL, Harden TK, Garrison JC. Selective activation of phospholipase C by recombinant G-protein α- and βγ-subunits. J Biol Chem 1994;269:2814–9.

Coburn RF, Labelle EF, Griffiths T, Baron CB. Smooth muscle sarcolemma-associated phospholipase C-β2; agonist-evoked translocation. J Cell Physiol 1997;171:271–83.

Davis HP, Squire LR. Protein synthesis and memory: a review. Psychol Bull 1984;96:518–59.

Divecha N, Banfic H, Irvine RF. The polyphosphoinositide cycle exists in the nuclei of Swiss 3T3 cells under the control of a receptor (for IGF-I)

in the plasma membrane, and stimulation of the cycle increases nuclear diacylglycerol and apparently induces translocation of protein kinase C to the nucleus. EMBO J 1991;10:3207–14.

Divecha N, Rhee SG, Letcher AJ, Irvine RF. Phosphoinositide signalling enzymes in rat liver nuclei: phosphoinositidase C isoform $\beta 1$ is specifically, but not predominantly, located in the nucleus. Biochem J 1993; 289:617–20.

Faenza I, Matteucci A, Bavelloni A, Marmiroli S, Martelli AM, Gilmour RS, et al. Nuclear PLCβ_1 acts as a negative regulator of p45/NF-E2 expression levels in Friend erythroleukemia cells. Biochim Biophys Acta 2002;1589:305–10.

Fanselow MS, Bolles RC. Naloxone and shock-elicited freezing in the rat. J Comp Physiol Psychol 1979;93:736–44.

Filtz TM, Cunningham ML, Stanig KJ, Paterson A, Harden TK. Phosphorylation by protein kinase C decreases catalytic activity of avian phospholipase C-β. Biochem J 1999;338:257–64.

Homma Y, Takenawa T, Emori Y, Sorimachi H, Suzuki K. Tissue- and cell type-specific expression of mRNAs for four types of inositol phospholipid-specific phospholipase C. Biochem Biophys Res Commun 1989; 164:406–12.

Igaz LM, Vianna MRM, Medina JH, Izquierdo I. Two time periods of hippocampal mRNA synthesis are required for memory consolidation of fear-motivated learning. J Neurosci 2002;22:6781–9.

Irvine RF. Nuclear lipid signalling. Nat Rev, Mol Cell Biol 2003;4:1–12.

Jhon D-Y, Lee H-H, Park D, Lee C-W, Lee K-H, Yoo OJ, et al. Cloning, sequencing, purification, and G_q-dependent activation of phospholipase C-$\beta 3$. J Biol Chem 1993;268:6654–61.

Kelley GG, Reks SE, Ondrako JM, Smrcka AV. Phospholipase Cϵ: a novel Ras effector. EMBO J 2001;20:743–54.

Laroche S, Redini-Del Negro C, Clements MP, Lynch MA. Long-term activation of phosphoinositide turnover associated with increased release of amino acids in the dentate gyrus and hippocampus following classical conditioning in the rat. Eur J Neurosci 1990;2:534–43.

Lattal KM, Abel T. Different requirements for protein synthesis in acquisition and extinction of spatial preferences and context-evoked fear. J Neurosci 2001;21:5773–80.

Lee SB, Rhee SG. Molecular cloning, splice variants, expression, and purification of phospholipase C-$\beta 4$. J Biol Chem 1996;271:25–31.

Lee C-W, Lee K-H, Lee SB, Park D, Rhee SG. Regulation of phospholipase C-$\beta 4$ by ribonucleotides and the α subunit of G_q. J Biol Chem 1994;269:25335–8.

Litosch I. G-protein $\beta\gamma$ subunits antagonize protein kinase C-dependent phosphorylation and inhibition of phospholipase C-β_1. Biochem J 1997;326:701–7.

Majerus PW, Ross TS, Cunningham TW, Caldwell KK, Jefferson AB, Bansal VS. Recent insights in phosphatidylinositol signaling. Cell 1990;63:459–65.

Manzoli L, Billi AM, Rubbini S, Bavelloni A, Faenza I, Gilmour RS, et al. Essential role for nuclear phospholipase C β_1 in insulin-like growth factor I-induced mitogenesis. Cancer Res 1997;57:2137–9.

Mao L, Wang JQ. Metabotropic glutamate receptor 5-regulated Elk-1 phosphorylation and immediate early gene expression in striatal neurons. J Neurochem 2003;85:1006–17.

Marmiroli S, Zini N, Bavelloni A, Faenza I, Ognibene A, Maraldi NM. Transfected Saos-2 cells overexpressing phosphoinositidase C β_1 isoform accumulate it within the nucleus. Biol Cell 1996;86:121–6.

Morgan MA, LeDoux JE. Differential contribution of dorsal and ventral medial prefrontal cortex to the acquisition and extinction of conditioned fear in rats. Behav Neurosci 1995;109:681–8.

Morris AJ, Scarlata S. Regulation of effectors by G-protein α- and $\beta\gamma$-subunits. Recent insights from studies of the phospholipase C-β isozymes. Biochem Pharmacol 1997;54:429–35.

Morrow BA, Elsworth JD, Inglis FM, Roth RH. An antisense oligonucleotide reverses the footshock-induced expression of Fos in the rat medial prefrontal cortex and the subsequent expression of conditioned fear-induced immobility. J Neurosci 1999;19:5666–73.

Nishizuka Y. The protein kinase C family and lipid mediators for transmembrane signaling and cell regulation. Alcohol, Clin Exp Res 2001;25(5 Suppl):3S–7S.

Paulssen RH, Woodson J, Liu Z, Ross EM. Carboxyl-terminal fragments of phospholipase C-$\beta 1$ with intrinsic Gq GTPase-activating protein (GAP) activity. J Biol Chem 1998;271:26622–9.

Quevedo J, Vianna MRM, Roesler R, de-Paris F, Izquierdo I, Rose SPR. Two time windows of anisomycin-induced amnesia for inhibitory avoidance training in rats: protection from amnesia by pretraining but not pre-exposure to the task apparatus. Learn Mem 1999;6:600–7.

Raymond CR, Thompson VL, Tate WP, Abraham WC. Metabotropic glutamate receptors trigger homosynaptic protein synthesis to prolong long-term potentiation. J Neurosci 2000;20:969–76.

Rhee SG. Regulation of phosphoinositide-specific phospholipase C. Annu Rev Biochem 2001;70:281–312.

Ross CA, MacCumber MW, Glatt CE, Snyder SH. Brain phospholipase C isozymes: differential mRNA localizations by in situ hybridization. Proc Natl Acad Sci U S A 1989;86:2923–7.

Ryu SH, Kim UH, Wahl MI, Brown AB, Carpenter G, Huang KP, et al. Feedback regulation of phospholipase C-β by protein kinase C. J Biol Chem 1990;265:17941–5.

Sacchetti B, Baldi E, Lorenzini CA, Bucherelli C. Differential contribution of some cortical sites to the formation of memory traces supporting fear conditioning. Exp Brain Res 2002;146:223–32.

Sanders MJ, Wiltgen BJ, Fanselow MS. The place of the hippocampus in fear conditioning. Eur J Pharmacol 2003;463:217–23.

Smith MR, Ryu S-H, Suh P-G, Rhee S-G, Kung H-F. S-phase induction and transformation of quiescent NIH 3T3 cells by microinjection of phospholipase C. Proc Natl Acad Sci U S A 1989;86:3659–63.

Smrcka AV, Sternweis PC. Regulation of purified subtypes of phosphatidylinositol-specific phospholipase C β by G protein α and $\beta\gamma$ subunits. J Biol Chem 1993;268:9667–74.

Stiedl O, Palve M, Radulovic J, Birkenfeld K, Spiess J. Differential impairment of auditory and contextual fear conditioning by protein synthesis inhibition in C57BL/6N mice. Behav Neurosci 1999;113:496–506.

Sun B, Murray NR, Fields AP. A role for nuclear phosphatidylinositol-specific phospholipase C in the G_2/M phase transition. J Biol Chem 1997;272:26313–7.

Takenawa T, Homma Y, Emori Y. Properties of phospholipase C isozymes. Methods Enzymol 1991;197:511–8.

Ventura C, Maioli M. Protein kinase C control of gene expression. Crit Rev Eukaryot Gene Expr 2001;11:243–67.

Vitale M, Matteucci A, Manzoli L, Rodella L, Mariani AR, Zauli G, et al. Interleukin 2 activates nuclear phospholipase Cβ by mitogen-activated protein kinase-dependent phosphorylation in human natural killer cells. FASEB J 2001;15:1789–91.

Wahl MI, Jones GA, Nishibe S, Rhee SG, Carpenter G. Growth factor stimulation of phospholipase C-$\gamma 1$ activity. Comparative properties of control and activated enzymes. J Biol Chem 1992;267:10447–56.

Watanabe M, Nakamura M, Sato K, Kano M, Simon MI, Inoue Y. Patterns of expression for the mRNA corresponding to the four isoforms of phospholipase Cβ in mouse brain. Eur J Neurosci 1998;10:2016–25.

Weeber EJ, Savage DD, Sutherland RJ, Caldwell KK. Fear conditioning-induced alterations of phospholipase C-$\beta 1$a protein level and enzyme activity in rat hippocampal formation and medial frontal cortex. Neurobiol Learn Mem 2001;76:151–82.

West AE, Chen WG, Dalva MB, Dolmetsch RE, Kornhauser JM, Shaywitz AJ, et al. Calcium regulation of neuronal gene expression. Proc Natl Acad Sci U S A 2001;98:11024–31.

Williams RL. Mammalian phosphoinositide-specific phospholipase C. Biochim Biophys Acta 1999;1441:255–67.

Zini N, Sabatelli P, Faenza I, Ognibene A, Maraldi NM. Interleukin-1α induces variations of the intranuclear amount of phosphatidylinositol 4,5-bisphosphate and phospholipase C β_1 in human osteosarcoma Saos-2 cells. Histochem J 1996;28:495–504.

Fear conditioning is associated with altered integration of PLC and ERK signaling in the hippocampus

Colin T. Buckley and Kevin K. Caldwell
Department of Neurosciences
University of New Mexico School of Medicine
Albuquerque, NM

Proofs should be sent to:
Kevin K. Caldwell
Department of Neurosciences
MSC08 4740
1 University of New Mexico
Albuquerque, NM 87131-0001

Corresponding author's information:
Telephone: 505-272-0033
Fax: 505-272-8082
e-mail: kcaldwell@salud.unm.edu

Running title: PLC – ERK2 interactions

ABSTRACT

The extracellular signal-regulated protein kinases (ERKs) are proline-directed, serine/threonine kinases that regulate a variety of cellular functions, including proliferation, differentiation, and plasticity. In the present report, we provide evidence that ERK2 and phosphatidylinositol-specific phospholipase C (PLC)-β and -γ isozymes interact in the rat hippocampal formation. We found that anti-PLC-β1a, -β2, -β4, -γ1 and –γ2, but not –β3, immune complexes isolated from rat hippocampal formation postnuclear fractions contain anti-ERK2 immunoreactivity. Further, we show that PLC catalytic activity is associated with anti-ERK2 immunoprecipitates isolated from the hippocampal formation, and that the amount of enzyme activity is significantly increased following fear-conditioned learning. The observed interactions may be mediated by consensus sequences conforming to an ERK2 docking site, termed a D-domain, that we identified in PLC-β1a, -β2, -β4 -γ1 and -γ2. Based on these results, we propose that PLC-β and PLC-γ isozymes form signaling complexes with ERK2 in rat brain, and these complexes play critical roles in learning and memory, as well as a variety of other neuronal functions.

Key words: docking, hippocampal formation, PLC, MAPK, fear conditioning

INTRODUCTION

Cells possess a variety of means to integrate diverse extracellular stimuli into coordinated cellular responses. Both direct and indirect interactions between the components of signal transduction pathways are important means of signal integration (Pawson and Nash 2000). Several published studies reveal that there is substantial crosstalk between phosphatidylinositol-specific phospholipase C (PLC)-dependent and mitogen-activated protein kinase (MAPK)-dependent signaling systems in cells. Three of these studies demonstrate that direct, protein-protein interactions between components of these pathways can occur: Xu et al. (2001) found that PLC-β1 associates with both extracellular signal-regulated protein kinase 1 (ERK1) and ERK2 in cells over-expressing PLC-β1, Barr et al. (2002) demonstrated that PLC-β2 binds to p38 protein kinase, and we have shown that PLC-γ1 directly binds to ERK2 (Buckley et al. 2004). In the present studies we tested the hypothesis that PLC-β and PLC-γ isozymes interact with ERK2 in rat brain.

ERKs comprise one of the major families of MAPKs; c-Jun amino-terminal kinases (JNKs, also called stress-activated protein kinases) and p38 stress-activated protein kinases are the other major families of MAPKs. Multiple members of the ERK family have been cloned (Pearson et al. 2001, Johnson and Lapadat 2002); of these, ERK1 and ERK2 are the most abundant in brain. Although ERK1 and ERK2 possess high sequence homology (90% identical; Boulton et al. 1991), they display similar, but distinct, subcellular distributions in the rat forebrain (Suzuki et al. 1995), they perform unique roles in synaptic functioning (Mazzucchelli et al. 2002), and disruption of the mouse ERK2 gene produces embryonic lethality (Hatano et al. 2003), whereas ERK1 knockout

3

mice are viable (Mazzucchelli et al 2002). We chose to focus our studies on hippocampal formation ERK2, which has shown to play a prominent role in synaptic plasticity (English and Sweatt 1997, Davis et al. 2000, Watabe et al. 2000, Selcher et al. 2003 Ying et al. 2002) and processes important for spatial and associative learning (Selcher et al. 1999, Atkins et al. 1998, Sweatt 2001).

PLC isozymes catalyze the hydrolysis of phosphatidylinositol 4,5-bisphosphate (PtdIns(4,5)P$_2$), into the important intracellular messengers, inositol 1,4,5-trisphosphate (Ins(1,4,5)P$_3$, "IP$_3$") and 1,2-diacylglycerol (1,2-DAG) (Majerus et al. 1990; Williams 1999). Eleven distinct mammalian PLC isozymes, with multiple subtypes, and in some instances splice variants of these subtypes, have been identified (Rhee 2001). These 11 PLC isozymes have been grouped into four types: PLC-β, PLC-δ, PLC-γ, and PLC-ϵ. Each of the known PLC-β (Watanabe et al. 1998) and PLC-γ (Homma et al. 1989) isozymes has been reported to be present in brain. Growing evidence implicates PLC isozymes as important components of signal transduction processes involved in brain functioning. Several lines of research indicate that PLC-β1 may participate in various forms of synaptic plasticity, including fear-conditioned learning and memory (see Weeber et al. 2001 and references therein). To our knowledge, there are no published studies that have implicated PLC-β2 in brain functioning. PLC-β3 has been reported to play a role in μ-opioid receptor-dependent responses (Xie et al. 1999). PLC-β4 coupling to metabotropic glutamate receptors in the cerebellum (Kim et al. 1997) may account for its role in delay eyeblink conditioning and cerebellar synaptic plasticity (Kishimoto et al. 2001; Miyata et al. 2001). PLC-γ isozymes have been implicated in the control of various

4

neuronal responses, including neuronal plasticity (Minichiello et al. 2002) and nerve growth cone guidance (Ming et al. 1999).

In the present studies, we found that PLC-β and PLC-γ isozymes interact with ERK2 in the rat hippocampal formation. This interaction is a mechanism through which PLC- and ERK2-dependent signaling may be integrated. Further, we provide evidence that the interaction of PLC and ERK2 may play an important role in hippocampal-dependent learning and memory.

MATERIALS AND METHODS

Animals

Female Sprague-Dawley rats (150-200 days old) were maintained as described in Weeber et al. (2001). The rats were given unlimited access to standard rat chow and tap water. All procedures employed for the housing, handling, fear conditioning and sacrificing of rats were approved by the University of New Mexico Health Sciences Center Laboratory Animal Care and Use Committee

Tissue preparation and subcellular fractionation

Rats were sacrificed by decapitation. The hippocampal formations were rapidly removed and were homogenized in 1.5mL of ice-cold homegenization buffer (HB): 20 mM Tris-HCl, pH 7.4, 1mM EDTA, 320 mM sucrose, 40 µg leupeptin/mL, 20 µg aprotonin/mL, 30 µM calpain inhibitor III, 0.5 mM AEBSF, and 200 µM sodium orthovanadate, as described in Weeber et al. (2001). Hippocampal formation homogenates were frozen in liquid nitrogen, and stored at −80°C for further fractionation. The homogenates were thawed, and then centrifuged (1,000 xg, 7 min, 4°C). The supernatant was decanted; the pellet was resuspended in 0.5 mL HB, homogenized and centrifuged as before. The supernatant was combined with the supernatant from the first centrifugation to form the S1 fraction, and centrifuged (200,000 x g, 30 min, 4°C.). The soluble (S2) fraction was decanted and the pellet (P2) fraction was resuspended in 500 µL of extraction buffer [HB supplemented with 75 mM NaCl, 75 mM KCl, and 1% (v/v) Triton X-100], homogenized as described above, and stored on ice. After 20 minutes, the mixture was spun (200,000 x g, 20 min, 4°C). The Triton X-100 soluble material (herein referred to as the "P2"

fraction) was decanted, aliquoted into storage tubes, frozen in liquid nitrogen, and stored at -80°C until further use. Protein determinations were performed as described in Weeber et al. (2001).

Immunoprecipitation

Anti-PLC isozyme immune complexes were isolated as follows. Hippocampal formation P2 preparations (100 µg protein) were incubated with 6 µg of rabbit anti-PLC isozyme antibody overnight with mixing at 4°C. The immune complexes were recovered with protein A – Sepharose beads as described in Weeber et al. (2001) and washed twice with 1 mL of extraction buffer. Anti-ERK2 immune complexes were isolated as follows. Fifteen µg of rat hippocampal formation P2 proteins were incubated with 4 µg of mouse anti-ERK2 antibody. Immune complexes were recovered using 100 µL protein A – Sepharose beads and washed twice with 1.25X PLC activity assay buffer.

Immunoblotting

Anti-ERK2 immunoreactivity associated with anti-PLC immune complexes was measured as follows. Immune complexes were released from the beads by adding 50 µL of 2X SDS-PAGE sample buffer (125 mM Tris, pH 6.8, 0.005 % bromophenol blue, 100 mM DTT, 17.5 % glycerol, 4.0 % SDS) and boiling for 5 minutes. Eluted proteins were separated using 7.5% SDS PAGE gels prior to transfer to polyvinylidene fluoride (PVDF) membranes. Membranes were blocked in 5% (w/v) fat-free milk in Tris buffered saline (TBS), and blotted with mouse anti-ERK2 (1:1000) antibody, or mouse anti-phospho-ERK1/2 (1:2000) antibody followed by anti-mouse horseradish peroxidase-

conjugated (1:20,000) antibody. The immunoreactive proteins were detected using enhanced chemiluminescene from Amersham Pharmacia Biotech, Inc (Piscataway, NJ).

In vitro treatment of anti-PLC immune complexes with phospho-ERK2

Biotinylated goat anti-rabbit IgG (100 µl of 10.0 µg IgG/mL PBS) was coated onto a streptavidin coated well, using 8-well strips. Each strip was incubated overnight at 4°C, and then washed three times with PBS at room temperature (5 min each). Rabbit anti-PLC-β1a, PLC-β4, and PLC-γ2 were diluted in PBS to a concentration of 2 µg/mL and incubated (100 µL per well) with the biotinylated goat anti-rabbit IgG-coated streptavidin strips overnight at 4°C. Control wells were processed in a similar fashion except normal rabbit IgG (2 µg/mL) was substituted for anti-PLC antibody. The next day, the strips were washed with PBS three times (for five minutes) at room temperature. Hippocampal P2 fraction extracts were diluted with PBS to a final concentration of 30 µg/100 µL, added to each well, and incubated overnight at 4°C. Unbound proteins were removed with three washes with PBS (5 min per wash). Captured PLC was treated (20 min, 35 °C) with one of the following: 1) Assay Dilution Buffer I (ADBI): 20 mM [3-(N-Morpholino)propanesulfonic acid], pH 7.2, 25mM β-glycerol phosphate, 5mM EGTA, 1mM sodium orthovanadate, 1mM dithiothreitol, 20µM PKC inhibitor peptide, 2µM PKA inhibitor peptide, and 20 µM Compound R24571; 2) ADBI with 90 µM ATP, 13.5 mM MgCl$_2$; 3) ADBI with 0.4 U of recombinant phospho-ERK2 (Upstate Biotechnology); 4) ADBI containing 0.4 U of recombinant phospho-ERK2 and 90 µM ATP, 13.5 mM MgCl$_2$. Next, the wells were washed three times (5 minutes each at room temperature) with 1.25X PLC assay buffer (43.75 mM sodium phosphate, pH 6.8, 87.5

8

mM KCl, 1.0 mM EGTA, 1.0 mM $CaCl_2$) prior to quantification of PLC activity (see below).

Immune complex PLC activity measurement

Immune complex-associated PLC activities were quantified as described in Buckley and Caldwell (2003). Activity was calculated as nmol (or pmol) $Ins(1,4,5)P_3$ product formed / min / mg protein present within the well from which the enzyme was affinity captured.

Fear conditioning

One trial, delay fear conditioning was performed essentially as described by Weeber et al. (2001) except that the conditioning apparatus was a Habitest System equipped with a Precision Regulated Shocker (Coulbourn Instruments, Allentown, PA). Rats were randomly assigned to either the one-trial fear-conditioned (paired tone-shock, PTS) group or the unpaired control (UPC) group. Thirty minutes following shock delivery, rats were sacrificed, their hippocampal formation was removed, and the postnuclear particulate (P2) fraction was isolated as described above.

Materials

Rabbit polyclonal antibodies against PLC-β1a, -β2, -β3, -β4a, -γ1, and -γ2, mouse monoclonal antibody to ERK2, goat polyclonal antibodies against ERK1, and biotinylated goat anti-rabbit IgG were purchased from Santa Cruz Biotechnology, Inc. (Santa Cruz, CA). HRP labeled goat anti-mouse IgG secondary antibody and [^{3}H] $PtdIns(4,5)P_2$ were purchased from PerkinElmer Life Sciences (Boston, MA). Mouse monoclonal anti-phospho-ERK1/2 antibody was purchased from Cell Signaling Technology (Beverly, MA. Streptawells®, streptavidin coated microtiter plates and Triton X-100 were purchased from Roche Applied Science (Indianapolis, IN). SDS-

PAGE gels and buffers and PVDF membranes were from BioRad Laboratories (Hercules, CA). Protein A-Sepharose CL-4B and ECL Plus Western Blotting Detection System were obtained from Amersham Pharmacia Biotech, Inc (Piscataway, NJ). Leupeptin, AEBSF, aprotinin, calpain inhibitor III, and recombinant, activated and non-activated ERK2 from rat, were purchased from Calbiochem (San Diego, CA). All other chemicals and supplies were purchased from commercial sources.

RESULTS

ERK2 co-immunoprecipitates with PLCs

In order to test the hypothesis that PLC-β and -γ isozymes associate with ERK2 in rat brain, anti-PLC-β and anti-PLC-γ immune complexes were isolated from rat hippocampal formation postnuclear membrane (P2) extracts and probed for anti-ERK2 immunoreactivity. We found that ERK2 co-immunoprecipitated with PLC-β1a, -β2, -β4 (Figure 1A), -γ1 and -γ2 (Figure 1B). In contrast, the amount of anti-ERK2 immunoreactivity associated with anti-PLC-β3 immunoprecipitates (Figure 1A) was not different from the background (i.e., IgG control). When anti-PLC-β and PLC-γ immunoprecipitates were probed for anti-ERK1 immunoreactivity, no signals were detected, whereas anti-phospho-ERK1/2 immunoreactivities were minimal, or no signals were detected (data not shown).

Fear conditioning increases the amount of PLC activity associated with anti-ERK2 immunoprecipitates

We questioned whether associations between ERK2 and PLC isozymes are changed by physiologic stimuli that signal through ERK-dependent pathways. ERK2 has been implicated as important for learning and memory in several paradigms, including contextual fear conditioning (Atkins et al., 1998); thus, we sought to determine whether one-trial, delay fear conditioning exerted an effect on PLC-ERK2 interactions. Anti-ERK2 immune complexes were isolated from the hippocampal formation of rats that had either undergone one-trial fear conditioning (paired tone-shock, PTS) or an "unpaired" control (UPC) paradigm, and assayed for associated PLC activity (Figure 2A). First, it

11

should be noted that these results demonstrate that one or more of the PLCs associated with anti-ERK2 immunoprecipitates were catalytically active. Further, 30 minutes following fear conditioning there was a significant increase in the amount of PLC activity associated with ERK2 (Figure 2B). We have obtained similar results in studies employing anti-ERK2 immune complexes isolated from mouse hippocampal formation P2 fraction 30 minutes following fear conditioning or a behavioral control (immediate shock) procedure (data not shown).

In vitro treatment of affinity captured phospholipase C β1a, β4, and γ2 with phospho-ERK2

We sought to determine whether phospho-ERK2 treatment exerted an effect on PLC lipase activity. Affinity purified phospholipase C-β1a, -β4, and -γ2 were incubated under conditions that allowed for substrate phosphorylation (i.e., in the presence of Mg^{2+} and ATP), or not, prior to measuring the catalytic activity of each isozyme. *In vitro* treatment of anti-PLC-β1 (Figure 3A) and anti-PLC-β4 (Figure 3B) immune complexes with phospho-ERK2 in the absence of Mg^{2+}-ATP did not alter phospholipase activity, whereas the same treatment of anti-PLC-γ2 (Figure 3C) immune complexes reduced PLC activity. Incubation of both anti-PLC-γ2 and anti-PLC-β4 immune complexes with Mg^{2+}-ATP stimulated lipase activity. This is similar to results that we reported for anti-PLC-γ1 immune complexes (Buckley and Caldwell 2003). Treatment of captured PLC-γ2 and PLC-β4 with phospho-ERK2 and Mg^{2+}-ATP opposed this ATP-dependent stimulation. PLC-β2 demonstrated only negligible lipase activity under the conditions used in these assays; therefore, the affect of phospho-ERK2 could not be reliably assed. Phospho-

ERK2-dependent regulation of PLC-γ1 enzyme activity is addressed in a separate report (Buckley et al. 2004).

Identification of MAPK docking motifs in PLC isozymes

The identification of sequence motifs that mediate protein-protein interactions, when combined with available protein amino acid sequence data, allows for the identification of putative protein binding pairs. Two ERK-binding motifs have been identified by Kornfeld and colleagues (Jacobs et al. 1999; Fantz et al. 2001): 1) the FXFP motif, having the consensus sequence of F-X-F-P, and 2) the D-domain motif, having two possible consensus sequences: either (K/R)-X-(X/K/R)-(K/R)-X$_{(1-4)}$-(L/I)-X-(L/I) or (K/R)-(K/R)-(K/R)-X$_{(1-5)}$-(L/I)-X-(L/I). We searched PLC-β, PLC-γ, PLC-δ and PLC-ε isozymes for amino acid sequences that fit these consensus sequences and found that PLC-β1, -β2, -β4, -γ1, -γ2, -δ1, -δ3, and -ε each contain at least one putative D-domain, while PLC-β3 is the only isozyme in which we identified an FXFP motif (Table 1).

DISCUSSION

We have made several important observations in these studies. First, we demonstrated that ERK2 associates with PLC-β1a, -β2, -β4, -γ1 and –γ2 isozymes in the rat hippocampal formation. Previously, Xu et al. (2001) demonstrated that, in 3T3 cells overexpressing PLC-β1, an association between ERK2 and PLC-β1 could be detected. We found that the association is not specific for PLC-β1, but also occurs with other PLC-β, as well as PLC-γ isozymes. Further, this interaction is not unique to PLC-β1 within the nucleus, as reported by Xu et al. (2001). Second, we were unable to detect an association between any of the PLC-β or -γ isozymes and ERK1. This result is in contrast to results of Xu et al. (2001), who reported that PLC-β1 was associated with phospho-ERK1. Our studies indicate that either ERK2 and ERK1 differ in their affinities for PLC isozymes or ERK1 and PLC isozymes are differentially compartmentalized in the rat hippocampal formation. Third, the finding that there was an increase in the amount of PLC activity associated with anti-ERK2 immunoprecipitates following fear-conditioned learning indicates that the association of ERK2 and PLC isozymes is of physiologic significance. Fourth, ATP-stimulated PLC-γ2 lipase activity is completely reversed in the presence of phospho-ERK2. The simplest explanation for this observation is that it is an effect that is secondary to phospho-ERK2-catalyzed phosphorylation of PLC-γ2. However, we have found that PLC-γ2 is a relatively poor *in vitro* substrate for phospho-ERK2, at least under conditions that allow for the robust phosphorylation of PLC-γ1 (Buckley et al. 2004). These results support, instead, a mechanism in which phospho-ERK2 either indirectly regulates PLC-γ2 enzyme activity (e.g., secondary to effects on one or more regulatory

14

proteins, such as a protein kinase, that are associated with the anti-PLC-γ2 immune complex) or directly regulates PLC-γ2 catalytic activity by a phosphorylation-independent mechanism. This latter proposal is supported by the observation that the effect of phospho-ERK2 was observed in the absence of Mg^{2+}-ATP (Figure 3C) and by reports showing that ERKs regulate the catalytic activity of other enzymes (e.g., MAPK phosphatase-3, Camps et al. 1998; phosphotyrosine-specific phosphatase PTP-SL, Buschbeck et al. 2002) by a mechanism that is dependent on direct interaction between ERK and the phosphatase, but is independent of ERK catalytic activity. Finally, employing consensus sequences reported by Kornfeld and colleagues (Jacobs et al. 1999; Fantz et al. 2001), we identified putative ERK2 binding sites in nine of the 11 known types of PLC. These identifications have not previously been reported.

We have not yet identified which PLC isozyme(s) underlies the observed increase in ERK2-associated PLC activity in fear-conditioned animals. Preliminary experiments have shown that the amount of particulate-associated ERK2-PLC-γ2 complex is significantly increased 30 minutes following fear conditioning, implicating PLC-γ2 as an important contributor to the observed increase in ERK2-associated PLC activity (data not shown).

We identified D-domain sequences in PLC isozymes employing consensus sequences defined by Kornfeld and colleagues (Jacobs et al. 1999; Fantz et al. 2001). Other investigators (e.g., Pearson et al. 2001) have identified different, but similar, docking motifs for MAPKs. In general, binding motifs for MAPKs are composed of approximately 20 amino acids. In contrast to specifying consensus sequences, Sharrocks and colleagues (Barsyte-Lovejoy et al. 2002) have proposed models for MAPK docking

15

domains that define regions of sequence similarity: basic, LXL, hydrophobic. These regions play differing roles in determining specificity for interactions with ERK, JNK and p38 family members. Each of the D-domains that we identified consists of a basic region and an L-X-L motif. Further, an adjacent hydrophobic region is readily identifiable in several PLC isozymes (e.g., PLC-γ1, ^{953}LVV; PLC-γ2, ^{187}VSGI). Thus, it is possible that, in addition to binding ERK2, the D-domains of PLC isozymes bind MAPKs belonging to the p38 and/or JNK families. We have begun studies aimed at addressing this possibility. In support of this proposal is the demonstration by Barr et al (2002) that p38 binds to PLC-β2. The PLC-β2 D-domain that we identified is within the portion of PLC-β2 that they identified (amino acids 774-1181) as mediating the interaction. Differential coupling of PLC-β and PLC-γ isozymes to members of the MAPK family could explain how different cellular responses (e.g., growth, differentiation, apoptosis, neurite outgrowth) are elicited by enzymes (i.e., PLC isozymes) that perform the same catalytic function (i.e., Ins(1,4,5)P$_3$ and DAG production). The formation of PLC-MAPK signaling complexes is likely to facilitate, and restrict, the transduction of PLC-dependent signals to specific MAPK signaling pathways. Peptide versions of these docking sites may prove to be important pharmacologic tools in the treatment of a variety of diseases.

In conclusion, we provide evidence that PLC-β and PLC-γ isozymes interact with ERK2 in rat hippocampal formation. These interactions may play an important role in hippocampal-dependent learning and memory. These studies provide the basis to hypothesize that behavioral challenge elicits spatial and temporal alterations in the

integration of PLC- and ERK-dependent signaling in the rat brain, and that errors in the

coordination of these signals may lead to cognitive and behavioral impairments.

ACKNOWLEDGEMENTS

REFERENCES

Atkins, C. M.; Selcher, J. C.; Petraitis, J. J.; Trzaskos, J. M.; Sweatt, J. D. The MAPK cascade is required for mammalian associative learning. Nat.Neurosci. 1: 602-609; 1998.

Barr, A. J.; Marjoram, R.; Xu, J.; Snyderman, R. Phospholipase C-beta 2 interacts with mitogen-activated protein kinase kinase 3. Biochem.Biophys.Res.Commun. 293: 647-652; 2002.

Barsyte-Lovejoy, D.; Galanis, A.; Sharrocks, A. D. Specificity determinants in MAPK signaling to transcription factors. J.Biol.Chem. 277: 9896-9903; 2002.

Boulton, T. G.; Nye, S. H.; Robbins, D. J.; Ip, N. Y.; Radziejewska, E.; Morgenbesser, S. D.; DePinho, R. A.; Panayotatos, N.; Cobb, M. H.; Yancopoulos, G. D. ERKs: a family of protein-serine/threonine kinases that are activated and tyrosine phosphorylated in response to insulin and NGF. Cell 65: 663-675; 1991.

Buckley, C.T. and Caldwell, K.K. (2003) Two-layer antibody capture of enzymes on the surface of microtiter plates: application to the study of the regulation of phospholipase C-γ1 catalytic activity Anal. Biochem. 320: 193-198.

Buckley, C.T., Sekiya, F., Kim, Y.J., Rhee, S.G., Caldwell K.K. (2004) Identification of phospholipase C-γ1 as a mitogen-activated protein kinase substrate. J. Biol. Chem. 279, 41807-41814.

Buschbeck, M., Eickhoff, J., Sommer, M. N., Ullrich, A. Phosphotyrosine-specific phosphatase PTP-SL regulates the ERK5 signaling pathway. J. Biol. Chem. 277: 29503-29509; 2002.

19

Camps, M., Nichols, A., Gillieron, C., Antonsson, B., Muda, M., Chabert, C., Boschert, U., Arkinstall, S. Catalytic activation of the phosphatase MKP-3 by ERK2 mitogen-activated protein kinase. Science 280: 1262-1265; 1998.

Davis, S., Vanhoutte, P., Pagès, C., Caboche, J., Laroche, S. The MAPK/ERK cascade targets both Elk-1 and cAMP response element-binding protein to control long-term potentiation-dependent gene expression in the dentate gyrus *in vivo*. J. Neurosci. 20: 4563-4572; 2000.

English, J.D., Sweatt, J.D. A requirement for the mitogen-activated protein kinase cascade in hippocampal long term potentiation. J. Biol. Chem. 272: 19103-19106; 1997.

Fantz, D. A.; Jacobs, D.; Glossip, D.; Kornfeld, K. Docking sites on substrate proteins direct extracellular signal-regulated kinase to phosphorylate specific residues. J.Biol.Chem. 276: 27256-27265; 2001.

Hatano, N., Mori, Y., Oh-hora, M., Kosugi, A., Fujikawa, T., Nakai, N., Niwa, H., Miyazaki, J. Hamaoka, T., Ogata, M. Essential role for ERK2 mitogen-activated protein kinase in placental development. Genes Cells. 8:847-856; 2003.

Homma, Y.; Takenawa, T.; Emori, Y.; Sorimachi, H.; Suzuki, K. Tissue- and cell type-specific expression of mRNAs for four types of inositol phospholipid-specific phospholipase C. Biochem.Biophys.Res.Commun. 164: 406-412; 1989.

Jacobs, D.; Glossip, D.; Xing, H.; Muslin, A. J.; Kornfeld, K. Multiple docking sites on substrate proteins form a modular system that mediates recognition by ERK MAP kinase. Genes Dev. 13: 163-175; 1999.

20

Johnson, G. L.; Lapadat, R. Mitogen-activated protein kinase pathways mediated by ERK, JNK, and p38 protein kinases. Science 298: 1911-1912; 2002.

Kim, D.; Jun, K. S.; Lee, S. B.; Kang, N. G.; Min, D. S.; Kim, Y. H.; Ryu, S. H.; Suh, P. G.; Shin, H. S. Phospholipase C isozymes selectively couple to specific neurotransmitter receptors. Nature 389: 290-293; 1997.

Kishimoto, Y.; Hirono, M.; Sugiyama, T.; Kawahara, S.; Nakao, K.; Kishio, M.; Katsuki, M.; Yoshioka, T.; Kirino, Y. Impaired delay but normal trace eyeblink conditioning in PLCbeta4 mutant mice. Neuroreport 12: 2919-2922; 2001.

Lee, S. B., Rhee, S. G. Molecular cloning, splice variants, expression, and purification of phospholipase C-δ4. J. Biol. Chem. 271: 25-31; 1996.

Majerus, P. W.; Ross, T. S.; Cunningham, T. W.; Caldwell, K. K.; Jefferson, A. B.; Bansal, V. S. Recent insights in phosphatidylinositol signaling. Cell 63: 459-465; 1990.

Mazzucchelli, C., Vantaggiato, C., Ciamei, A., Fasano, S., Pakhotin, P., Krezel, W., Welzl, H., Wolfer, D. P., Pagès, G., Valverde, O., Marowsky, A., Porrazzo, A., Orban, P.C., Maldonado, R., Ehrengruber, M. U., Cestari, V., Lipp, H.-P., Chapman, P. F., Pouysségur, J., Brambilla, R. Knockout of ERK1 MAP kinase enhances synaptic plasticity in the striatum and facilitates striatal-mediated learning and memory. Neuron 34: 807-820; 2002.

Ming, G.; Song, H.; Berninger, B.; Inagaki, N.; Tessier-Lavigne, M.; Poo, M. Phospholipase C-gamma and phosphoinositide 3-kinase mediate cytoplasmic signaling in nerve growth cone guidance. Neuron 23: 139-148; 1999.

Minichiello, L.; Calella, A. M.; Medina, D. L.; Bonhoeffer, T.; Klein, R.; Korte, M. Mechanism of TrkB-mediated hippocampal long-term potentiation. Neuron 36: 121-137; 2002.

Miyata, M.; Kim, H. T.; Hashimoto, K.; Lee, T. K.; Cho, S. Y.; Jiang, H.; Wu, Y.; Jun, K.; Wu, D.; Kano, M.; Shin, H. S. Deficient long-term synaptic depression in the rostral cerebellum correlated with impaired motor learning in phospholipase C beta4 mutant mice. Eur.J.Neurosci. 13: 1945-1954; 2001.

Pawson, T., Nash, P. Protein-protein interactions define specificity in signal transduction. Genes Dev. 14: 1027-1047; 2000.

Pearson, G.; Robinson, F.; Beers, G. T.; Xu, B. E.; Karandikar, M.; Berman, K.; Cobb, M. H. Mitogen-activated protein (MAP) kinase pathways: regulation and physiological functions. Endocr.Rev. 22: 153-183; 2001.

Rhee, S. G. Regulation of phosphoinositide-specific phospholipase C. Annu.Rev.Biochem. 70: 281-312; 2001.

Selcher, J. C., Atkins, C. M., Trzaskos, J. M., Paylor, R., Sweatt, J.D. A necessity for MAP kinase activation in mammalian spatial learning. Learn. Mem. 6: 478-490; 1999.

Selcher, J. C., Weeber, E. J., Christian, J., Nekrasova, T., Landreth, G. E., Sweatt, J. D. A role for ERK MAP kinase in physiologic temporal integration in hippocampal area CA1. Learn. Mem. 10: 26-39; 2003.

Suzuki, T.; Okumura-Noji, K.; Nishida, E. ERK2-type mitogen-activated protein kinase (MAPK) and its substrates in postsynaptic density fractions from the rat brain. Neurosci.Res. 22: 277-285; 1995.

Sweatt, J. D. The neuronal MAP kinase cascade: a biochemical signal integration system subserving synaptic plasticity and memory. J.Neurochem. 76: 1-10; 2001.

Watabe, A. M., Zaki, P. A., O'Dell, T. J. Coactivation of β-adrenergic and cholinergic receptors enhances the induction of long-term potentiation and synergistically activates mitogen-activated protein kinase in the hippocampal CA1 region. J. Neurosci. 20: 5924-5931; 2000.

Watanabe, M.; Nakamura, M.; Sato, K.; Kano, M.; Simon, M. I.; Inoue, Y. Patterns of expression for the mRNA corresponding to the four isoforms of phospholipase Cbeta in mouse brain. Eur.J.Neurosci. 10: 2016-2025; 1998.

Weeber, E. J.; Savage, D. D.; Sutherland, R. J.; Caldwell, K. K. Fear conditioning-induced alterations of phospholipase C-beta1a protein level and enzyme activity in rat hippocampal formation and medial frontal cortex. Neurobiol.Learn.Mem. 76: 151-182; 2001.

Williams, R. L. Mammalian phosphoinositide-specific phospholipase C. Biochim.Biophys.Acta 1441: 255-267; 1999.

Xie, W.; Samoriski, G. M.; McLaughlin, J. P.; Romoser, V. A.; Smrcka, A.; Hinkle, P. M.; Bidlack, J. M.; Gross, R. A.; Jiang, H.; Wu, D. Genetic alteration of phospholipase C beta3 expression modulates behavioral and cellular responses to mu opioids. Proc.Natl.Acad.Sci.U.S.A 96: 10385-10390; 1999.

Xu, A.; Suh, P. G.; Marmy-Conus, N.; Pearson, R. B.; Seok, O. Y.; Cocco, L.; Gilmour, R. S. Phosphorylation of nuclear phospholipase C beta1 by extracellular signal-regulated kinase mediates the mitogenic action of insulin-like growth factor I. Mol.Cell Biol. 21: 2981-2990; 2001.

Ying, S.-W., Futter, M., Rosenblum, K., Webber, M. J., Hunt, S. P., Bliss, T. V. P., Bramham, C. R. Brain-derived neurotrophic factor induces long-term potentiation in intact adult hippocampus: requirement for ERK activation coupled to CREB and upregulation of *Arc* synthesis. J. Neurosci. 22: 1532-1540; 2002.

Figure 1 ERK2 co-immunoprecipitates with (A) PLC-β1, -β2 and -β4, but not -β3, and (B) PLC-γ1 and -γ2 . Hippocampal membrane proteins were incubated with rabbit polyclonal antibody specific for each of the designated PLC isozymes or with normal rabbit IgG. Immune complexes were recovered using protein A - Sepharose beads, washed to remove nonspecific proteins, and then separated on SDS-PAGE gels. Gels were also loaded with rat hippocampal membrane protein to serve as internal blotting control (Control). Samples were then transferred to PVDF membranes and were blotted with mouse monoclonal antibody specific for ERK2. The blots shown are representative of at least three blots for each isozyme.
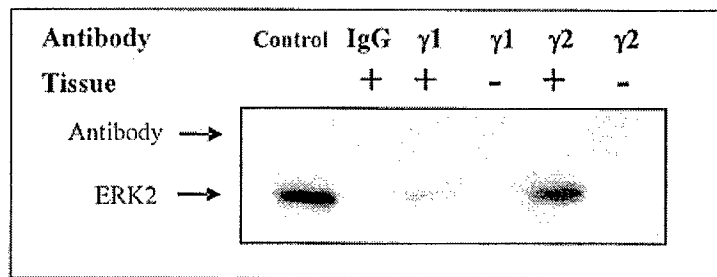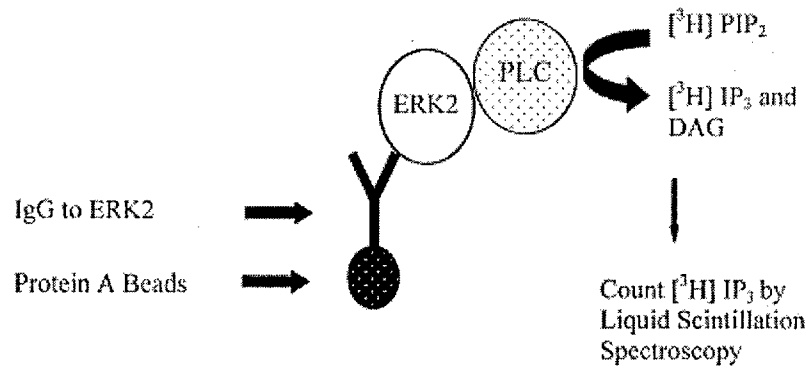
FIGURE 1

A
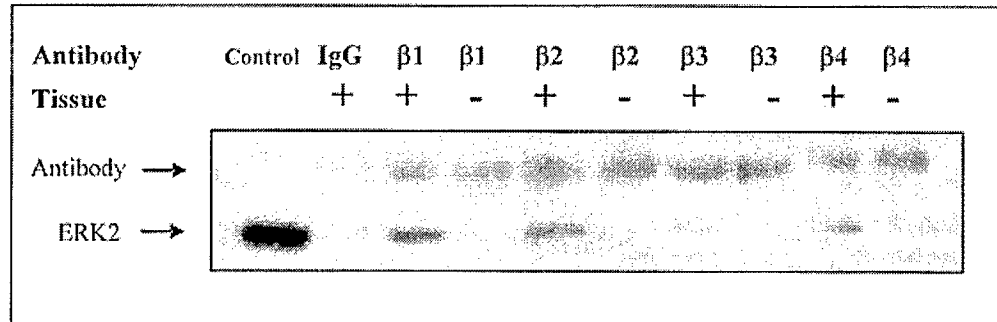
B

Figure 2. PLC activity present in anti-ERK2 immunoprecipitates isolated from rat hippocampal formation postnuclear membrane fractions. A.) Schematic representation of Enzyme Linked Immunosorbent Assay (ELISA) of PLC co-immunoprecipitating with ERK2. ERK2 was affinity captured with an anti-ERK2 monoclonal antibody bound to protein A-Sepharose beads. The beads were washed, then incubated in the presence of substrate, $[^3H]PtdIns(4,5)_2$ ($[^3H]PIP_2$). $[^3HIns(1,4,5)P_3$, $[^3H]IP_3$, product formation was measured by liquid scintillation spectroscopy. Background measurements were taken using a matching non-immune mouse IgG and treated similarly to anti-ERK2 immune complexes. Activity specific to the anti-ERK2 immune complex was measured as lipase activity present in the anti- ERK2 immune complexes minus lipase activity within the non-immune IgG sample. *B.)* The hippocampal formation was isolated from adult rats 30 min. following completion of the fear conditioning (paired tone-shock, PTS) or behavioral control (unpaired control, UPC) paradigm. Postnuclear membrane fractions were prepared and ERK2 was immunoprecipitated as described in the Methods. Immune complex PLC activity was measured and expressed as pmol $Ins(1,4,5)P_3$ product formed / min / mg tissue. N=6 for UPC and n=9 for PTS; asterisk designates significance determined by Student's t-test ($p < 0.02$).

FIGURE 2

A

B

28
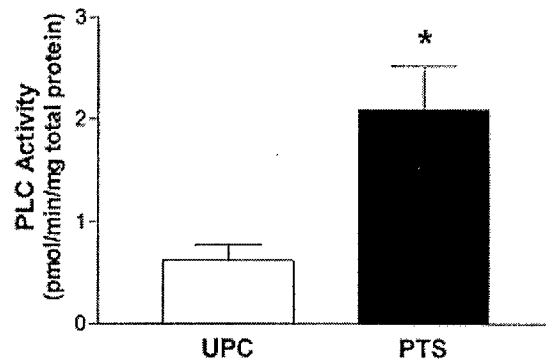
Figure 3. Effects of phospho-ERK2 treatment on anti-PLC-β1a (top), -β4 (middle), and -γ2 (bottom) immune complex PLC activity. Affinity captured PLC isozymes were treated with buffer, buffer with phospho-ERK2, buffer plus ATP, or buffer with phospho-ERK2 and ATP; subsequently, PLC activity was determined as described in the Materials and Methods section. Data are from 6 replicates and are representative of two experiments for PLC-β1a and PLC-β4 and three experiments for PLC-γ2.

FIGURE 3

A

B

C
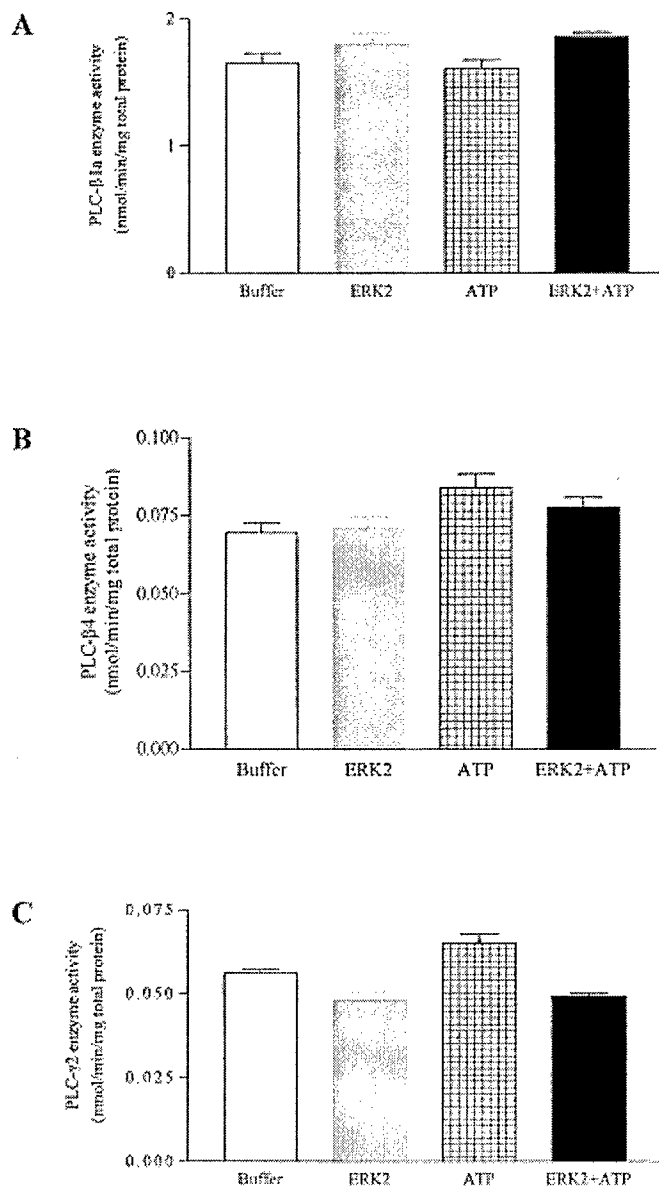
Table 1 Identification of peptide sequences within PLC isozymes that conform to consensus sequences of the D-domain and the FXFP motif. D-domain and FXFP motifs were identified employing consensus sequences identified by Kornfeld and colleagues (Jacobs et al. 1999; Fantz et al. 2001). Brackets indicate that two L/I-X-L/I motifs were identified at the C-terminal of the peptide. The position of the amino-terminal residue in the protein is identified as a superscript numeral. Sequences employed for these determinations were accession numbers P10687 (PLC-β1a), NP004564 (PLC-β2), NP032900 (PLC-β3), AAB28484 (PLC-β4a), P10686 (PLC-γ1), P24135 (PLC-γ2), P10688 (PLC-δ1), S14113 (PLC-δ2), NP542419 (PLC-δ4), and BAC00906 (PLC-ε); the sequence for PLC-δ3 was taken from Lee and Rhee (1996).

TABLE 1

PLC isozyme	FXFP motif	D-domain motif
-β1	none	[777]R-N-E-R-N-Q-P-L-M-L [1028]K-Y-Q-K-R-E-H-I-K-L [1153]K-F-K-R-L-P-L-E-I
-β2	none	[977]R-E-L-K-D-R-L-E-L(-E-L)
-β3	[782]F-D-F-P	none
-β4	none	[985]K- K-K-G-G-S-N-C-L-E-I
-γ1	none	[945]R-R-K-K-I-A-L-(E-L)
-γ2	none	[164]R-E-L-K-T-I-L-P-L
-δ1	none	[102]K-D-Q-R-N-T-L-D-L [335]K-G-C-R-C-L-E-L
-δ2	none	none
-δ3	none	[93]R-R-K-N-L-D-L
-δ4	none	none
-ε	none	[1369]R-E-N-K-K-D-L-Q-L-(P-L) [1941]R-G-Y-R-H-L-Q-L

Identification of Phospholipase C-γ1 as a Mitogen-activated Protein Kinase Substrate*

Colin T. Buckley‡, Fujio Sekiya§, Yeun Ju Kim§, Sue Goo Rhee§, and Kevin K. Caldwell‡¶

From the ‡Department of Neurosciences, University of New Mexico Health Sciences Center, Albuquerque, New Mexico 87131 and the §Laboratory of Cell Signaling, NHLBI, National Institutes of Health, Bethesda, Maryland 20892

The discovery of sequence motifs that mediate protein-protein interactions, coupled with the availability of protein amino acid sequence data, allows for the identification of putative protein binding pairs. The present studies were based on our identification of an amino acid sequence in phosphatidylinositol-specific phospholipase C-γ1 (PLC-γ1) that fits the consensus sequence for a mitogen-activated protein kinase (MAPK) binding site, termed the D-domain. Extracellular signal-regulated kinase 2 (ERK2), an MAPK, and phospho-ERK2 were bound by an immobilized peptide sequence containing the identified PLC-γ1 D-domain. Furthermore, a peptide containing the PLC-γ1 D-domain was able to competitively inhibit the *in* vitro phosphorylation of recombinant PLC-γ1 by recombinant phospho-ERK2, whereas a control peptide derived from a distant region of PLC-γ1 was ineffective. Similarly, the peptide containing the PLC-γ1 D-domain, but not the control peptide, competitively inhibited the *in vitro* phosphorylation of Elk-1 and c-Jun catalyzed by recombinant phospho-ERK2 and phospho-c-Jun N-terminal kinase 3 (phospho-JNK3), another type of MAPK, respectively. Incubation of anti-PLC-γ1 immunocomplexes isolated from rat brain with recombinant phospho-ERK2 opposed the increase in PLC-γ1-catalyzed hydrolysis of phosphatidylinositol 4,5-P_2 (PtdIns(4,5)P_2), which was produced by a tyrosine kinase associated with the immunocomplexes, whereas *in vitro* phosphorylation of recombinant PLC-γ1 by recombinant phospho-ERK2 did not alter PLC-γ1-catalyzed PtdIns(4,5)P_2 hydrolysis. These studies have uncovered a previously unidentified mechanism for the integration of PLC-γ1- and ERK2-dependent signaling.

Mitogen-activated protein kinases (MAPKs)[1] are proline-directed, serine/threonine kinases having a minimal consensus

¶ To whom correspondence should be addressed: Dept. of Neurosciences, MSC08 4740, 1 University of New Mexico, Albuquerque, NM 87131-0001. Tel.: 505-272-0033; Fax: 505-272-8082; E-mail: kcaldwell@salud.unm.edu.

[1] The abbreviations used are: MAPK, mitogen-activated protein kinase; ERK, extracellular signal-regulated protein kinase; JNK, c-Jun N terminal kinase; p38, p38 stress-activated protein kinase; MEK, MAPK/ERK kinase; PLC-γ1, phosphatidylinositol-specific phospholipase C-γ1; PtdIns(4,5)P_2, phosphatidylinositol 4,5-P_2; Ins(1,4,5)P_3, inositol 1,4,5-trisphosphate; 1,2-DAG, 1,2-diacylglycerol; GST, glutathione S-transferase; SH2, Src homology 2; SH3, Src homology 3; PKC, protein kinase C; PKA, protein kinase A; MOPS, 3-(N-morpholino)propanesulfonic acid; PVDF, polyvinylidenedifluoride.

substrate sequence of (S/T)P, where S, T, and P represent the amino acids serine, threonine, and proline, respectively (1). The presence of a proline residue in the −2 position is favorable and yields the optimal consensus substrate sequence of PX(S/T)P, where X is any amino acid (1). Three families of MAPK have been identified: extracellular signal-regulated protein kinase (ERK), c-Jun N-terminal kinase (JNK, also called stress-activated protein kinase), and p38 stress-activated protein kinase (p38; also called RK/CSBP). Multiple members of each of these MAPK families have been cloned. MAPKs exist in an inactive, unphosphorylated form and an active, phosphorylated form. MAPKs are converted to the active, phosphorylated form by dual-specificity kinases termed MAPK kinases or MAPK/ERK kinases (MEKs), which phosphorylate threonine and tyrosine (Y) residues in the enzymes (2–4).

It has been estimated that ~90% of all proteins contain an (S/T)P sequence, yet, not all of these proteins are substrates for MAPKs (5). This indicates that MAPK-dependent phosphorylation of a substrate involves the interaction (docking) of the kinase with a site on the substrate that is distinct from the phosphoacceptor site. Kornfeld and colleagues (5–6) have identified two ERK binding motifs: 1) the FXFP motif and 2) the D-domain motif. In addition to conferring specificity, docking domains may increase the efficiency of substrate phosphorylation (7–11). The location of the MAPK docking site can be either N- or C-terminal to the phosphorylation site (10, 12). The sites on ERKs that are involved in substrate binding have also been identified: the common docking site, which binds the D-domain of the substrate (13), and a distinct hydrophobic pocket for FXFP binding formed between the MAP kinase insert, the $p + 1$ site, and an αF helix (14).

Phosphatidylinositol-specific phospholipase C (PLC) isozymes catalyze the hydrolysis of phosphatidylinositol 4,5-bisphosphate (PtdIns(4,5)P_2), yielding the intracellular messengers, inositol 1,4,5-trisphosphate (Ins(1,4,5)P_3) and 1,2-diacylglycerol (1,2-DAG) (15–16). Complementary DNA clones have been isolated for 11 distinct mammalian PLC isozymes (17). Comparison of the predicted amino acid sequences of these clones reveals that PLC isozymes may be grouped into four types: PLC-β, PLC-δ, PLC-γ, and PLC-ε; the present studies focus on PLC-γ1. Growing evidence implicates PLC-γ1 as an important component of signal transduction processes involved in various cellular processes, including mitogenesis, differentiation, transformation, and neuronal plasticity (18). It is important to note that some PLC-γ-mediated cellular responses have been shown to be independent of PLC-γ lipase activity (19–22), indicating that PLC-γ isozymes function through interactions (direct or indirect) with other signaling molecules, in addition to functioning via Ins(1,4,5)P_3- and 1,2-DAG-dependent signaling pathways.

Cross-talk between the MAPK signaling cascade and PLC-γ1 has been demonstrated in many studies. For example,

Morrison *et al.* (23) showed that the MEK, Raf, co-immunoprecipitates with, as well as phosphorylates, PLC-γ1. Rong *et al.* (24) reported that activation of the Raf/MEK/MAPK pathway in PC12 cells by nerve growth factor requires PLC-γ1 enzyme activity. We demonstrate that ERK2 and phospho-ERK2 interact with PLC-γ1 both *in vitro* and within rat brain and that this interaction has functional significance.

EXPERIMENTAL PROCEDURES

Animals—Female Sprague-Dawley rats (150–200 days old) were maintained as described in Weeber *et al.* (25). The rats were given unlimited access to standard rat chow and tap water. All procedures employed for the housing, handling, and sacrificing of rats were approved by the University of New Mexico Health Sciences Center Institutional Animal Care and Use Committee.

Peptide Synthesis—All peptides and peptide columns were commercially synthesized by BIOSOURCE International (Hopkinton, MA). Both of the peptides used in the kinase inhibition assays demonstrated the same solubility in water. Neither peptide altered the pH of the reaction buffers in these assays.

PLC-γ1 D-domain Peptide Pull-down Assay—Peptides containing the sequence of the PLC-γ1 D-domain (RRKKIALELSELVVYC, rat PLC-γ1 amino acids 945–960) or a control sequence form PLC-γ1 (FLETNTLRTGERPELC, rat PLC-γ1 amino acids 232–247) were synthesized (>90% purity) and coupled to thiol agarose (1 mg of peptide per ml of resin). Binding of recombinant ERK2 (unactive) and phospho-ERK2 (active) to the peptide-coupled agarose was performed employing a procedure adapted from Zhang *et al.* (26). Briefly, 5 ng of ERK2, or 50 ng of phospho-ERK2, per 100 μl of binding buffer (20 mM Tris-HCl, pH 7.4, 1 mM EDTA, 320 mM sucrose, 75 mM NaCl, 75 mM KCl, and 16 mM (1%, v/v) Triton X-100) were incubated with 50 μl (packed volume) of D-domain or control peptide agarose at 4 °C for 2 h with mixing. The agarose was collected by centrifugation (14,000 × g, 4 min, room temperature) and washed four times with 1 ml of binding buffer. Bound proteins were eluted by boiling in 2× SDS-PAGE loading buffer, separated by SDS-PAGE (7.5% w/v polyacrylamide gels), transferred to polyvinylidene fluoride (PVDF) membrane, and probed for anti-ERK2 or anti-phospho-ERK2 immunoreactivity as described below.

In Vitro Phosphorylation of PLC-γ1—Recombinant PLC-γ1 and PLC-γ2 were prepared essentially as described in Park *et al.* (27). One microgram of recombinant PLC-γ1 or PLC-γ2 preparation was incubated (30 °C, 20 min, and 25-μl final volume) in kinase reaction buffer (for phospho-ERK2: Assay Dilution Buffer I (20 mM MOPS, pH 7.2, 25 mM β-glycerol phosphate, 5 mM EGTA, 1 mM sodium orthovanadate, 1 mM dithiothreitol, and 0.01% (v/v) Brij-35); for phospho-JNK3: 75 mM Tris-HCl, pH 7.5, 3.6 mM MOPS, pH 7.2, 4.5 mM β-glycerol phosphate, 1.05 mM EGTA, 3.2 mM dithiothreitol, 0.18 mM sodium orthovanadate, 0.5 mg BSA/ml, 0.015% (v/v) Brij-35; and for phospho-p38γ: 30 mM Tris-HCl, 0.03 mM EGTA, 0.1 mg BSA/ml, and 2 mM dithiothreitol), 13.5 mM MgCl$_2$, and 90 μM [γ-^{32}P]ATP (15 μCi) in the absence or presence of recombinant phospho-ERK2 (100 ng), phospho-JNK3 (100 ng), or phospho-p38γ (250 ng). Control reactions were incubated in the absence of protein kinase. Peptide competition studies were performed by preincubating (10 min, 30 °C) 50 ng phospho-ERK2 in the presence of 100 μM PLC-γ1 D-domain (MERRKKIALELSELVVYCRPVPFD, rat PLC-γ1 amino acids 943–966) or PLC-γ1 Control (YSAQKTMDLPFLETNTL-RTGERPEL, rat PLC-γ1 amino acids 222–246) peptide in kinase reaction buffer/MgCl$_2$/ATP solution (see above). Control reactions were performed in the absence of phospho-ERK2 and peptide. Reactions were initiated by addition of recombinant PLC-γ1 (1 μg/reaction) and continued for 30 min at 30 °C. Reactions were terminated by the addition of 8 μl of 4× SDS-PAGE sample buffer followed by heating (100 °C, 6 min). The entire mixture was subjected to SDS-PAGE (7.5% w/v polyacrylamide gels) then transferred to PVDF, and ^{32}P-labeled PLC-γ1 was detected by autoradiography. In addition, the membrane was stained with Coomassie Brilliant Blue R-250 to measure protein loading. Briefly, the PVDF membrane was immersed in a 0.025% (w/v) Brilliant Blue R-250 solution containing 40% (v/v) methanol for 5 min at room temperature, then destained for 15 min in 40% (v/v) methanol.

Phosphorylation of c-Jun and Elk-1—MAPK-dependent phosphorylation of c-Jun and Elk-1 was preformed employing a procedure based on a method described by Ho *et al.* (28). Phosphorylation of Elk-1 was performed as follows. His-tagged phospho-ERK2 (12.5 ng) was incubated (20 min, 30 °C, 25-μl reaction volume) with 1 μg of recombinant fusion protein of GST-tagged Elk-1, residues 301–428, in phospho-ERK2 kinase reaction buffer (see above), 13.5 mM MgCl$_2$, and 90 μM [γ-^{32}P]ATP (15 μCi) in the absence or presence of the PLC-γ1 D-domain peptide (in a 1:2 dilution series starting at 100 μM and ending at 12.5 μM) or 100 μM PLC-γ1 control peptide. The phospho-ERK2 was preincubated with the appropriate peptide for 10 min at 30 °C prior to adding the substrate to initiate the kinase reaction. The peptide sequences for the PLC-γ1 D-domain and Control peptides were the same as used in the PLC-γ *in vitro* phosphorylation studies. Reactions were terminated and processed as described above for *in vitro* phosphorylation of PLC-γ1. Equal loading of PVDF membranes was assessed using Brilliant Blue R-250 staining as described above.

Kinase reactions (25 μl) for phospho-JNK3 (1 ng) phosphorylation of GST-c-Jun (300 ng) were performed in JNK3 kinase reaction buffer (see above), 13.5 mM MgCl$_2$, 90 μM [γ-^{32}P]ATP (15 μCi), and the indicated concentration of peptide. Again, phospho-JNK3 kinase was preincubated with the appropriate peptide for 10 min at 30 °C prior to adding the substrate. Reactions were incubated for 10 min at 30 °C and were analyzed as described above.

Tissue Preparation and Subcellular Fractionation—Preparation of Triton X-100 extracts of rat whole brain postnuclear (S1) fraction and hippocampal formation postnuclear membrane (P2) fraction were performed as described in Buckley and Caldwell (29) except buffers also contained 20 mM β-glycerophosphate, 20 mM sodium pyrophosphate, and 10 mM sodium fluoride.

Affinity Capture of Anti-PLC-γ1 Immune Complexes—Anti-PLC-γ1 immunocomplexes were isolated as follows. For determinations of anti-ERK2 immunoreactivities, whole rat brain S1 fraction (100 μg of protein) was incubated with 6 μg of rabbit anti-PLC-γ1 antibody overnight with mixing at 4 °C. The immunocomplexes were recovered with protein A-Sepharose beads and washed twice with 1 ml of extraction buffer supplemented with 20 mM β-glycerophosphate, 20 mM sodium pyrophosphate, and 10 mM sodium fluoride, as described in Weeber *et al.* (25). For GST pull-down assays, whole rat brain S1 fraction (100 μg of protein) was incubated with glutathione-agarose precoupled to a GST fusion protein of the PLC-γ1 SH2-SH2-SH3 domains or glutathione-agarose control beads for 4 h at 4 °C. The beads were collected by centrifugation, and the supernatant was decanted and incubated with 6 μg of rabbit anti-PLC antibodies or non-immune rabbit IgG. The immunocomplexes and controls were processed as described above. For *in vitro* PLC activity measurements, anti-PLC-γ1 immunocomplexes were immobilized on 96-well plates, as described elsewhere (29).

Immunoblotting—Anti-ERK2 immunoreactivity associated with anti-PLC-γ1 immunocomplexes or bound by immobilized D-domain peptides was measured as follows. Fifty microliters of 2× SDS-PAGE sample buffer was added to the sample, and the mixture was boiled for 5 min. Eluted proteins were separated using 7.5% (w/v) SDS-PAGE gels prior to transfer to PVDF membranes. Membranes were blocked in 5% (w/v) fat-free milk in Tris-buffered saline and blotted with mouse anti-ERK2 antibody (1:1000) followed by anti-mouse horseradish peroxidase-conjugated antibody (1:3000). The immunoreactive proteins were detected using enhanced chemiluminescence.

In Vitro Treatment of Anti-PLC-γ1 Immunocomplexes with Phospho-ERK2—Anti-PLC-γ1 immunocomplexes were captured from 20 μg of rat hippocampal P2 preparation, then incubated (20 min, 35 °C) in the presence of one of the following buffers: *A*) Assay Dilution Buffer I plus 20 μM protein kinase C (PKC) inhibitor peptide, 2 μM protein kinase A (PKA) inhibitor peptide, and 20 μM Compound R24571; *B*) Buffer A containing 0.4 unit of recombinant phospho-ERK2; *C*) Buffer A supplemented with 13.5 mM MgCl$_2$ and 90 μM ATP; or *D*) Buffer C with 0.4 unit of recombinant phospho-ERK2. The wells were washed three times (5 min each) with 1.25× PLC assay buffer (43.75 mM sodium phosphate, pH 6.8, 87.5 mM KCl, 1.0 mM EGTA, 1.0 mM CaCl$_2$) prior to quantification of PLC activity (see below). The *in vitro* treatment of recombinant PLC-γ1 with recombinant phospho-ERK2 was performed as described for the anti-PLC-γ1 immunocomplexes captured from rat hippocampal P2 preparation, except 100 ng of recombinant PLC-γ1 was first captured onto the microtiter plate prior to the *in vitro* treatment, or not, with recombinant phospho-ERK2. In addition, incubation of recombinant PLC-γ1 with Buffer C was omitted due to the failure of detecting [γ-^{32}P]phosphate incorporation in the absence of kinase (Fig. 3*A*). Recombinant PLC-γ1 lipase activity was then quantified as described below.

Immunocomplex PLC Activity Measurement—PLC activity associated with anti-PLC-γ1 immunocomplexes was quantified as described in Buckley and Caldwell (29). Activity was calculated as nanomoles of Ins(1,4,5)P$_3$ product formed/min/mg of protein present in the sample from which the enzyme was affinity captured.

A

```
   1 MAGVGTPCAN GCGPSAPSEA EVLHLCRSLE VGTVMTLFYS KKSQRPERKT FQVKLETRQI
  61 TWSRGADKIE GSIDIREIKE IRPGKTSRDF DRYQEDPAFR PDQSHCFVIL YGMEFRLKTL
 121 SLQATSEDEV NMWIKGLTWL MEDTLQAATP LQIERWLRKQ FYSVDRNRED RISAKDLKNM
 181 LSQVNYRVPN MRFLRERLTD FEQRSGDITY GQFAQLYRSL MYSAQKTMDL PFLETNTLRT
 241 GERPELCQVS LSEFQQFLLE YQGELWAVDR LQVQEFMLSF LRDPLREIEE PYFFLDELVT
 301 FLFSKENSVW NSQLDAVCPE TMNNPLSHYW ISSSHNTYLT GDQFSSESSL EAYARCLRMG
 361 CRCIELDCWD GPDGMPVIYH GHTLTTKIKF SDVLHTIKEH AFVASEYPVI LSIEDHCSIA
 421 QQRNMAQHFR KVLGDTLLTK PVDIAADGLP SPNQLRRKIL IKHKKLAEGS AYEEVPTSVM
 481 YSENDISNSI KNGILYLEDP VNHEWYPHYF VLTSSKIYYS EETSSDQGNE DEEEPKEASG
 541 STELHSSEKW FHGKLGAGRD GRHIAERLLT EYCIETGAPD GSFLVRESET FVGDYTLSFW
 601 RNGKVQHCRI HSRQDAGTPK FFLTDNLVFD SLYDLITHYQ QVPLRCNEFE MRLSEPVPQT
 661 NAHESKEWYH ASLTRAQAEH MLMRVPRDGA FLVRKRNEPN SYAISFRAEG KIKHCRVQQE
 721 GQTVMLGNSE FDSLVDLISY YEKHPLYRKM KLRYPINEEA LEKIGTAEPD YGALYEGRNP
 781 GFYVEANPMP TFKCAVKALF DYKAQREDEL TFTKSAIIQN VEKQDGGWWR GDYGGKKQLW
 841 FPSNYVEEMI NPAILEPERE HLDENSPLGD LLRGVLDVPA CQIAIRPEGK NNRLFVFSIS
 901 MPSVAQWSLD VAADSQEELQ DWVKKIREVA QTADARLTEG KMMERRKKIA LELSELVVYC
 961 RPVPPFDEEKI GTERACYRDM SSFPETKAEK YVNKAKGKKF LQYNRLQLSR IYPKGQRLDS
1021 SNYDPLPMWI CGSQLVALNF QTPDKPMQMN QALFMAGGHC GYVLQPSTMR DEAFDPFDKS
1081 SLRGLEPCVI CIEVLGARHL PKNGRGIVCP FVEIEVAGAE YDSTKQRTEF VVDNGLNPVW
1141 PAKPFHFQIS NPEFAFLRFV VYEEDMFSDQ NFLAQATFPV KGLKTGYRAV PLKNNYSEDL
1201 ELASLLIKID IFPAKENGDL SPFSGTSLRE RASDASSQLF HVRAREGSFE ARYQQPFEDF
1261 RISQEHLADH FDSRERRAPR RTRVNGDNRL
```

B

```
  1 MAAAAAAGPE MVRGQVFDVG PRYTNLSYIG EGAYGMVCSA YDNLNKVRVA IKKISPFEHQ
 61 TYCQRTLREI KILLRFRHEN IIGINDIIRA PTIEQMKDVY IVQDLMETDL YKLLKTQHLS
121 NDHICYFLYQ ILRGLKYIHS ANVLHRDLKP SNLLLNTTCD LKICDFGLAR VADPDHDHTG
181 FLTEYVATRW YRAPEIMLNS KGYTKSIDIW SVGCILAEML SNRPIFPGKH YLDQLNHILG
241 ILGSPSQEDL NCIINLKARN YLLSLPHKNK VPWNRLFPNA DSKALDLLDK MLTFNPHKRI
301 EVEQALAHPY LEQYYDPSDE PIAEAPFKFD MELDDLPKEK LKELIFEETA RFQPGYRS
```

FIG. 1. **Phospholipase C-γ1 and Erk2 amino acid sequences.** *A*, PLC-γ1 sequence. Putative D-domain and MAPK phosphoacceptor sites are marked: one D-domain (*blue, bold,* and *underlined letters*); seven MAPK phosphorylation sites (*red, bold,* and *underlined sequence*). *B*, ERK2 sequence. Putative PLC-γ1 interaction motifs are marked: minimum SH3 domain binding motif (*green, bold,* and *underlined sequence*), β$_{1A}$ integrin PLC-γ binding motif (*underlined sequence*). Accession numbers: PLC-γ1 (P10686) and ERK2 (AAA41124).

MATERIALS AND METHODS

Rabbit polyclonal and mouse monoclonal antibodies against PLC-γ1, mouse monoclonal antibody to ERK2, biotinylated goat anti-rabbit antibodies, glutathione agarose, glutathione *S*-transferase (GST) fusion protein comprising the SH2-SH2-SH3 domains of PLC-γ1 pre-coupled to agarose, as well as each of the three individual domains pre-coupled to agarose, were purchased from Santa Cruz Biotechnology, Inc. (Santa Cruz, CA). Horseradish peroxidase-labeled goat anti-mouse IgG secondary antibody, [γ-^{32}P]ATP, and [^{3}H]PtdIns(4,5)P$_2$ were purchased from PerkinElmer Life Sciences. Mouse monoclonal anti-phospho-ERK1/2 antibody, GST-tagged c-Jun (amino acids 1–89), and GST-tagged Elk-1 (amino acids 301–428) were purchased from Cell Signaling Technology (Beverly, MA). PtdIns(4,5)P$_2$ was purchased from Avanti Polar Lipids (Alabaster, AL). Streptawells®, streptavidin-coated microtiter plates, and Triton X-100 was purchased from Roche Applied Science. All electrophoresis supplies and PVDF membranes were from Bio-Rad. Protein A-Sepharose CL-4B and ECL Plus Western blotting Detection System were obtained from Amersham Biosciences. Recombinant phospho-ERK2, recombinant phospho-JNK3, recombinant phospho-p38γ, Assay Dilution Buffer I, Kinase Inhibitor Mixture, rabbit polyclonal anti-MAP kinase/ERK2 antibody, and magnesium/ATP mixture were from Upstate Biotechnology (Lake Placid, NY). Leupeptin, 4-(2-aminoethyl)benzenesulfonylfluoride hydrochloride, aprotinin, calpain inhibitor III, recombinant ERK2, and recombinant phospho-ERK2 were purchased from Calbiochem (San Diego, CA). Coomassie Brilliant Blue R-250 was from Fisher Biotech (Fairlawn, NJ). All other chemicals and supplies were purchased from commercial sources.

RESULTS

Identification of a Putative MAPK Docking Motif in PLC-γ1— We searched the primary structure of PLC-γ1 (Fig. 1A) for one or more amino acid motifs that fit the consensus sequences of ERK docking sites, as identified by Kornfeld and colleagues (5–6): 1) the FXFP motif, having the consensus sequence of FXFP and 2) the D-domain, having two possible consensus sequences: (K/R)X(X/K/R)(K/R)X$_{(1-4)}$(L/I)X(L/I) or (K/R)(K/R)(K/R)X$_{(1-5)}$(L/I)X(L/I). We did not find an FXFP sequence but did identify overlapping

sequences that conform to the two consensus D-domain sequences: ^{945}RRKKIAL(EL). In addition, we searched for potential ((S/T)P) and optimal (PX(S/T)P) MAPK phosphorylation sites in the primary sequence of PLC-γ1 (Fig. 1A). Seven (S/T)P sequences were identified, but none fit the optimal sequence for MAPK phosphorylation. We also searched the primary structure of ERK2 (Fig. 1B) for possible PLC-γ1-interacting domains. We identified a sequence (^{224}PIFP) that fits the minimum consensus sequence (PXXP) of an SH3 domain binding motif (30). In addition, we identified a sequence (^{112}KLLKTQHLSNDHI) that demonstrates homology to a PLC-γ1 binding site (KLLMIIH-DRREFA) on the cytoplasmic domain of integrin β$_{1A}$ (31).

Rat Brain ERK2 Co-immunoprecipitates with PLC-γ1— We found that anti-ERK2 immunoreactivity is associated with anti-PLC-γ1 immunocomplexes isolated from rat whole brain postnuclear (S1) fractions (Fig. 2A), as well as hippocampal formation postnuclear membrane (P2) preparations (data not shown). We detected only minimal anti-phospho-ERK2 immunoreactivity associated with anti-PLC-γ1 immunocomplexes (data not shown).

We tested the hypothesis that ERK2 found associated with anti-PLC-γ1 immunoprecipitates was bound, either directly or indirectly (*i.e.* mediated by a second, intermediary protein), to the SH2 and/or SH3 domains of PLC-γ1. We performed preliminary experiments in which we incubated rat whole brain S1 fraction (100 μg) with a fusion protein comprising the N-terminal SH2, C-terminal SH2, and SH3 domains of rat PLC-γ1 pre-coupled to agarose (50 μg), or with each of these three domains individually coupled to agarose (50 μg). These studies demonstrated specific binding of ERK2 to the combined SH2-SH2-SH3 agarose, as well as the C-terminal SH2 domain, but not with the N-terminal SH2 domain or the SH3 domain (data not shown). ERK2 within rat brain S1 extracts failed to bind to
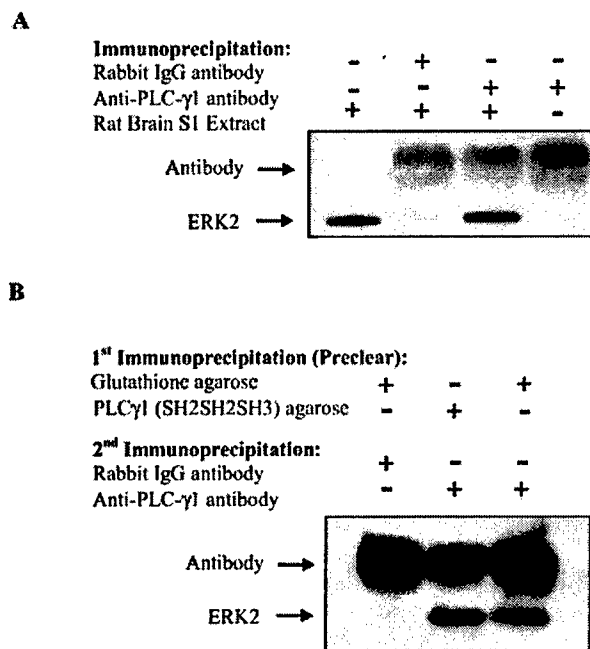
A

Immunoprecipitation:

Rabbit IgG antibody	-	+	-	-
Anti-PLC-γl antibody	-	-	+	+
Rat Brain S1 Extract	+	+	+	-

Antibody ➝

ERK2 ➝

B

1ˢᵗ Immunoprecipitation (Preclear):

Glutathione agarose	+	-	+
PLCγl (SH2SH2SH3) agarose	-	+	-

2ⁿᵈ Immunoprecipitation:

Rabbit IgG antibody	+	-	-
Anti-PLC-γl antibody	-	+	+

Antibody ➝

ERK2 ➝

FIG. 2. **Co-immunoprecipitation of PLC-γ1 and ERK2 is not affected by preclearing rat brain S1 preparations of proteins that bind to PLC-γ1 SH2 and SH3 domains.** *A*, rat brain S1 fraction was incubated overnight with PLC-γ1 rabbit polyclonal antibodies, or normal rabbit IgG. Immunocomplexes were recovered using Protein A-coated Sepharose beads and washed three times with buffer. Bound proteins were eluted with SDS-PAGE loading buffer, fractionated on SDS-polyacrylamide gels, and transferred to PVDF membrane. Anti-ERK-2 immunoreactivity was determined as described under "Experimental Procedures." *B*, rat brain S1 fraction was mixed with either glutathione-agarose or agarose-bound fusion protein consisting of the PLC-γ1 N-SH2, C-SH2, and SH3 domains fused with glutathione *S*-transferase. The beads were collected by centrifugation, the supernatant was removed, and PLC-γ1 was immunoprecipitated as in *A*. For both *A* and *B* the results are representative of three independent experiments.

AUTORADIOGRAM

A

	No kinase	+pERK2	+ pp38 γ⁻	+pJNK3
PLC-γl ➝				

COOMASSIE STAIN

	No kinase	+pERK2	+ pp38 γ	+pJNK3
PLC-γl ➝				

B

AUTORADIOGRAM

	No kinase	+pERK2	+ pp38 γ	+pJNK3
PLC-γ2 ➝				

COOMASSIE STAIN

	No kinase	+pERK2	+ pp38 γ	+pJNK3
PLC-γ2 ➝				

FIG. 3. **MAPKs catalyze the phosphorylation of recombinant PLC-γ1.** Recombinant PLC-γ1 (*A*) or PLC-γ2 (*B*) was incubated *in vitro* with [γ-³²P]ATP and either without (*lane 1*, no kinase) or with recombinant phospho-ERK2 (*lane 2*, +pERK2), phospho-p38γ (*lane 3*, + pp38γ), or phospho-JNK3 (*lane 4*, + pJNK3). The reactions were terminated and resolved by SDS-PAGE. Proteins were transferred to PVDF and radioactivity was detected by autoradiography (*top*) or protein was stained with Coomassie blue (*bottom*). The results are representative of three experiments for phospho-ERK2 and phospho-JNK3 phosphorylation of PLC-γ1. Phospho-p38γ phosphorylation of recombinant PLC-γ1 was tested twice.

C-terminal SH2 beads following pre-clearing of the extracts with the C-terminal SH2 beads (50 μg), even though a significant amount of ERK2 was still present within the sample (data not shown). These studies demonstrated that rat brain ERK2 indirectly binds to the PLC-γ1 C-terminal SH2 domain *in* vitro. However, pre-clearing of rat whole brain S1 preparations (100 μg) with an excess (50 μg) of agarose-coupled GST-SH2-SH2-SH3 domains of PLC-γ1 prior to isolation of anti-PLC-γ1 immunocomplexes did not dissociate the ERK2·PLC-γ1 complex (Fig. 2*B*). This approach is analogous to a procedure described by Snyder and colleagues (32), who reported that in the presence of 10 μg of GST-PLC-γ1 SH3 domain co-immunoprecipitation of PLC-γ1 and phosphoinositide 3-kinase enhancer is blocked. Thus, these studies demonstrate that, although ERK2 can bind indirectly to the PLC-γ1 C-terminal SH2 domain *in vitro*, the PLC-γ1 SH2 and SH3 domains do not significantly contribute to the binding of ERK2 within anti-PLC-γ1 immunocomplexes isolated from rat brain.

Phospho-ERK2 Directly Interacts with and Phosphorylates PLC-γ1 in Vitro—The identification of a putative ERK2 docking site in PLC-γ1 and co-immunoprecipitation of PLC-γ1 and ERK2 indicated that the two proteins may directly bind to each other. To test this hypothesis and to determine whether PLC-γ1 is a substrate for phospho-ERK2-catalyzed phosphorylation, we incubated recombinant PLC-γ1 and PLC-γ2 with recombinant phospho-ERK2 in the presence of [γ-³²P]ATP. We also sought to determine whether other MAPKs, specifically p38γ and JNK3, were able to phosphorylate PLC-γ1. Fig. 3*A* shows that PLC-γ1 serves as an *in vitro* substrate for phospho-ERK2, as well as
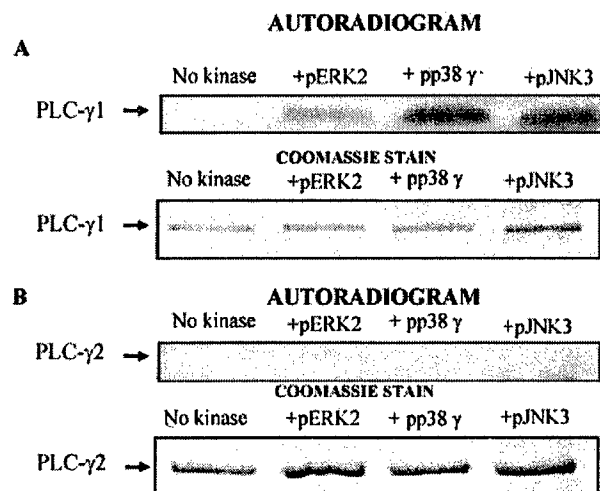
phospho-p38γ and phospho-JNK3, whereas negligible phosphorylation of PLC-γ2 was detected in the presence of these MAPKs (Fig. 3*B*). Control reactions incubated in the absence of recombinant MAPK demonstrated that the phosphorylation of PLC-γ1 was catalyzed by the recombinant MAPK.

Recombinant ERK2 and Phospho-ERK2 Bind to Immobilized PLC-γ1 D-domain Peptide in Vitro—To determine whether the identified PLC-γ1 D-domain sequence is capable of binding ERK2, the sequence of the PLC-γ1 D-domain (Fig. 4*A*) and a control peptide sequence outside of the PLC-γ1 D-domain (Fig. 4*A*) were coupled to thiol-agarose and incubated with recombinant ERK2. Similarly, we incubated the immobilized peptides with recombinant phospho-ERK2. Both recombinant ERK2 (Fig. 4*B*) and recombinant phospho-ERK2 (Fig. 4*C*) were capable of binding to the immobilized D-domain peptide. In contrast, neither ERK2 nor phospho-ERK2 was bound by the PLC-γ1 control peptide, confirming that the binding was specific for the D-domain.

The PLC-γ1 D-domain Inhibits the MAPK-catalyzed Phosphorylation of MAPK Substrates—To substantiate the claim that the peptide sequence that we identified in PLC-γ1 functions as a putative D-domain, we assessed the ability of a peptide containing the PLC-γ1 D-domain (Fig. 5*A*) to competitively inhibit the phosphorylation of a known phospho-ERK2 substrate, Elk-1, and a known JNK substrate, c-Jun. Several investigators (*e.g.* Refs. 8–10) have demonstrated that D-domain peptides competitively inhibit the binding of MAPKs to their substrates *in vitro*. The PLC-γ1 D-domain peptide inhibited both c-Jun phosphorylation by active JNK-3 (Fig. 5*B*) and Elk-1 phosphorylation by active ERK2 (Fig. 5*C*) in a concentration-dependent manner, whereas the PLC-γ1 control peptide did not inhibit either Elk-1 or c-Jun phosphorylation by the appropriate kinase. The Elk-1 substrate contains multiple MAPK phosphorylation sites, accounting for the appearance of three phosphorylated bands in the autoradiogram. The PLC-γ1 D-domain peptide inhibited the phosphorylation of the upper two bands, whereas it did not alter labeling of the lower, least phosphorylated band, suggesting that it may result from phos-
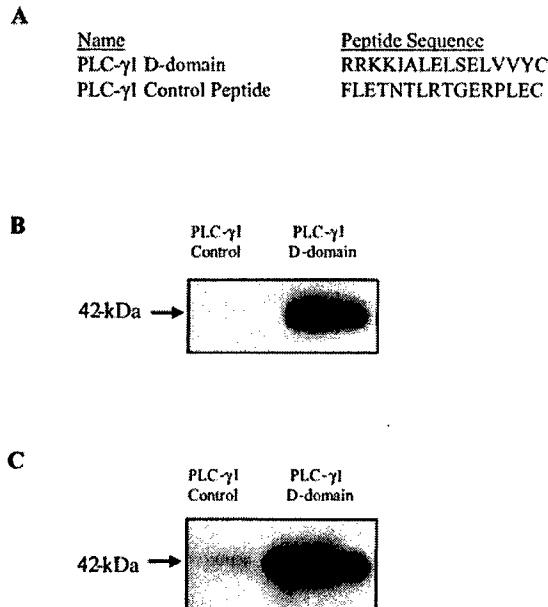
A

Name	Peptide Sequence
PLC-γl D-domain	RRKKIALELSELVVYC
PLC-γl Control Peptide	FLETNTLRTGERPLEC

B

C

FIG. 4. **Immobilized PLC γ1 D-domain binds recombinant ERK2 and recombinant phospho-ERK2.** *A*, amino acid sequences of synthetic peptides corresponding to the putative PLC-γ1 D-domain or a PLC-γ1-control peptide which contain a C-terminal cysteine for coupling to agarose were incubated with unphosphorylated ERK2 (*B*) or phospho-ERK2 (*C*). The agarose was collected by centrifugation and washed with buffer. Bound protein was eluted with SDS-PAGE loading buffer, separated by SDS-PAGE, and transferred to PVDF membrane, and the blot was probed for anti-ERK2 or anti-phospho-ERK2 immunoreactivity as described under "Experimental Procedures." Each result is representative of at least three separate experiments.

A

Name	Peptide Sequence
PLC-γl D-domain	MERRKKIALELSELVVYCRPVPFD
PLC-γl Control Peptide	YSAQKTMDLPFLETNTLRTGERPEL

B

C

FIG. 5. **PLC-γ1 D-domain competitively inhibits phospho-JNK3-dependent phosphorylation of c-Jun and phospho-ERK2-dependent phosphorylation of Elk-1.** *A*, amino acid sequences of synthetic peptides containing the putative PLC-γ1 D-domain or a PLC-γ1-control peptide. *B*, phospho-JNK3 was incubated with GST-c-Jun and [γ-^{32}P]ATP in the absence or presence of the PLC-γ1 D-domain peptide (50 μM to 3.125 μM) or control peptide at a concentration of 50 μM. The proteins were separated using SDS-PAGE, transferred to PVDF, and visualized using autoradiography. *C*, recombinant Erk2 was incubated with a recombinant protein fusion of GST-tagged Elk-1 and [γ-^{32}P]ATP in the absence or presence of the PLC-γ1 D-domain peptide (100 μM to 12.5 μM) or control peptide at a concentration of 100 μM. Phosphorylation was analyzed as in *B*. The results shown in *B* and *C* are representative of four independent experiments.

phorylation of phosphoacceptor sites independent of interaction of phospho-ERK2 with the D-domain of Elk-1. Similar results have been reported by Bardwell *et al.* (10).

The PLC-γ1 D-domain Inhibits the Phospho-ERK2-catalyzed Phosphorylation of PLC-γ1—In the presence of the PLC-γ1 D-domain peptide, the phospho-ERK2-catalyzed phosphorylation of PLC-γ1 was blocked, whereas the PLC-γ1 control peptide did not affect the phosphorylation of PLC-γ1 (Fig. 6*A*). Coomassie staining of the membrane demonstrated equal loading of the recombinant PLC-γ1 (Fig. 6*B*).

Treatment of Anti-PLC-γ1 Immunocomplexes with Phospho-ERK2 Reverses the Tyrosine Kinase-dependent Stimulation of Immunocomplex PLC Activity—Phospho-ERK2 phosphorylation of recombinant PLC-γ1 did not alter lipase activity (Fig. 7*A*). In contrast, phospho-ERK2 exerted significant effects on anti-PLCγ1 immunocomplex PLC activity (Fig. 7*B*). Anti-PLC-γ1 immunocomplexes were isolated from rat hippocampal formation P2 preparations, then treated with or without ATP and with or without phospho-ERK2. Subsequently, PLC activity was measured. PLC-γ1 enzyme activity was significantly increased by treatment with ATP alone. We have shown previously that this effect of ATP is produced by a tyrosine kinase that is associated with the anti-PLC-γ1 immunocomplex (29). In the absence of ATP, phospho-ERK2 did not significantly alter PLC-γ1 enzyme activity. In the presence of ATP, phospho-ERK2 significantly reduced, but did not completely reverse, the increase in PLC-γ1 enzyme activity that was produced by a tyrosine kinase associated with the immunocomplexes.

DISCUSSION

We have made several important and novel observations in these studies. First, we provide evidence that PLC-γ1 associates with ERK2 in rat brain extracts and that dual phosphorylation of ERK2 in its activation loop is not critical for the
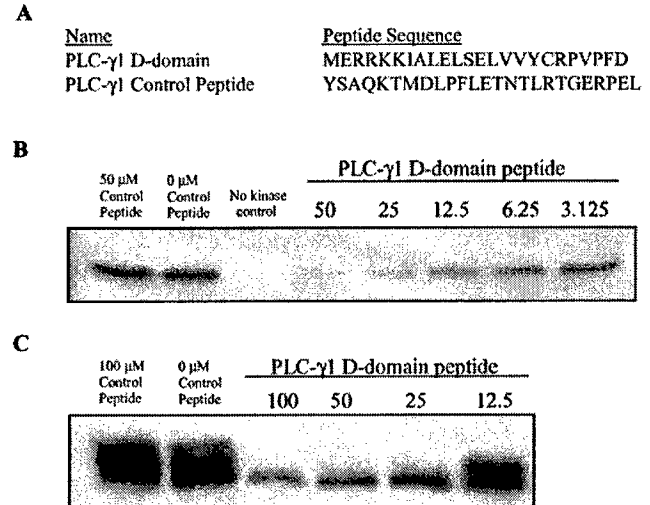
association as demonstrated by minimal immunoreactivity of a phospho-specific antibody for ERK1/2 in a Western blot of PLC-γ1 immunoprecipitates. This association, therefore, was probably not mediated via binding to a phosphoacceptor site found within the PLC-γ1 sequence due to conformational constraints imposed on ERK2 by the non-phosphorylated "activation lip" of ERK2. However, the interaction of PLC-γ1 with phospho-ERK2 was direct, because recombinant PLC-γ1 was a substrate for recombinant phospho-ERK2 *in vitro*. This, in turn, is a second novel finding; *i.e.* PLC-γ1 is a MAPK substrate. The finding that PLC-γ2 was minimally phosphorylated by MAPKs under the same conditions demonstrated specificity of the kinase reactions. Although our results demonstrate that PLC-γ2 is a poor phospho-MAPK substrate, it is possible that MAPK-dependent phosphorylation of PLC-γ2 may occur under other conditions: *e.g.* after PLC-γ2 has been phosphorylated by another protein kinase. Third, using both peptide-binding and MAPK substrate phosphorylation assays, we identified a peptide sequence within the primary sequence of PLC-γ1 that conforms to the consensus sequence for an ERK-docking site, a D-domain. A peptide version of the PLC-γ1 D-domain inhibited the *in vitro* phosphorylation of PLC-γ1 by phospho-ERK2. This result demonstrates that the interaction between PLC-γ1 and phospho-ERK2 is dependent on the common docking domain of phospho-ERK2 and strongly implicates the D-domain of PLC-γ1 as the ERK2-binding site on PLC-γ1. Furthermore, it indicates that interactions between other sites on phospho-ERK2 (*e.g.* putative PLC-γ1 interaction motifs shown in Fig. 1*B*) and PLC-γ1 do not play a significant role in PLC-γ1-phospho-ERK2 binding. Finally, phospho-ERK2 treatment of anti-PLC-γ1 immunocomplexes under conditions allowing for substrate phosphorylation revealed that phospho-ERK2 opposes tyrosine kinase-dependent stimulation of PLC-γ1 enzyme activity, whereas phosphorylation of recombinant

MAPK Phosphorylation of PLC-γ1

PLC-γ1 by phospho-ERK2 under similar conditions did not affect the lipase activity of PLC-γ1.

Identification of the PLC-γ1 D-domain sequence was based on consensus sequences defined by Kornfeld and colleagues (5–6). Other investigators (*e.g.* Refs. 3, 12–13, 33) have identified similar, but different, MAPK docking sequence motifs. In general, MAPK binding motifs consist of peptide sequences of ~20 amino acids, or less. Rather than specifying consensus

A

AUTORADIOGRAM OF PLC-γ1

B

COOMASSIE STAIN OF PLC-γ1

FIG. 6. **PLC-γ1 D-domain peptide inhibits phospho-ERK2-catalyzed phosphorylation of recombinant PLC-γ1.** *A,* recombinant PLC-γ1 was incubated *in vitro* with [γ-^{32}P]ATP and without (*lane 1,* no kinase) phospho-ERK2 or with recombinant phospho-ERK2 (*lanes 2–4,* +ERK2) in the absence (*lane 4*) or presence of the PLC-γ1 D-domain peptide (*lane 2*) or the PLC-γ1 control peptide (*lane 3*). Proteins were transferred to PVDF, and radioactivity was detected by autoradiography (*A*) or protein was stained with (*B*) Coomassie stain. The results shown are representative of three separate experiments.

sequences, Sharrocks and colleagues (34) have developed models of MAPK docking domains that identify regions of sequence similarity: specifically, basic, L*X*L, and hydrophobic motifs. These regions play differing roles in dictating specificity for interactions with members of the ERK, JNK, and p38 stress-activated protein kinase families. The p38 kinases bind proteins that have a basic region and hydrophobic region, whereas the intervening LXL motif is dispensable; ERKs require the presence of all motifs, although the hydrophobic motif is less important than the other two regions (34). The PLC-γ1 D-domain that we identified consists of a basic region and an (L/I)XL motif; in addition, an adjacent hydrophobic region (^{953}LVV) is readily identifiable. This indicates that, in addition to binding ERKs, the PLC-γ1 D-domain may bind p38 and JNK family members. In support of this proposal, we have found that PLC-γ1 is an *in vitro* substrate for p38γ and JNK3.

PLC-γ1·ERK2 protein complexes were immunoprecipitated from rat brain lysates, indicating that the observed interactions between recombinant proteins are not simply *in vitro* artifacts. However, we were able to detect only minimal anti-phospho-ERK2 immunoreactivity associated with anti-PLC-γ1 immunocomplexes. It is worth noting that, similar to our data, Husi *et al.* (35) reported that the *N*-methyl-D-aspartic acid receptor is isolated in association with ERK2, but not phospho-ERK2, and Loeb *et al.* (36) reported that the TrkA receptor is found in association with ERK1, but not phosph-ERK1, or either form of ERK2. Interestingly, PLC-γ1 has been shown to co-immunoprecipitate with an unidentified protein of molecular mass of ~42,000 Da, and the amount of phosphorylated protein (molecular mass ~ 42,000 Da) associated with anti-PLC-γ1 immunoprecipitates is significantly increased following receptor activation (37, 38). Our results indicate that this protein may be ERK2.

Results of the experiments in which we assessed the effects of phospho-ERK2 pretreatment on *in vitro* PLC activity indicate that PLC-γ1 is regulated, either directly or indirectly, by phospho-ERK2. Phospho-ERK2 treatment opposed stimulation of PLC-γ1 enzyme activity by a tyrosine kinase that co-immunoprecipitated with PLC-γ1. Two possible mechanisms may underlie this effect. Phospho-ERK2-catalyzed phosphorylation
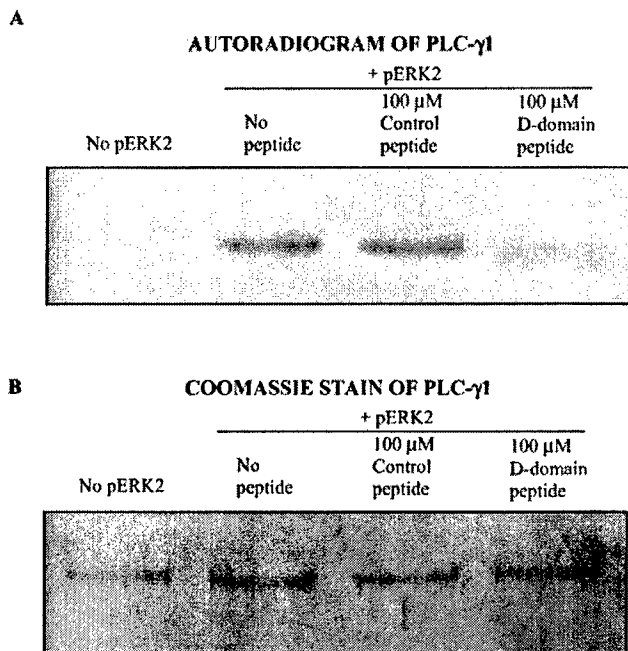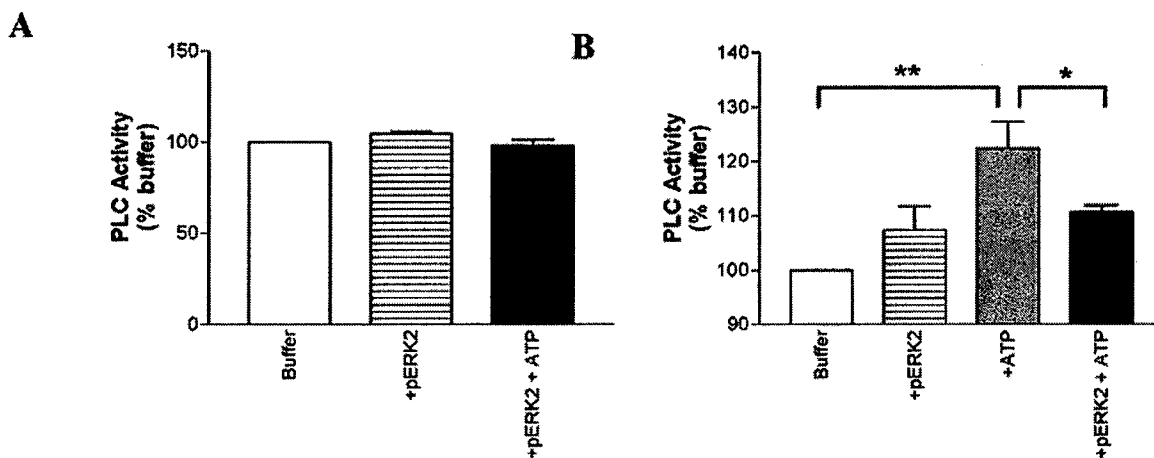
A

B

FIG. 7. **Phospho-ERK2 treatment significantly reduces ATP-dependent stimulation of immunocomplex PLC-γ1 catalytic activity.** PLC-γ1 was affinity captured as recombinant PLC-γ1 (*A*), or from rat hippocampal formation postnuclear particulate (P2) fraction (*B*). Captured recombinant PLC-γ1 was treated with one of the following: buffer, buffer containing recombinant phospho-ERK2 (+*pERK2*); or buffer containing recombinant phospho-ERK2 and ATP (+*pERK2* + *ATP*). Captured PLC-γ1 from rat hippocampal formation postnuclear particulate (P2) fraction was treated with buffer; buffer containing ATP (+*ATP*); buffer containing recombinant phospho-ERK2 (+*pERK2*); or buffer containing recombinant phospho-ERK2 and ATP (+pERK2 + ATP). Subsequently, PLC activity associated with the immunocomplex was determined. PLC activity is calculated as nanomoles of Ins(1,4,5)P$_3$ product formed/min/mg of protein, then expressed within each experiment as a percentage of the mean of the buffer value. Each point is the average ± S.E. (*n* = 3 preparations) after background subtraction. In *B,* one-way analysis of variance revealed a significant overall effect of treatment F (3, 11) = 12.61, p < 0.002. Newman-Kuels multiple comparison test revealed p < 0.01 (**) for buffer *versus* +ATP and p < 0.05 for +ATP *versus* +pERK2+ATP.
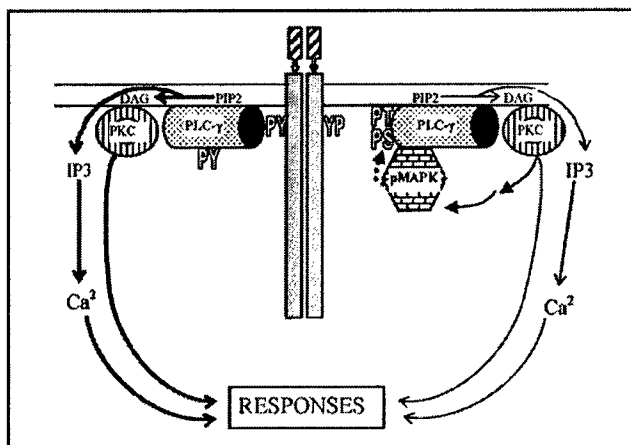
FIG. 8. **Model showing proposed mechanism of MAPK-dependent opposition of tyrosine kinase-dependent activation of PLC-γ1.** Upon binding of ligand to a tyrosine kinase receptor, transphosphorylation of tyrosine residues of the receptor creates a phosphotyrosine (*PY*) binding site for the N-terminal SH2 domain of PLC-γ1 on the receptor cytoplasmic tail. The receptor then phosphorylates PLC-γ1 on tyrosine residue(s), increasing the catalytic efficiency of the enzyme toward its substrate, PI(4,5)P$_2$ (*PIP2*). Consequently, there is an increase in the formation of the products 1,2-diacylglycerol (*DAG*), which activates certain forms of protein kinase C (*PKC*), and Ins(1,4,5)P$_3$, which mobilizes Ca^{2+} from intracellular stores. PKC and Ca^2 elicit a variety of cellular responses. The *darker lines* indicate elevated flux through the pathway, relative to lighter lines. On the *right side* of the receptor, PKC is shown to lead to the activation of PLC-γ1-associated MAPK via a multistep pathway. Alternative mechanisms of MAPK activation are also possible. The activated MAPK (*pMAPK*) phosphorylates threonine and/or serine, yielding phosphothreonine (*PT*), and phosphoserine (*PS*), respectively, on PLC-γ1, which opposes activation of PLC-γ1 by the ligand-bound tyrosine kinase receptor. For ease of interpretation, the PT/PS-phosphorylated PLC-γ1 is shown dissociated from the tyrosine kinase receptor.

of PLC-γ1 may oppose tyrosine kinase-dependent phosphorylation of the enzyme, similar to the mechanism proposed by Rhee and colleagues (39) for the regulation of PLC-γ1 activity by PKA and PKC. Tyrosine phosphorylation, and consequent activation, of PLC-γ1 may be reduced either as the result of reduced efficiency of PLC-γ1 phosphorylation by one or more tyrosine kinases or increased efficiency of PLC-γ1 dephosphorylation by one or more tyrosine phosphatases. Alternatively, phospho-ERK2 may indirectly decrease PLC-γ1 enzyme activity as the result of inhibiting the catalytic activity of the tyrosine kinase that is responsible for the genistein-inhibited activation of the isozyme. Studies aimed at testing these possibilities are being conducted in our laboratory. Finally, it should be noted that, because PLC-γ1 is commonly positioned early within a signal transduction pathway, relatively small changes in PLC-γ1 enzyme activity become amplified, often producing 2- to 4-fold changes in physiologic responses (*e.g.* functioning of ion channels, changes in gene expression) (40).

The physiologic significance of associations between PLC-γ1 and MAPKs is currently uncertain. Several possibilities exist. First, MAPKs may regulate the catalytic activity of PLC-γ1. Our results support a model (see Fig. 8) in which phospho-ERK2 acts to oppose tyrosine kinase-dependent activation of PLC-γ1, indicating that MAPKs, at least phospho-ERK2, may act to down-regulate PLC-γ1 signaling. This is in contrast to the reported stimulatory effect of phospho-ERK1/2 on PLC-β1 (41). A second possible significance of MAPK interactions with PLC-γ1 is that PLC-γ1 may target MAPKs to signaling complexes containing components (*e.g.* PKC, Raf, and MEK) of pathways that produce MAPK activation, thus increasing the efficiency of transducing signals from PLC-γ1 to MAPKs. Once activated, the phospho-MAPK may, or may not, dissociate from

PLC-γ1 and regulate downstream effectors (*e.g.* transcription factors). In support of this proposal are reports of PLC-γ1 association with PKC-α (42) and Raf (23), and the identified roles of PLC-γ1 in the control of cellular processes that are dependent on gene transcription (43–45). Third, association of a MAPK with a PLC isozyme may allow for the MAPK to gain access to, and phosphorylate, a protein (*e.g.* one bound to the SH2 and/or SH3 domains of PLC-γ1) that does not itself directly bind to the MAPK. This is analogous to the demonstration that JNK can phosphorylate proteins lacking JNK-binding sites but that are bound to c-Jun (46).

PLC-γ1 has been reported to directly interact with various classes of cellular proteins, including receptor and non-receptor tyrosine kinases (26, 47–48), ion channel-forming receptors (49), phospholipase D2 (50), the synaptic vesicle protein, synaptojanin (51), the p21Ras-specific guanine nucleotide exchange factor SOS1 (21), and the serine/threonine kinase Raf1 (23). Our studies demonstrate that ERK2 and phospho-ERK2 can be added to this list. Thus, in addition to regulating cellular functions via controlling Ins(1,4,5)P$_3$ and 1,2-DAG production, PLC-γ1 appears to act as a scaffolding protein, which may account for the observations that some PLC-γ1-mediated cellular responses are independent of catalytic activity (19–22). Additional studies are needed to determine whether MAPK-dependent phosphorylation of PLC-γ1 regulates its functioning as a scaffolding protein.

REFERENCES

1. Davis, R. J. (1993) *J. Biol. Chem.* **268**, 14553–14556
2. Kolch, W. (2000) *Biochem. J.* **351**, 289–305
3. Pearson, G., Robinson, F., Beers, G. T., Xu, B. E., Karandikar, M., Berman, K., and Cobb, M. H. (2001) *Endocr. Rev.* **22**, 153–183
4. Johnson, G. L., and Lapadat, R. (2002) *Science* **298**, 1911–1912
5. Fantz, D. A., Jacobs, D., Glossip, D., and Kornfeld, K. (2001) *J. Biol. Chem.* **276**, 27256–27265
6. Jacobs, D., Glossip, D., Xing, H., Muslin, A. J., and Kornfeld, K. (1999) *Genes Dev.* **13**, 163–175
7. Yang, S. H., Whitmarsh, A. J., Davis, R. J., and Sharrocks, A. D. (1998) *EMBO J.* **17**, 1740–1749
8. Yang, S. H., Yates, P. R., Whitmarsh, A. J., Davis, R. J., and Sharrocks, A. D. (1998) *Mol. Cell. Biol.* **18**, 710–720
9. Galanis, A., Yang, S. H., and Sharrocks, A. D. (2001) *J. Biol. Chem.* **276**, 965–973
10. Bardwell, A. J., Abdollahi, M., and Bardwell, L. (2003) *Biochem. J.* **370**, 1077–1085
11. Espanel, X., Walchli, S., Ruckle, T., Harrenga, A., Huguenin-Reggiani, M., and van Huijsduijnen, R. H. (2003) *J. Biol. Chem.* **278**, 15162–15167
12. Seidel, J. J., and Graves, B. J. (2002) *Genes Dev.* **16**, 127–137
13. Tanoue, T., Yamamoto, T., and Nishida, E. (2002) *J. Biol. Chem.* **277**, 22942–22949
14. Lee, T., Hoofnagle, A. N., Kabuyama, Y., Stroud, J., Min, X., Goldsmith, E. J., Chen, L., Resing, K. A., and Ahn, N. G. (2004) *Mol. Cell* **14**, 43–55
15. Majerus, P. W., Ross, T. S., Cunningham, T. W., Caldwell, K. K., Jefferson, A. B., and Bansal, V. S. (1990) *Cell* **63**, 459–465
16. Williams, R. L. (1999) *Biochim. Biophys. Acta* **1441**, 255–267
17. Rhee, S. G. (2001) *Annu. Rev. Biochem.* **70**, 281–312
18. Carpenter, G., and Ji, Q. (1999) *Exp. Cell Res.* **253**, 15–24
19. Smith, M. R., Liu, Y. L., Matthews, N. T., Rhee, S. G., Sung, W. K., and Kung, H. F. (1994) *Proc. Natl. Acad. Sci. U. S. A.* **91**, 6554–6558
20. Huang, P. S., Davis, L., Huber, H., Goodhart, P. J., Wegrzyn, R. E., Oliff, A., and Heimbrook, D. C. (1995) *FEBS Lett.* **358**, 287–292
21. Kim, M. J., Chang, J. S., Park, S. K., Hwang, J. I., Ryu, S. H., and Suh, P. G. (2000) *Biochemistry* **39**, 8674–8682
22. Patterson, R. L., van Rossum, D. B., Ford, D. L., Hurt, K. J., Bae, S. S., Suh, P. G., Kurosaki, T., Snyder, S. H., and Gill, D. L. (2002) *Cell* **111**, 529–541
23. Morrison, D. K., Kaplan, D. R., Rhee, S. G., and Williams, L. T. (1990) *Mol. Cell. Biol.* **10**, 2359–2366
24. Rong, R., Ahn, J. Y., Chen, P., Suh, P. G., and Ye, K. (2003) *J. Biol. Chem.* **278**, 52497–52503
25. Weeber, E. J., Savage, D. D., Sutherland, R. J., and Caldwell, K. K. (2001) *Neurobiol. Learn. Mem.* **76**, 151–182
26. Zhang, X., Chattopadhyay, A., Ji, Q. S., Owen, J. D., Ruest, P. J., Carpenter, G., and Hanks, S. K. (1999) *Proc. Natl. Acad. Sci. U. S. A.* **96**, 9021–9026
27. Park, D., Jhon, D. Y., Kriz, R., Knopf, J., and Rhee, S. G. (1992) *J. Biol. Chem.* **267**, 16048–16055
28. Ho, D. T., Bardwell, A. J., Abdollahi, M., and Bardwell, L. (2003) *J. Biol. Chem.* **278**, 32662–32672

29. Buckley, C. T., and Caldwell, K. K. (2003) *Anal. Biochem.* **320,** 193–198
30. Alexandropoulos, K., Cheng, G., and Baltimore, D. (1995) *Proc. Natl. Acad. Sci. (U. S. A.)* **92,** 3110–3114
31. Vossmeyer, D., Hofmann, W., Loster, K., Reutter, W., and Danker, K. (2002) *J. Biol. Chem.* **277,** 4636–4643
32. Ye, K., Aghdasi, B., Luo, H. R., Moriarity, J. L., Wu, F. Y., Hong, J. J., Hurt, K. J., Bae, S. S., Suh, P. G., and Snyder, S. H. (2002) *Nature* **415,** 541–544
33. MacKenzie, S. J., Baillie, G. S., McPhee, I., Bolger, G. B., and Houslay, M. D. (2000) *J. Biol. Chem.* **275,** 16609–16617
34. Barsyte-Lovejoy, D., Galanis, A., and Sharrocks, A. D. (2002) *J. Biol. Chem.* **277,** 9896–9903
35. Husi, H., and Grant, S. G. (2001) *J. Neurochem.* **77,** 281–291
36. Loeb, D. M., Tsao, H., Cobb, M. H., and Greene, L. A. (1992) *Neuron* **9,** 1053–1065
37. Wahl, M. I., Nishibe, S., Suh, P. G., Rhee, S. G., and Carpenter, G. (1989) *Proc. Natl. Acad. Sci. U. S. A.* **86,** 1568–1572
38. Park, D. J., Rho, H. W., and Rhee, S. G. (1991) *Proc. Natl. Acad. Sci. U. S. A.* **88,** 5453–5456
39. Park, D. J., Min, H. K., and Rhee, S. G. (1992) *J. Biol. Chem.* **267,** 1496–1501
40. Hoek, J. B. and Kholodenko, B. N. (1998) *Alcohol. Clin. Exp. Res.* **22,** 224S–230S
41. Vitale, M., Matteucci, A., Manzoli, L., Rodella, L., Mariani, A. R., Zauli, G., Falconi, M., Billi, A. M., Martelli, A. M., Gilmour, R. S., and Cocco, L. (2001) *FASEB J.* **15,** 1789–1791
42. Lee, I. H., You, J. O., Ha, K. S., Bae, D. S., Suh, P. G., Rhee, S. G., and Bae, Y. S. (2004) *J. Biol. Chem.* **279,** 26645–26653
43. Choi, D. Y., Toledo-Aral, J. J., Segal, R., and Halegoua, S. (2001) *Mol. Cell. Biol.* **21,** 2695–2705
44. Yang, J. M., Vassil, A. D., and Hait, W. N. (2001) *Mol. Pharmacol.* **60,** 674–680
45. Liao, H. J., Ji, Q. S., and Carpenter, G. (2001) *J. Biol. Chem.* **276,** 8627–8630
46. Kallunki, T., Deng, T., Hibi, M., and Karin, M. (1996) *Cell* **87,** 929–939
47. Nakanishi, O., Shibasaki, F., Hidaka, M., Homma, Y., and Takenawa, T. (1993) *J. Biol. Chem.* **268,** 10754–10759
48. Plattner, R., Irvin, B. J., Guo, S., Blackburn, K., Kazlauskas, A., Abraham, R. T., York, J. D., and Pendergast, A. M. (2003) *Nat. Cell Biol.* **5,** 309–319
49. Gurd, J. W., and Bissoon, N. (1997) *J. Neurochem.* **69,** 623–630
50. Jang, I. H., Lee, S., Park, J. B., Kim, J. H., Lee, C. S., Hur, E. M., Kim, I. S., Kim, K. T., Yagisawa, H., Suh, P. G., and Ryu, S. H. (2003) *J. Biol. Chem.* **278,** 18184–18190
51. Ahn, S. J., Han, S. J., Mo, H. J., Chung, J. K., Hong, S. H., Park, T. K., and Kim, C. G. (1998) *Biochem. Biophys. Res. Commun.* **244,** 62–67